Extended theoretical and experimental studies
of the calcium looping process for carbon dioxide capture

Von der Fakultät Energie-, Verfahrens- und Biotechnik der Universität Stuttgart

zur Erlangung der Würde eines Doktor-Ingenieurs (Dr.-Ing.)

genehmigte Abhandlung

Vorgelegt von

Glykeria Duelli geb. Varela

aus Kastrosikia, Preveza, Griechenland

Hauptberichter: Univ.-Prof. Dr. techn. Günter Scheffknecht

Mitberichter: Prof. Dr. Piero Salatino

Tag der mündlichen Prüfung: 3. März 2017

Institut für Feuerungs- und Kraftwerkstechnik der Universität Stuttgart

2017

Acknowledgements

For Christian and our daughter Nina

Table of Contents

Nomenclature

Latin Alphabets Formula Symbols

Symbol	Unit	Meaning
D_P	µm	Sauter mean particle diameter
D	M	Reactor diameter
$D50$	µm	Volume basis median particle diameter
$D10$	µm	Volume basis particle diameter below which 10% of particles distribution lie
$D90$	µm	Volume basis particle diameter below which 90% of particles distribution lie
f	-	Fraction of particles
H	M	Height
H	J	Enthalpy
k	1/s	Kinetic constant
k_{Attr}	1/(kgs)	Attrition rate constant
K_{Attr}	m²/(kgs³)	Overall attrition rate constant
k_{Deac}	-	Limestone deactivation constant
M	Kg	Mass in the DFB system
N	Mol	Amount of material
$\dot{N}$	mol/s	Molar flux
N	-	Number of carbonation calcination cycles
$\dot{R}$	1/s	Reaction rate
R_{Attr}	%$_{wt}$/h	Attrition rate by weight
T	K	Temperature
t	S	Time
$t_{crit,Carb}$	S	Time for sorbent carbonation conversion up to $X_{max, Ave}$

$t_{crit,Calc}$	S	Time for complete limestone calcination
u	m/s	Superficial gas velocity
u_{mf}	m/s	Minimum fluidization velocity
$X_{max,\,Ave}$	-	Maximum average carbonation conversion
X	-	Sorbent carbonate content
x	kg/kg	Mass fraction
y	m^3/m^3	Volume fraction

Greek Alphabets Formula Symbols

Symbol	Unit	Meaning
Δ	-	Difference
η	-	Efficiency
κ	-	Limestone deactivation coefficient
ξ_{CaL}	-	Calcium looping ratio
τ	S	Space time
ϕ	-	Specific parameter facility related

Subscript Indices

Subscripts	Meaning
Act	Active in terms of availability to react
Attr	Attrition
Ave	Average
bal	Balance
bed	Bed material
loss	With reference to the amount of Ca collected in the cyclones
Ca	Calcium

Carb	Carbonation
CR	Carbonator reactor
Calc	Calcination
CO₂	Carbon dioxide
crit	Critical
out	Emitted, outlet
in	Inlet flow
i	Index number
Deac	Deactivation
diff	Diffusion
dry	Dry
eq	Equilibrium
G	Flue gas
g	Gas
kin	Kinetic
m	Mean
mf	Minumum fluidization
MU	Make-up
max	maximum
meas	measurement
Norm	Normalized
P	Particle
L	Lean
R	Rich
Resi	Residual
RR	Regenerator reactor
rec	Recirculation
S	Solid
st	Water vapor
th	Thermal
theo	Theoretical
wt	Weight

vol	Volumetric
0	Initial conditions relative to the empty system state

Superscript Indices

Superscripts	Meaning
$\cdot$	Time derivative

List of Acronyms

Acronym	Meaning
AC	Avoided costs
AComb	Air-combustion
AFOLU	Agriculture, forest and other land use
ASU	Air separation unit
BECCS	Bioenergy carbon capture and storage
BET	Brunauer-Emmett-Teller theory
BFB	Bubbling fluidized bed
CaL	Calcium looping
CCS	Carbon capture and storage
CFB	Circulating fluidized bed
CFD	Computational fluid dymamics
CFBC	Circulating fluidized bed combustion
CFPP	Coal fired power plant
CHP	Combined heat and power
COE	Cost of electricity
COP	Conference of the parties
CPU	Compression and purification unit
DFB	Dual fluidized bed
EMMS	Energy minimization and multi-scale analysis

EPA	Environmental protection agency
EOR	Enhanced oil recovery
FGD	Flue gas desulphurization
GHG	Greenhouse gas
GT	Gas turbine
IEA	International energy agency
IGCC	Intergrated gasification combined cycle
K-L	Kunii- Levenspiel
LHV	Lower caloric value
LR	Ca looping ratio
LS	Limestone
NGFPP	Natural gas fired power plant
NGCC	Natural gas combined cycle
OComb	Oxy-combustion
TFM	Eulerian-Eulerian two-fluid model
TPES	Total primary energy supply
TGA	Thermogravimetric analyzer
TFB	Turbulent fluidized bed
TRL	Technology readiness level
UNIPCC	United nations intergovernmental panel on climate change
2DS	Two degrees celcius scenario

Abstract

The world is at a critical juncture in its efforts to combat climate change. Since the first Conference of the Parties (COP) in 1995, greenhouse-gas (GHG) emissions have risen by more than one-quarter and the atmospheric concentration of these gases has increased steadily to 435 parts per million carbon-dioxide equivalent (ppm CO_2-eq) in 2012 [1]. The international commitment to keep the increase in long-term average temperatures below two degrees Centigrade, compared to pre-industrial levels, requires substantial and sustained reductions in global emissions. Given the dominant role that fossil fuels continue to play in primary energy consumption followed by the continuously increasing global energy demand, the deployment of carbon capture and storage technologies (CCS) is imperative [1]. The individual component technologies required for CO_2 capture, transport and storage are generally well-understood and, in some cases, technologically mature.

The largest challenge for CCS deployment is the integration of component technologies into large-scale (demonstration) projects. In this direction simulation and modeling works allow a cost effective investigation of the feasibility and the applicability of the prototype technology as well as its development and optimization. In addition, complete process approach allows determination of the impact that integration of the CO_2 capture plant imposes on the power plant. However, a reliable assessment of the process performance requires the process models to be validated with experimental data.

In this work, one of the major CCS technologies, the calcium looping process is realized, investigated and evaluated at a 10 kW_{th} dual fluidized bed (DFB) continuously operating facility at the University of Stuttgart. The performance of the process in terms of CO_2 capture in the carbonator and sorbent calcination in the regenerator is studied. Natural limestones were used. The process was realised in presence of water vapor in both carbonator and regenerator reactor. The calcination took place in high CO_2 concentration representative of the oxy-fuel combustion in the regenerator. Synthetic

flue gas was used while both reactors were electrically heated with supplementary CH_4 combustion in the regenerator when necessary. The Ca flow circulating between the reactors as well as the Ca mass in the reactors were varied. The regenerator and the carbonator temperatures were varied. The sorbent CO_2 capture ability was studied through thermogravimetric analysis of the samples taken during experimentation. Attrition phenomena were studied by measuring the particle size distribution and weighting the material collected from the cyclones of the DFB facility.

The experimentation was successfully performed with reliable data and the trends observed are in good agreement with previous works. It was shown that CO_2 capture efficiencies of more than 90% can be achieved at conditions closer to the industrial ones. The CO_2 capture efficiency was improving by increasing bed inventory and looping ratio. The sorbent calcination degree is a decreasing function of the carbonate content of the incoming solid flow and an increasing function of the particle residence time and reactor temperature. In presence of water vapor, CO_2 capture efficiencies of more than 90% and complete sorbent calcination were achieved for looping ratios of around 8. The temperatures were for the regenerator not more than 1193K and for the carbonator around 903K. The sorbent carbonation conversion was retained at about 0.2 $mol_{CaCO3}/mol_{CaO,}$ constant for many hours of operation. The material loss was measured to be around 4.5%$_{wt}$/h based on the total system inventory while the mean particle size of the sorbent decreased to around 400 μm and remained constant for many hours of operation.

Simplified semi-empirical models were successfully implemented in the experimental results. Kinetic and attrition constants were calculated and a good agreement between the predicted and the actual data is shown. Design parameter of active space time was found to be 30s for the carbonator and 0.11h for the regenerator with efficiencies of more than 90% in both reactors.

Kurzfassung

Die Welt ist an einem kritischen Punkt in ihren Bemühungen zur Bekämpfung des Klimawandels. Seit der ersten Konferenz der Klimaschutz-Vertragsparteien im Jahr 1995 haben die Treibhausgasemissionen um mehr als ein Viertel zugenommen und die atmosphärische Konzentration dieser Gase hat sich stetig erhöht, bis auf 435 Teile pro Million Kohlendioxid-Äquivalent (ppm CO_2 äquivalent) im Jahr 2012 [1]. Um die Erhöhung des langfristigen durchschnittlichen Temperaturanstieges im Vergleich zum vorindustriellen Niveau unter zwei Grad Celsius zu halten, ist es erforderlich, mit internationalem Engagement eine erhebliche und nachhaltige Senkung der globalen Emissionen zu erreichen. Die vorherrschende Rolle, welche die fossilen Brennstoffe beim Primärenergieverbrauch weiterhin einnehmen, sowie die Tatsache eines stetig ansteigenden weltweiten Energiebedarfs legen den Einsatz von Kohlendioxid-Abscheidung und Speicherung (CCS) nahe [1]. Die erforderlichen Technologien der einzelnen Komponenten zur CO_2-Abscheidung, zum Transport und zur Lagerung sind im Allgemeinen gut bekannt und in einigen Fällen bereits technisch ausgereift.

Die größte Herausforderung für den CCS-Einsatz ist die Integration der Einzelkomponenten in größere Demonstrationsanlagen-Projekte. Vor diesem Hintergrund ermöglichen Simulations- und Modellierungsarbeiten eine kostengünstige Ermittlung der Machbarkeit und der Anwendbarkeit sowie die Entwicklung und Optimierung der Technologie. Darüber hinaus lassen sich mit einer Gesamtprozessbetrachtung mögliche Auswirkungen, welche die Integration der CO_2-Abscheidungsanlage auf das Kraftwerk hat, bestimmen. Allerdings erfordert eine zuverlässige Beurteilung der Leistungsfähigkeit des Prozesses eine Validierung der Prozessmodelle mittels experimentellen Daten.

Für diese Arbeit wurde eine der wesentlichen CCS-Technologien, das Calcium (Ca)-Looping-Verfahren, in einer kontinuierlich arbeitenden dualen $10kW_{th}$-Wirbelschichtanlage (DFB) der Universität Stuttgart, untersucht und evaluiert. Dabei wurden sowohl die Leistungsfähigkeit des CO_2-Abscheidungsprozesses im Karbonator als auch die Sorbent-Kalzinierung im Regenerator untersucht. Natürliche Kalksteine

wurden verwendet. Die Kalzinierung erfolgte bei hoher CO_2-Konzentration, was repräsentativ ist für die Oxy-fuel-Verbrennung im Regenerator. Außerdem wurde ein synthetisches Rauchgas inklusive Wasserdampf verwendet und beide Reaktoren wurden elektrisch beheizt, im Bedarfsfall auch mit Methan-Zusatzfeuerung im Regenerator. Die Feststoff-Zirkulation zwischen beiden Reaktoren sowie das Inventar in den Reaktoren wurde verändert. Auch die Regenerator- und die Karbonator-Temperaturen wurden variiert. Die CO_2-Abscheidefähigkeit des Sorbens wurde durch eine thermogravimetrische Untersuchung der während der Experimente genommenen Proben untersucht. Die Untersuchung von Abrieb-Phänomenen erfolgte durch Messungen der Partikelgrößen-Verteilung und Gewichtung des aus den Zyklonen der DFB-Anlage gesammelten Materials.

Die Experimente wurden erfolgreich durchgeführt und die beobachteten Trends stimmen gut mit früheren Arbeiten überein. Es konnte gezeigt werden, dass mit Bedingungen, die den industriellen Gegebenheiten sehr ähnlich sind, CO_2-Abscheidungsgrade von mehr als 90% erreicht werden. Die CO_2-Abscheidungsgrade verbesserten sich bei Erhöhung der Karbonatorbettmasse und bei höherem Ca-Looping-Ratio. Der Sorbens-Kalzinierungsgrad ist eine abnehmende Funktion des Karbonatgehalts des eingehenden Feststoffstromes und eine mit der Partikelverweilzeit und der Reaktortemperatur ansteigende Funktion. In Gegenwart von Wasserdampf wurden CO_2-Abscheidungsgrade von mehr als 90% und eine komplette Sorbens-Kalzinierung bei einem Ca-Looping-Ratio von etwa 8 erreicht. Die maximalen Temperaturen für den Regenerator lagen bei 1193K und die des Karbonators lagen bei etwa 903K. Die Sorbens-Karbonatisierung wurde für die Dauer von mehreren Betriebsstunden bei etwa 0,2 mol_{CaCO3}/mol_{CaO} konstant gehalten. Der gemessene Materialverlust betrug etwa 4,5%$_{wt}$/h des gesamten Systeminventars und die durchschnittliche Partikelgröße des Sorbents verringerte sich auf etwa 400 µm und blieb dann für mehrere Betriebsstunden konstant.

Vereinfachte semi-empirische Modelle wurden mit den experimentellen Ergebnissen erfolgreich validiert. Die angepassten kinetischen Konstanten und Abriebkonstanten zeigen, dass die tatsächlichen Daten gut mit den vorhergesagten

Daten übereinstimmen. Wirkungsgrade von mehr als 90% in beiden Reaktoren wurden bei aktiven Raumzeiten von 30s im Karbonator und 0,11h im Regenerator erreicht.

1 Introduction

Countries have already recognised that climate change, which is closely related to the growth of CO_2 emissions from human activities in both energy and industry sectors, presents an ever growing threat to development, poverty eradication efforts and the welfare of their citizens [2]. Each of the last three decades has been successively warmer at the earth's surface than any preceding decade since 1850 [2]. The impacts of climate change are already being felt on each continent by means of extreme phenomena such as sea level rise, desertification and extreme weather events. Warming is expected to exhibit interannual-to-decadal variability and will not be regionally uniform while it may affect part of the earth population not responsible [2].

According to the UN Intergovernmental Panel on Climate Change (UNIPCC), the world's greenhouse gas emissions are continuing to increase. Carbon dioxide from human activities, the major greenhouse gas, is continuously growing (40% since pre-industrial times and 2.2% per year for the period 2000-2010 compared to 1.3% per year for the previous three decades) [2]. In 2014 the concentration of CO_2 was about 40% higher than in the middle 1800's. On our current path, global temperature rise will far exceed the goal to limit it to two degrees centigrade that countries have agreed upon to avoid the fatal impacts of climate change [2].

In this direction, the International Energy Agency (IEA) proposed the so called 2°C Scenario (2DS) [3]. The 2DS describes an energy system consistent with an emissions trajectory that recent climate science research indicates would give an 80% chance of limiting average global temperature raise to 2°C. It sets the target of cutting energy-related CO_2 emissions by more than half in 2050 (compared with 2009) and ensuring that they continue to fall thereafter. To stop or at least to limit the negative consequences on climate change, the Paris Agreement is adopted on 7-8 December 2015 at the UN Climate Change Conference (COP21). In the Agreement, Parties committed to take ambitious actions to keep global temperature rise by the

end of the century below two degrees centigrade compared to pre-industrial levels, as adopted at Cancun 2010.

The mitigation strategies proposed by the UN IPCC may be categorized as follows: greenhouse gas (GHG) emissions intensity reduction, energy intensity reduction by improving technical efficiency, production and resource efficiency improvement as well as structural and systems efficiency improvement [4]. Furthermore, the UN IPCC mitigation options can be grouped into three broad sectors: (1) energy supply, (2) energy end-use sectors including transport, buildings, industry and (3) agriculture, forest and other land (AFOLU) [4]. Energy system related mitigation measures are categorized as follows: decarbonization of the energy supply sector, final energy demand reductions, and switch to low-carbon energy carriers, including electricity in the end-use sectors [4]. Especially, greater deployment of renewable energy, CCS, fuel switching within the group of fossil fuels, reduction of fugitive (methane) emissions in the fossil fuel chain would act for emissions intensity reduction. This goal can be achieved by improving the technical efficiency in (1) extraction, transport and conversion of fossil fuels, (2) electricity, heat and fuel transmission, distribution, and storage, (3) combined heat and power (CHP) or cogeneration [4]. Moreover, structural and systems efficiency improvement can be achieved by adressing integration needs [4].

Considering that fossil primary energy sources and its utilization in power generation are the primary CO_2 emitting sources, two mitigation measures are mainly considered: (1) efficiency improvement of the power plants and (2) separation of CO_2 from fuel or flue gas. Beyond efficiency-improving methods, for a further CO_2 reduction the decision on the method to be chosen need to be taken considering the most effective way. The 2DS acknowledges that transforming the energy sector is vital, but not the sole solution: the goal can only be achieved provided that CO_2 and GHG emissions in non-energy sectors are also reduced. The non-energy sectors include industrial sectors such as iron and steel, refining, petrochemical and cement manufacturing.

According to the IEA recent report, carbon capture and storage (CCS) is the only concept able to deliver significant emission reductions from the use of fossil fuels, not only from power generation, but also from industrial sectors [4]. The 2DS claims that CCS could deliver 13% of the cumulative emissions reductions needed by 2050 to limit the global temperature increase to 2°C. This represents the capture and storage of around 6 billion tones (Bt) of CO_2 emissions per year in 2050, nearly triple of India's energy sector emissions of today. Half of this captured CO_2 in the 2DS would come from industrial sectors, where there are currently limited or no alternatives for achieving substantial emission reductions. While there are alternatives to CCS in power generation, delaying or abandoning CCS would increase the required investment by 40% or more in the 2DS, and may place unrealistic demands on other low emission technology options [4]. Moreover, many models could not limit likely warming to below 2°C, if bioenergy, CCS and their combination (BECCS) are limited. Without CCS, long-term global climate goals may be unobtainable [5].

Calcium looping (CaL) is a techno-economically promising CO_2 capture technology based on separation of CO_2 with calcium-based solid sorbents (Figure 1) that can contribute to the challenge of dealing with global warming and simultaneously providing affordable energy. The process, which is already studied for syngas CO_2 removal from the 1960's, was firstly proposed by Heesink and Temmink in 1994 [6] as one of the zero emission coal technologies.
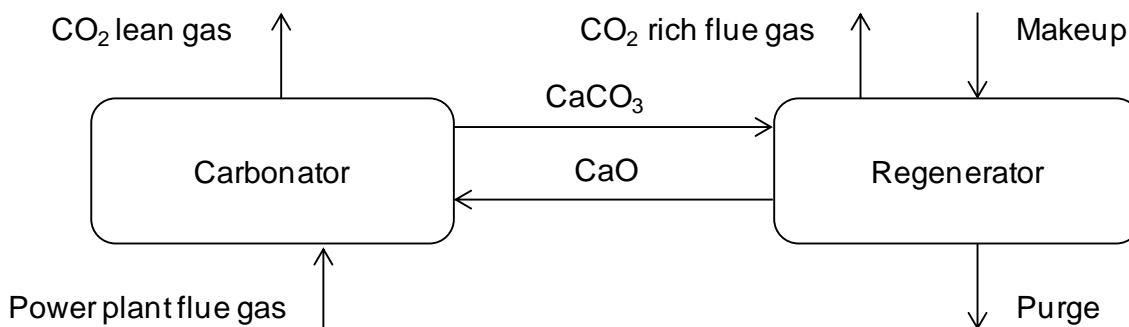
Figure 1: Main CaL process diagram

The CaL system utilizes limestone ($CaCO_3$) which is a natural well geographically distributed material that costs 10-30 $/tCaCO$_3$ [36]. The purged material has a great potential to be used in cement industry as well as in desulphurization units [8]. The nature of the material allows for post and/or pre-treatment of the sorbent. Thus, main sorbent disadvantages, i.e deactivation of the highly cycled sorbent CO_2 carrying capacity, may be counteracted [9]. Moreover, compared to solvents, $CaCO_3$ and CaO are much less hazardous to the operators' health and the environment [10]. In addition, the fluidized bed technology is applied to the system for the design of the reactors. This technology is already commercially used for coal combustion systems. Thus, the development process takes advantage of standard knowledge on fluid-dynamics and combustion. Additionally, the process has the potential to be used as a SO_2 scrubber thus the need of a flue gas desulphurization unit (FGD) might be overall eliminated [8]. Recent simulation work revealed that CaL seems to be the most appropriate technology for CO_2 capture in cement industry that accounts for almost 5% of CO_2 emissions worldwide [134].

Studies showed that heat can be recovered and used to generate an additional amount of high-pressure steam through the exothermic carbonation of lime at 923-973K and utilisation of available heat in the process streams [12,13]. Literature reports an overall efficiency decrease on the full system of 6.2 net points (from 45% LHV to 38.8%) [36]. Efficiency penalties associated with the calcination of the makeup flow of limestone required to maintain a given activity in the capture loop are considered zero, as it is assumed that an equivalent energy credit would be obtained from a cement plant or desulphurization plant using deactivated CaO from the CaL system [36]. The specific CO_2 emissions are reported to be 67 kgCO$_2$/MWh$_e$ [36]. With a further assumption of 10 $/ton of CO_2 to account for transport and storage a final set of reference cost figures of cost of electricity (COE)=0.075 $/kW$_e$ and avoided costs (AC)=40 $/tCO$_2$ can be estimated (they would be 0.086 $/kWe and 54.3 $/tCO$_2$ for the Oxy-CFB case) [36]. This is in line with other authors that mention predicted efficiency decrease 7 to 8% points, [13] with the CO_2 capture stage accounting for 2 to 3%, which is mainly due to the oxygen requirement [15]. Compared to an oxy-fuel

power plant less O_2 is required for oxy-combustion of fuel in the regenerator, leading to smaller ASU size [16], [14].

Besides, the average cost of avoided CO_2 is estimated to be 27-50 \$/tCO_2 which is more than 50% less than for amine scrubbing [18], [19], [20], [21], [22], [36]. Finally, exergy analysis revealed that although a considerable amount of the total exergy input (22.3%) is dissipated in the calcium looping process, the overall scheme is the most efficient in comparison to the amine scrubbing or the oxy-combustion [22].

The above mentioned aspects of the CaL system boost the research worldwide over the past decade and scaled up the process to TRL-6 (technology demonstrated in relevant environment: steady states at industrially relevant environment, pilots in the MW_{th} range) [36]. Research is performed with (1) an increased number of experimental work in testing facilities, (2) development of thermodynamic, mathematical, computational fluid dynamics (CFD) and process models as well as (3) integration works of the process into power generation systems (Table 1) [23]. However, the investigations performed up to now are mainly focused on the carbonator operation as well as the calcination reaction, while very few data are available for the regenerator operation [24]. In addition, most of the studies are performed under dry carbonator and air-fired conditions in the regenerator, while there is lack of data from a large scale facility where both reactors are operating under realistic process conditions [8], [24], [25], [26].

In this context, the scope of this work is to extend the knowledge on the calcium looping systems and to further validate tools which are useful for upscaling purposes as well as for interpretation of experimental results of pilot plants. Thus, this study reports experiments performed at the University of Stuttgart, in the 10 kW_{th} dual fluidized bed calcium looping facility under conditions closer to those expected industrially: wet flue gas in the carbonator reactor and atmospheres rich in CO_2 and H_2O_{st} in the regenerator reactor. The influence of main parameters, i.e temperature, CO_2 concentration, water vapor presence and Ca system inventory as well as mass flows circulating between the reactors, on CO_2 capture and release as well as sorbent CO_2 carrying capacity and mechanical stability, is discussed. Finally,

simplified kinetic and attrition models empirically oriented are implemented in the experimental results. Thus constants and characteristic parameters that can be used as a basis for design purposes are provided.

The work presented in this monograph is partly published by the author as follows: The effect of main process parameters on reactor and sorbent performance was published in the frame of the CALMOD "Modeling and experimental validation of calcium looping CO_2-capture process for near-zero CO_2-emission power plants" project in the final project report [131] as well as in the Deliverable of task 2.1 [107], in international conferences [132], [133] and in nominated international journals after peer review process [90], [105], [122]. Furthermore, system analysis by applying already existing models was published in an international well known journal after peer review process [112].

Glykeria Duelli (Varela) is the principal author and investigator in all the above mentioned publications. The principal author planned the experimental work while the coauthors assisted the principal author during the excecution of the experiments. Also, the principal author performed the analysis and the scientific interpretation of the results. Furthermore, the principal author worked on the documentation and the submitting/ reviewing process of the publications. Finally, the principal author is responsible for the experimental investigations and the application of the models as well as for the interpretation of the results.

Table 1: Review studies related to calcium looping

Reference	Subject
2005, Stanmore & Gilot [27]	Sintering, sulphation, particle fragmentation and attrition, correlations for mathematical modeling of carbonation, calcination, sulphation, sintering models for prediction of the aerodynamics and trajectories of particles, as well as reaction rates in fluidized beds
2008, Harrison et al [28]	Standard steam-methane reforming process and CaL process for H_2 production, thermodynamic analyses, sorbent durability, process configurations, experimental studies on H_2 production
2008, Florin et al [29]	Process configurations for enhanced H_2 production from biomass gasification, sorbent regeneration, sorbent activity decay, experimental work on H_2 production from carbonaceous fuels using calcium looping
2010, Blamey et al [30]	Carbonation, calcination, sintering and sorbent performance under cyclic operation, sorbent deactivation and reactivation techniques, calcium looping process applications, semi-empirical correlations for estimation of sorbent conversion.
2010, Dean et al [10]	Calcium looping cycle fundamentals, sorbent deactivation and sorbent performance, calcium looping thermodynamic and economic performance, application for cement and H_2 production, calcium looping pilot plants and operation up to 2011
2011, Anthony et al [9]	Natural and synthetic sorbents, sorbent performance improvements and reactivation strategies, calcium looping process applicability, experimental facilities
2012, Liu et al [31]	Enhancement of sorbent performance, methods for sintering-resistant sorbents
2013, Kierzkowska et al [32]	Carbonation reaction fundamentals, developments on synthetic Ca based sorbents
2013, Romano et al [33]	Calcium looping process simulations, suggestions for further modeling work
2014, Boot-Handford et al [34]	Process performance, sorbent deactivation/ regeneration, CaL pilot- plant work.
2015, Hanak et al [23]	Testing facilities: characteristics, operating conditions and experimental findings, reactor modeling, integration of calcium looping to power generation systems
2015, Abanades et al [36]	State of the art, low temperature solid sorbents and membranes CO_2 capture technologies, technical and economic aspects, process configurations, testing and pilot demonstration works, materials
2015, Fennell & Anthony [124]	Introduction, exergy-energy analysis, economics, sorbent enhancement, synthetic sorbents, spent sorbent utilization, reactor design, pilot plant experience, high pressure, low temperature solid CO_2 carriers

2 Background and CaL state of the art

2.1 Coal utilization and CO$_2$ emission

The use of energy in both power and industry sectors is responsible for almost two-thirds of all anthropogenic greenhouse-gas emissions (Figure 2) [36] while CO$_2$ resulting from oxidation of carbon in fuels during combustion dominates with 90% of total energy related emissions. In 2013, electricity and heat generation accounted for 42% of the total global CO$_2$ emissions. Energy demand is expected to grow by nearly one-third between 2013 and 2040 with a rate of 1.0% per year. The energy-related CO$_2$ emission is expected to grow by 16% from 2013 to 2040 (reaching 36.7 Gt) [37].
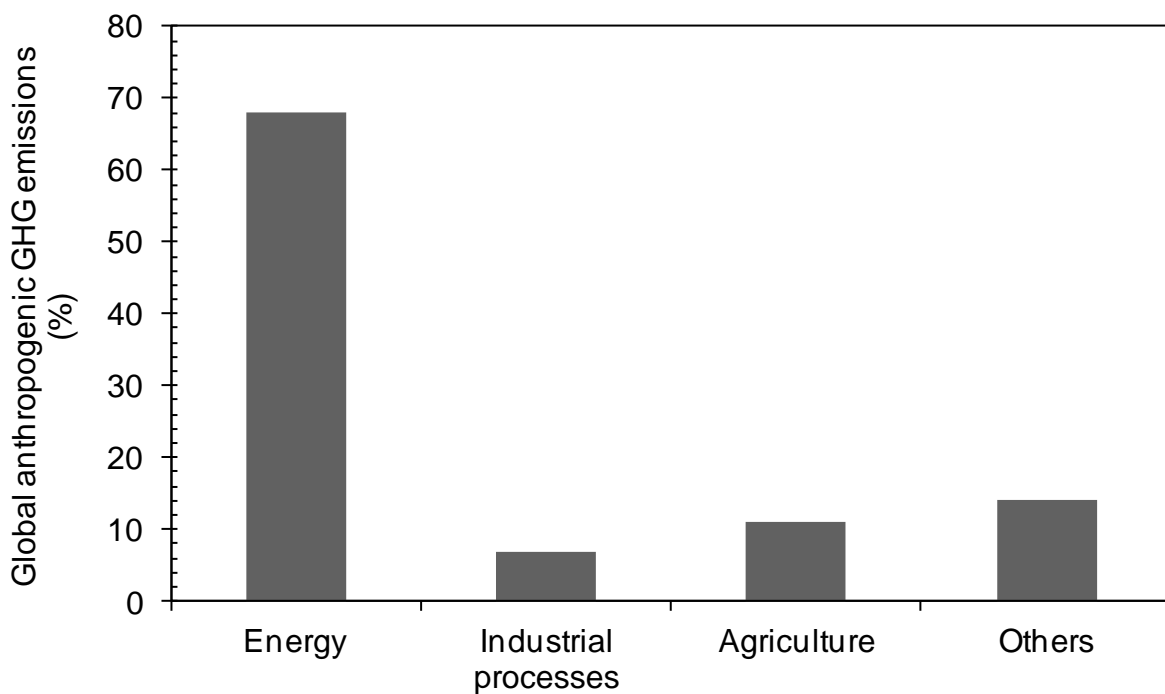
Figure 2: Share of global anthropogenic GHG emissions per sector in 2010 [37]

In 2013, coal represented 29% of the world total primary energy supply (TPES) and accounted for almost 46% of the global CO$_2$ emissions as shown in Figure 3. Currently, coal fills much of the growing energy demand of developing countries (such as China and India) where energy-intensive industrial production is

growing rapidly and large coal reserves exist with limited reserves of other energy sources. Worldwide policies are adapted to support the low-carbon technologies and improved energy efficiency, i.e. the US Clean Power Plan and China's carbon trading scheme to take effect in 2017, while the European Commission has set out a cost-effective pathway for achieving deep emission cuts of the order of 40% by 2030 and 60% by 2040 [38]. However, coal's share of total electricity generation is expected to be around 30% in 2040 [1].
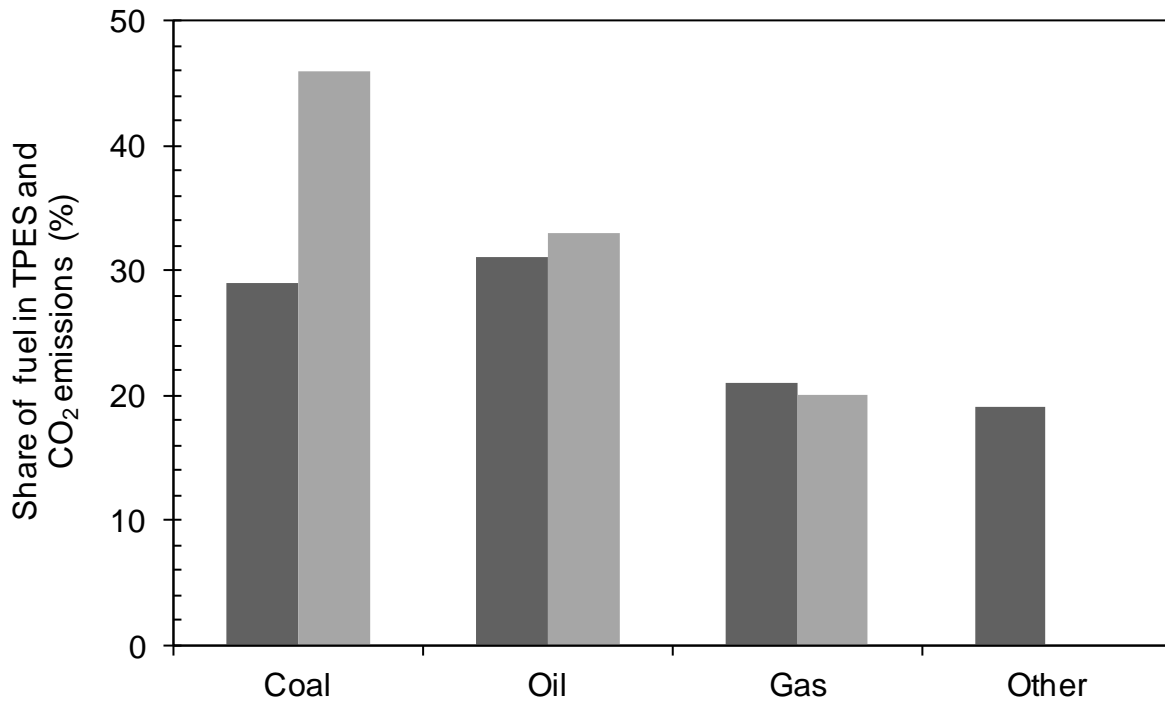
Figure 3: World primary energy supply (deep gray columns) and CO_2 emissions (light gray columns) by fuel in 2013 [37]

2.2   CO$_2$ mitigation measures

Reduction of the CO_2 emissions from heat and electricity production as well as energy intensive industries is imperative. United States Environmental Protection Agency (EPA) classifies these measures in 5 categories [39]. Increasing efficiency of power plants and fuel switching is one measure. Efficiencies of pulverised fuel-fired power plants, either hard coal or lignite, may be improved if the live steam

parameters are augmented and the individual components of the whole plant are systematically optimised [128]. This would allow the use of fossil fuels with lower greenhouse gas emissions. Furthermore, by switching to natural gas fired power plants, 40-50% less CO_2 would be emitted in comparison to the ones emitted when coal is used. Renewables is another measure to decarbonise the energy sector by increasing the share of total electricity generated from wind, solar, hydro, geothermal sources as well as from certain biofuel sources. Renewables make use of local resources and produce low or even zero greenhouse as well as toxic gas emission. Nuclear is also another way to product energy, since it involves no greenhouse gas emissions. Moreover, another measure may be increasing the energy efficiency of the end-use. This is realised by reducing energy demand and by increasing efficiency and conservation in residences, commercial and industrial buildings. Energy savings can reach a percentage of 10-20% [40]. It is noticeable that EPA's ENERGY STAR® partners removed over 300 million metric tons of greenhouse gases in 2014, and saved consumers and businesses over 34 billion $ on their utility bills. Finally, carbon can be further utilized with reduced emissions when carbon capture and storage is applied. The technology stands for capturing CO_2 as a by-product of fossil fuel combustion before it enters the atmosphere. Afterwards, the CO_2 is transferred to a long-term storage area, such as an underground geologic formation. This measure can reduce the amount of CO_2 emitted up to more than 80%.

The mentioned measures have restrictions in their application in commercial scale thus they need to be combined in order to decrease the carbon emissions. For example the applicability of the renewables may depend on local resources availability and cost. Besides, power production from these sources does not associate mature technologies while most current renewables energies are more expensive than conventional energy [40]. In addition, increasing efficiency of a power plant or fuel switching may impose more cost either due to the high gas price or due to the increased investment cost. Nuclear energy is, nevertheless, the only measure whose usage is controversial. Especially after the Fukushima accident in 2011 the development is worldwide hindered. Characteristically, Germany intends to shut down all the nuclear power plants by 2022. Finally, CCS includes technologies that

are not yet proven in commercial scale. It is, although, widely recognized as an exceptional technology in global mitigation, because of its huge potential of an 85% to 90% reduction of CO_2 emission in thermal power stations as well as energy intensive industries [41].

2.3   Carbon capture and storage (CCS)

Carbon capture and storage, or CCS, stands for the technologies and techniques that enable the capture of CO_2 emittted from fuel combustion or industrial processes, the transport of CO_2 via ships or pipelines, and its storage underground, in depleted oil and gas fields and deep saline aquifer formations. CCS technologies might be applied to various sectors such as coal/ gas fired power plants (CFPP/NGFPP), industrial sectors such as steel, cement, chemicals, fertiliser, hydrogen and refining, natural gas processing and enhanced oil recovery using CO_2 (CO_2-EOR).

CCS technologies can play a unique and vital role in the global transition to sustainable low-carbon economy, in both power generation and industry. However, they have not been yet commercially deployed in the power industry, with high equipment capital cost and drop of net thermal efficiency of the integrated system being main obstacles. Literature reports increase by 60–125% and 30–55% of the cost of electricity in the CFPPs and natural gas-fired combined cycle power plants respectively retrofitted with CCS [23]. Considering that the part of the CO_2 capture contributes to 70-80% of the total cost of the full CCS system [40], the need to find reliable, simple and cost efficient concepts and technologies for the CO_2 capture is imperative. There are four CO_2 carbon capture systems from fossil fuels, the pre-combustion capture, the oxy-fuel combustion capture, the capture from industrial processes and the post combustion capture. These systems are depicted in simplified form in Figure 4.
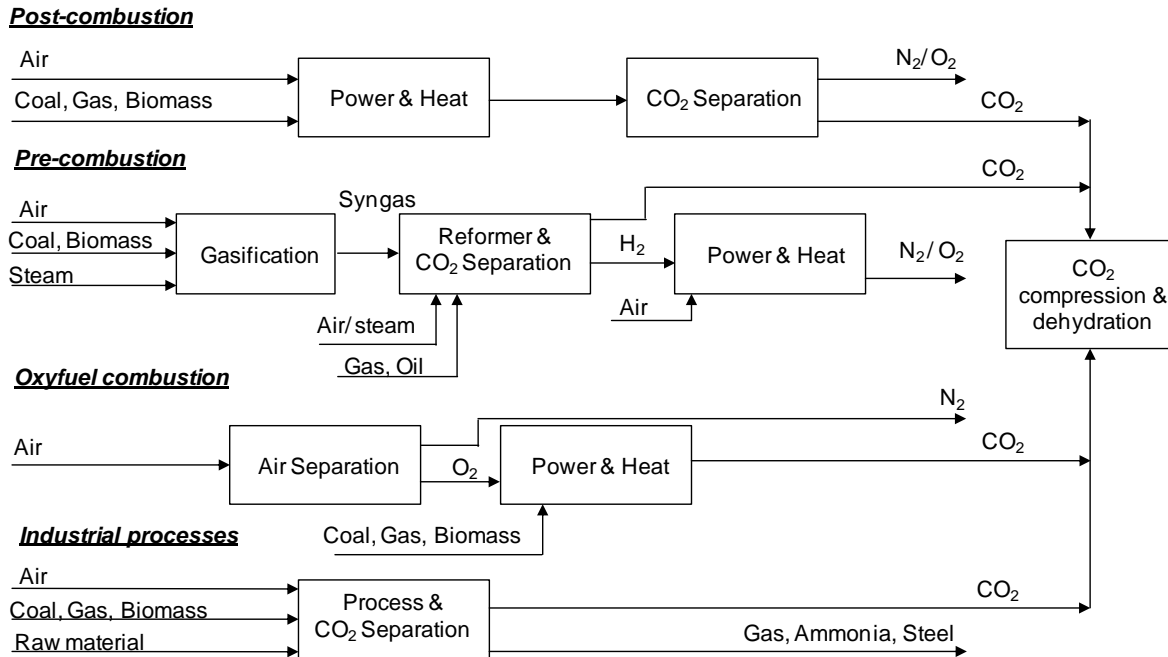
Figure 4: CO_2 capture systems (adapted by BP) [2]

The pre-combustion CO_2 capture system deals with the fuel, coal or natural gas, pretreatment before combustion. For the coal fuel case, the pretreatment involves a gasification process. A syngas is produced consisting mainly of CO and H_2. Trace elements of impurities i.e. sulfur that may be contained in the syngas are removed through further processing and either recovered or redirected to the gasifier. The syngas undergoes water gas shift reaction with steam forming H_2 and CO converting to CO_2. The highly concentrated (>20%) CO_2 produced can be easily separated by using physical, solid sorbents or membranes. The hydrogen is separated and can be burnt without producing any CO_2. Integrated gasification combined cycle (IGCC) power plants using coal as fuel are the main application of this technology. For the natural gas case, CH_4 that is the main gas contained, can be reformed to syngas containing H_2 and CO. The content of H_2 is increased by the water gas shift reaction while the rest of the process is the same as for the coal gasification. Analysis of an advanced combined cycle gas turbine plant operating with natural gas and a precombustion system showed a CO_2 capture of more than 80% with a CO_2 avoidage cost of 29 \$/tCO_2 [43].

The precombustion process is based on fully developed technology and is commercially applied in some industrial sectors. It can also be applied to retrofit power plants. However, main process disadvantages are: (1) temperature associated heat transfer problems and efficiency decay issues associated with the use of hydrogen-rich gas turbine fuel, (2) high parasitic power requirement for sorbent regeneration, (3) inadequate experience due to few gasification plants operated in the market, (4) high capital and operating costs for current sorption systems [40].

Oxy-fuel combustion capture system refers to production of a flue gas stream mainly composed of CO_2 and steam resulting from fuel combustion in a mixture of O_2-CO_2, in abscence of air-N_2. The combustion in pure oxygen increases significantly the flame temperature and reduces the flue gas volume with a negative impact on the temperature and heat flux profiles of the boiler. To overcome this problem, the flue gas is recycled back into the furnace. A significant advantage of this process is the substantially reduced NO_x emissions [43]. Although, the process is based on mature and technically feasible solutions, the energy intensive air separation unit requires about 60% of the power consumption for carbon capture and contributes significantly to the overall efficiency reduction of the plant of about 7-9 percentage points [45]. Furthermore the compression of captured CO_2 from atmospheric pressure to pipeline pressure requires additional parasitic energy. Moreover, many researchers expect elevated corrosion risks due to the increased concentrations of corrosive gases such as SO_2/SO_3, HCl, H_2O, and high pressure of CO_2 as well as due to the formation of sulphate deposits [129]. Worldwide there are a number of pilot scale facilities ranging between 0.3-30 MW_{th} [46] [129]. Recently, the Callide Oxy-fuel Project in Central Queensland, Australia, came to the end of its demonstration phase in March 2015 (with 11.000h of operation before the decomissioning phase) after having successfully demonstrated the application of the oxy-fuel and carbon capture technology in a pulverized coal unit producing a nominal 30 MW_e (25 MW_{th}) with low emissions [129]. It is considered as a large scale pilot plant and represents the latest achievement of TRL-7 (system prototype demonstration in operational environment: industrial pilots operating at over 10MW_{th}), demonstrating the use of oxy-fuel technology with electricity generation while the technology for CFPP aspires to

achieve a TRL-9 (actual system proven in operational environment: competitive manufacturing of full system) within 2016-2020 [129].

Post-combustion capture system stands for the separation of the CO_2 contained in the flue gas produced from a conventional stationary air-based combustion system. The flue gas is at atmospheric pressure and has a CO_2 concentration of 3-15 volume percent. Capturing CO_2 under these conditions is challenging because (1) the low pressure and dilute concentration dictate a high total volume of gas to be treated (2) trace impurities in the flue gas tend to reduce the effectiveness of the CO_2 separation processes and (3) compressing captured CO_2 from atmospheric pressure to pipeline pressure represents a large parasitic energy load [47]. The separation of the CO_2, is performed by: (1) absorption using solvents or solid sorbents, (2) cryogenic distillation and (3) membranes. The general scheme of the main separation processes is depicted in Figure 5.
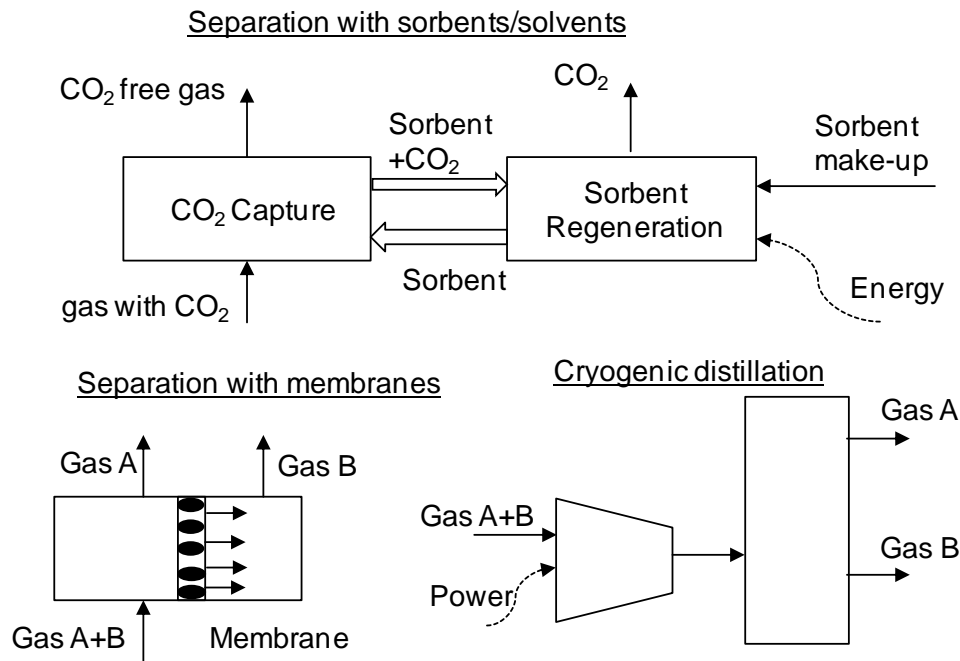
Figure 5: Post combustion main separation processes

The application of the cryogenic separation is ineffective due to the extremely energy intensive nature of the process, although it produces high purity liquid CO_2 ready for sequestration. On the other hand, the membrane separation process is

relatively simple but it is characterized by poor selectivity or low permeability with respect to CO_2 capture [49]. The process is currently under TRL-5 (technology validated in relevant environment: pilots operated at industrially relevant conditions at 0.05-1 MW_{th}) demonstrated at a capture rate of 1 tCO_2 per day using polymeric membranes [36]. The usage of chemical solvents and especially monoethanolamine (MEA) is the most mature and commercially available and can be adapted to existing power plants, downstream of the boiler without any significant changes to the original plant [40]. However, the demonstrated scale of operation (capture rate of 1 tCO_2 per year in the Boundary Dam project [36]) is significantly smaller than the typical size of power plants and severe penalties to the plant efficiency exist. Literature refers to a 10-14% point drop in the net effciency of the power plant [44]. Furthermore, the use of natural solvents, i.e limestone by implementing the calcium looping process is advantageous as already mentioned in section 1.

Finally, CO_2 capture from industrial processes is been performed for almost 80 years while most of the CO_2 emitted is vented to the atmosphere because there is no incentive or requirement to store [49]. Examples of CO_2 capture from process streams are purification of natural gas and production of H_2 containing syngas for the manufacture of ammonia, alcohols and synthetic liquid fuels. The techniques applied here are similar to the precombustion capture. Other industry process streams including CO_2 that is not captured are the cement and steel production as well as the fermentation processes for food and drink production. CO_2 could be captured by applying techniques common to post, pre or oxy-fuel combustion capture.

2.4   Worldwide ongoing and completed CCS projects

Worldwide there are 15 large-scale CCS projects capturing 27 million tons (Mt) of CO_2 every year. Besides, there are seven projects under construction expected to operate before 2018 with a CO_2 capturing capacity of around 13 million tons per year. These projects include the Gorgon carbon dioxide injection project in Australia, which will be the world's largest storage project with around 3.4 Mt of CO_2 stored annually. Another 10 large-scale CCS projects with a total CO_2 capture capacity of around 14 Mtpa are at the most advanced stage of development planning, the concept definition stage. Additionally, 12 large-scale CCS projects are in the evaluate and identify stages of development and have a total CO_2 capture capacity of around 25 Mtpa [50].

In Norway, the Sleipner oil and gas project since 1996, reports 20 years of successful operation, storing around 1 Mt of CO_2 per year from a natural gas processing facility with no trace of leakage [51]. In the United States, CO_2 has been used for enhanced oil recovery (EOR) for several decades, facilitated by an existing network of CO_2 transport pipelines of more than 6,600 km. In Canada, the Boundary Dam project became in October 2014 the first operating coal-fired power plant to apply CCS. Two additional projects in the power sector, the Kemper County project and the Petra Nova carbon capture project in USA, are due to come into operation in 2016. Finally, the Shell Quest CCS project, since November 2015, is the world's first CCS project to reduce emissions from oil sands upgrading.

All these projects provide valuable experience in operating large-scale CO_2 capture facilities, managing large CO_2 injection, and monitoring the behavior of CO_2 underground. The great benefit of these projects is that planning, construction and operation costs may be significantly reduced in future plants. For example, after only 12 months of operation, the Boundary Dam project owners believe they can reduce the cost of the next plant by 30% [50].

2.5   Calcium looping post combustion CO$_2$ capture

Calcium looping is one of the sorbent based post combustion alternatives. It is expected to be commercialized after 2020 and up to now it is demonstrated in the scale of 1.8 MW$_{th}$ that represents a TRL-6 (technology demonstrated in relevant environment: steady states at industrially relevant environments, pilots in the MW$_{th}$ range) [36]. Since 2005 several research groups have been intensively focused on performing theoretical and experimental studies to prove the competitiveness of the process as well as to identify critical design and operational parameters. The goal of all these studies is to aid in planning, constructing and operating pilot scale plants. Aspects that are partly covered in these works will be presented here in order to provide (a) the theoretical background of the experimental work and (b) the interpretation of the results as will be discussed in section 3.

2.5.1   General process description

The process is based on the mature technology of fluidized bed reactors that is convenient due to high reaction rate requirements and high enthalpy of the reactions involved. The CO$_2$ scrubber is the cheap and widely available non toxic natural product of limestone. The process makes use of the ability of calcium to capture and release CO$_2$ as per equation (1).

$$CaO_{(s)} + CO_{2(g)} \leftrightarrow CaCO_{3(s)} \qquad \Delta H_{25°C} = -178.2 \ kJ/mol \qquad (1)$$
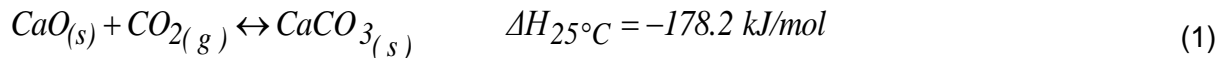
The reaction is already known for many centuries and is used in the cement industry as well as in various chemical processes. The forwards carbonation reaction is exothermic and proceeds in two phases: the reaction controlled and the diffusion limited. In the first phase, CO$_2$ diffuses into the pores and reacts into the active pore areas of CaO. The reaction is progressing and CaCO$_3$ is formed around the sorbent particles. In the second phase, the remaining active CaO is reacting with CO$_2$ with a

rate limited by the diffusion of the CO_2, through the product layer, to the active sorbent at the core of the particle. The first phase has a duration of around 1-2min while the second one will proceed until complete conversion. For the carbonation reaction to occur, the partial pressure of CO_2 in the vicinity of the solid surface must be higher than equilibrium pressure given by equation (2) and depicted in Figure 6 [119].

$$p_{CO_2,eq} = 4.137 \cdot 10^7 e^{\frac{-20474}{T}} \tag{2}$$

The conversion of the formed $CaCO_3$ to CaO, called calcination reaction is endothermic and proceeds rapidly up to full sorbent conversion under the condition that the temperature is above the temperature required by the equilibrium. For an increased value of CO_2 partial pressure higher temperatures are needed for the decomposition of $CaCO_3$.
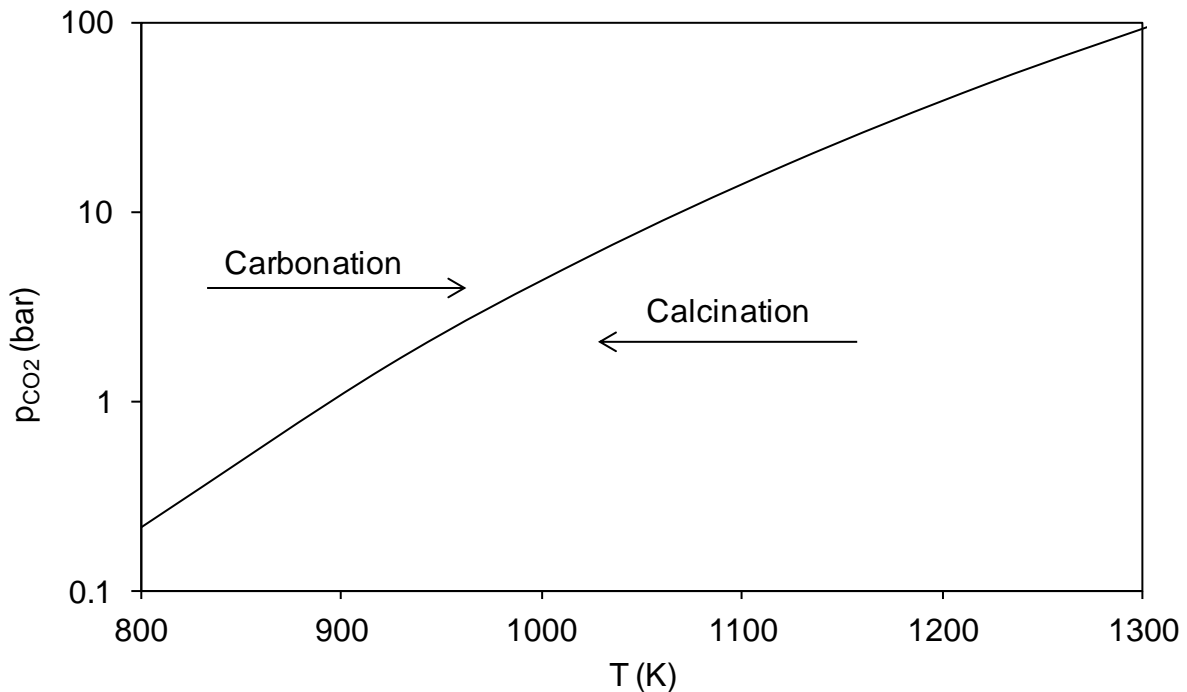
Figure 6: The equilibrium of CaO-$CaCO_3$

In 1994, Hirama et al [52] and in 1999, Shimizu et al [16] presented the conceptual design of the process as illustrated in Figure 7. The process is realized in

two interconnected fluidized bed reactors. Flue gas from fuel combustion in air, containing CO_2 between 4%$_{vol,dry}$ and 15%$_{vol,dry}$ is directed in the first reactor, the carbonator. There, separation of the CO_2 is done by means of the exothermic carbonation reaction of CaO so that $CaCO_3$ is formed and a CO_2 lean gas stream is produced.

The carbonation reaction at particle level could be expressed as follows [8]:

$$\dot{R}_{Carb} = k_{Carb}\, X_{max,Ave}\, (y_{CO_2} - y_{CO_2,eq}) \tag{3}$$

where $X_{max,Ave}$ is the maximum average carbonation conversion of the particles. It is a measurement of the sorbent activity [53], [54], [55]. It can be estimated in a thermogravimetric analyser (TGA) as the CO_2 that can be absorbed by CaO particles at the end of the fast reaction regime [56]. k_{Carb} is the kinetic constant characteristic of the limestone carbonation and is also derived from thermogravimetric analysis. $y_{CO_2,eq}$ is the equilibrium volume fraction of CO_2 and y_{CO_2} is the volume fraction of CO_2 in the reactor. The heat released by the reaction is used in a steam cycle that provides the necessary heat for the above mentioned carbonation reaction. The reaction may take place between 853K and 973K dependent on the reaction kinetics, the equilibrium driving forces as well as the desired parameters of the steam cycle.

The formed $CaCO_3$ is directed to the second reactor, the regenerator where CaO is produced by the endothermic calcination reaction. The calcination reaction model at particle level, which can be applied to all particles present in the regenerator reactor at any time, could be expressed according to the equation (4) as follows [57]:

$$\dot{R}_{Calc} = k_{Calc}\, (y_{CO_2,eq} - y_{CO_2}) \tag{4}$$

Where k_{Calc} is the kinetic constant characteristic of the limestone calcination and is derived from thermogravimetric analysis. The high temperature to drive the calcination reaction is provided by oxy-fuel combustion [16] in order to produce a high

CO_2 rich gas stream, which, after purification, is ready for transportation and storage. The combustion in pure oxygen imposes very high temperatures. Thus, a heat sink is required. In order to take advantage of the already well known technology of the air combustion systems, two thirds of the flue gas need to be recycled to obtain a temperature level in the furnace that is similar to that in the case of combustion with air. The flue gas in that case consists mainly of the combustion products CO_2 and steam leading to a CO_2 concentration of ~$90\%_{vol,dry}$ at best after dehumidification [45]. The remaining ballast gas consists of excess oxygen, necessary for adequate burnout of the coal, argon, nitrogen as well as sulphur species and nitrogen oxides. Adequate flue gas treatment measures may be used for purification of the gas stream. Afterwards, the refined CO_2 stream can be compressed and sequestered.
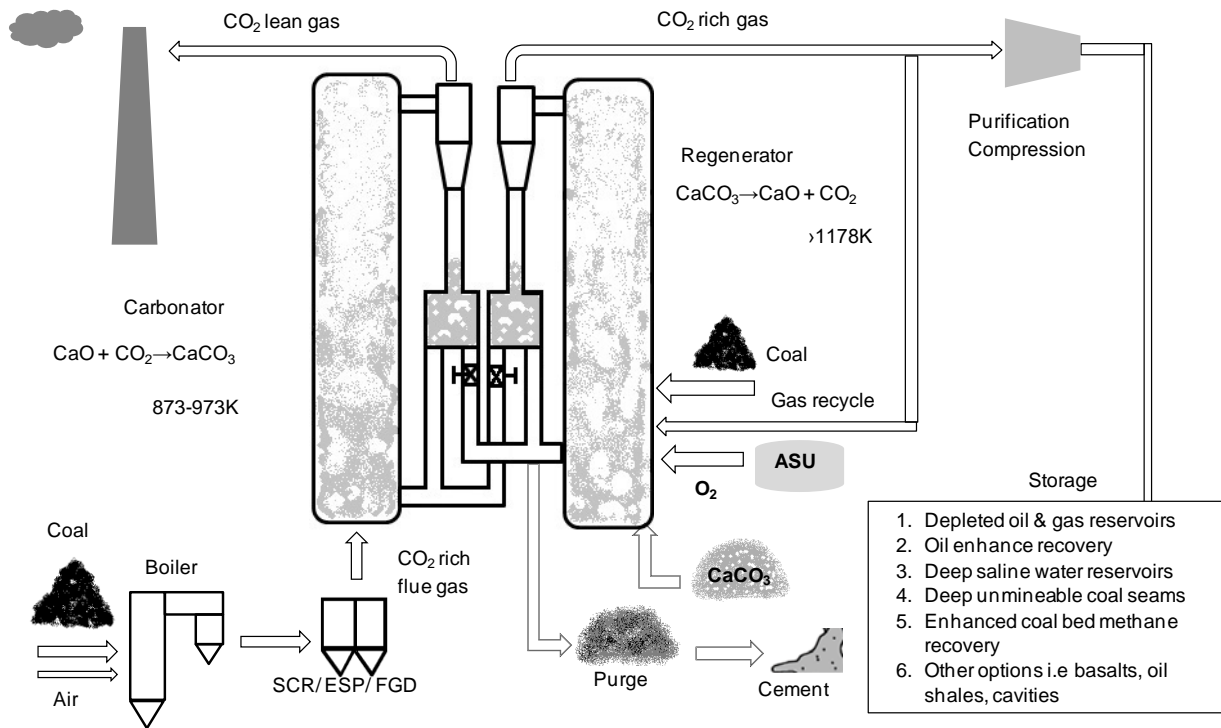
Figure 7: Ca-Looping general process schematic as applied in a coal fired power plant

2.5.2   Challenges of the CaL process

The oxy-fuel combustion process makes the technology economically competitive mainly due to lower auxiliary power and investment costs for O_2 production than in full oxy-fuel combustion power plants [11], [58], [59]. Nevertheless, the work performed up to now treats the part of the oxy-combustion on the regenerator in a simplified way, i.e. the flue gas recycle is excluded [33] while the influence of the oxy-combustion on sintering and limestone comminution behavior is not in detail investigated in bench scale testing facilities.

It is well known that the conversion of CaO to $CaCO_3$ referred also as carbon carrying capacity decays rapidly and achieves a value (referred as residual activity) of around 0.075 [54], [55]. For a sufficient flow of CO_2 from flue gas to be removed such a value imposes high solid transfer rates between the two reactors and a large bed inventory. In order to raise the lime average activity in the system, fresh limestone needs to be continuously fed to the system and spent material to be removed. In this way the average residence time of the sorbent in the system is reduced and thus higher average carrying capacities are achieved. On the other hand this increases operating as well as transport, handling and logistic costs. Dealing with reduced makeup rates is a key factor for the process economics and viability.

Sintering is one of the main issues that enhances the reduction of the carbonation conversion and need to be addressed [60]. The phenomenon stands for the morphological changes of the particles in terms of surface area and pore volume. Reduction of the CaO area available to react with CO_2 decreases the carrying capacity [54]. Literature shows that the majority of the sintering effects is enhanced when the sorbent is exposed to an environment that is characterized by high temperatures and gaseous atmospheres rich in carbon dioxide and steam [62], [63], [64], [65]. Several methods, i.e. doping the sorbents with a variety of acids or sorbent reactivation have been proposed to improve the sorbent activity [66], [67]. However,

these techniques increase the complexity of the process and cost as well as the potential of introducing toxic materials into the system.Taking into consideration that the oxy-combustion imposes an environment with elevated amount of CO_2 and steam, research is necessary to identify optimum operation system conditions. In that conditions sintering effects should be minimized and sorbent improvement methods should be avoided.

Moreover, it is well known that the particles in a calcium looping system are imposed to combined mechanical and thermal stresses while calcination or carbonation reaction takes place simultaneously [67], [68], [69]. The particle size is reducing and the particle size distribution is changing while the amount of the particles increase. Scala et al [68] performed detailed studies on a fluidized bed and identified three attrition/fragmentation mechanisms: the primary and secondary fragmentation and attrition by abrasion. The primary fragmentation occurs immediately after particles are injected in the hot reactor. It occurs due to the combined thermal stresses as well as the internal overpressures due to the CO_2 release. Both coarse and fine fragments are produced. The secondary fragmentation and attrition by abrasion are determined by mechanical stresses due to collisions among the particles and with the internal of the reactors. Secondary fragmentation generates coarser fragments while attrition by abrasion generates finer ones.

The behavior of the sorbent towards these mechanisms is necessary to be known for the design of the calcium looping system. A net Ca loss from the circulating loop adds to sorbent deactivation and contributes to the need of makeup of fresh sorbent, while fresh limestone need to be introduced in the system to compensate the material loss. Moreover, the fines that are generated are leaving the system and thus necessary filtering equipment is imposed. This aspect is related to the process economics but also to operation. Additionally, the size of the particles remaining in the system may affect the reactor hydrodynamics.

2.5.3   Steps to CaL process commercialization

For the industrialization of a technology, pre-design and construction of pilot plants, modeling work is required to minimize the financial risk of the construction of such a unit. In this direction, many research groups worldwide spent effort on investigating the process at several apparatus, small scale facilities and pilot plants while other scientific groups have proposed various models from simple process ones up to computational fluid dynamics (CFD) simulations [24], [36], [135].

At University of Stuttgart, the 10 kW$_{th}$[1] dual fluidized bed facility is in successful operation with CO_2 capture efficiencies of more than 90% since 2010. The carbonator reactor was characterized in detail by varying the main carbonator design parameters such as temperature, bed inventory, CO_2 inlet flow, as well as the solid circulation rate between the two reactors. Furthermore, a model that predicts the CO_2 capture efficiency of the carbonator was applied to the experimental data [8]. Parametric studies performed at this facility provided data useful for the design, construction and operation of the 200 kW$_{th}$[1] dual fluidized bed pilot plant at University of Stuttgart [136]. The pilot plant realized successful operation of the system for more than 600h. Wood pellets were burned in the regenerator with an oxygen air mixture up to 50%$_{vol}$ and with wet flue gas introduced in the carbonator. Full sorbent calcination as well as high CO_2 capture efficiencies improved by the water vapor presence were recorded. Material loss was measured to be between 2-5%$_{wt}$/h of the total system mass.

In a similar way, at INCAR-CSIC work performed at a 30 kW$_{th}$[1] DFB facility [36], [71], [72], [121]. Main difference between the two facilities was the coal combustion at the regenerator in presence of air to maintain the desired temperature. At that facility there was no specific controlling mechanism of the solids circulating between the reactors. The performance of the carbonator reactor was also studied in the presence of sulphur. Moreover, detailed sorbent attrition investigation was perfomed

---

[1] referred to carbonator

for both carbonator and regenerator reactor. The work was used for the design, construction and operation of the 1.7 MW$_{th}$[1] pilot plant of La-Pereda Hunosa. The plant was operated for more than 1800h with stable operation of the regenerator of more than 170h under oxy-fired coal combustion with off gas concentration measured around 85 %$_{vol,dry}$ [25], [73]. In comparison to the facilities mentioned, this plant operates with flue gas exiting from the nearby existing coal fired power plant.

Finally, two other research groups at CANMET and TU Darmstadt performed important work on process demonstration. At CANMET experimental work on a 75 kW$_{th}$ CANMET facility showed successful CO_2 capture of more than 90%. The regenerator was working under oxy-combustion of the fuel with flue gas recycle and an off gas CO_2 concentration of around 85%$_{vol,dry}$ [124]. In addition, at University of Darmstadt the 1 MW$_{th}$[2] dual fluidized bed facility successfully operated for nearly 400h [138]. The heat in the regenerator was provided by coal combustion in oxygen enriched air.

On the other side, the modeling work performed up to now is classified in three groups as per Ylätalo et al: the process scheme modeling (Table 2), the models incorporating spatial discretization (Table 3), and the CFD modeling work (Table 4) [74]. The process scheme models are the simplest mass and energy balance solver that can be used for a system. The calculation times are short and the parameter variation and investigation is easy. Nevertheless, many simplifications need to be done in order to describe the complex system. Many commercially available tools can be utilized thus facilitating the system analysis. The next step is modeling tools that include spatial discretization. In these models the domain of the existing modeling problem is divided into calculation cells enabling analysis of phenomena occurring inside the domain extent [74]. These models can be from 1 to 3D and usually include complex models for chemical reactions, heat transfer and solid entrainment. The phenomenon that is studied by these models is more accurate since the possibility of error sources is decreased. Finally, CFD modeling work of two phase flows is computationally challenging, especially when more than one reactor

---

[2] referred to regenerator

need to be included in the computer calculations. Thus, limited research studies are reported in the literature up to now.

Table 2: Summary of selected CaL process scheme modeling work

Reference	Model main characteristics
1999, Shimizu et al [16]	Semi predictive model with K-L hydrodynamics, conceptual study of the impact of Calcium looping plant integration on a supercritical CFPP
2008, Yang et al [75]	Investigation of heat integration with primary and secondary steam cycle
2009, Alonso et al [76]	Combination of residence time distribution functions with sorbent deactivation rates and reactivity, simplified fluid dynamics of solids and gase, carbonation rates are modeled defining the transition between fast and zero reaction rate regime, prediction of carbonation efficiency varying looping and makeup ratios
2013, Martinez et al [77]	Regenerator reactor model based on simple fluid-dynamic assumptions and calcination kinetics, evaluate the $CaCO_3$ content leaving the regenerator as a function of solid inventory, calciner temperature, solid circulation rate or fresh sorbent makeup flow
2012, Diego et al [78]	CFBCs models to predict the hydrodynamics of a postcombustion CaL system, compare the predicted solids circulation rates to those required for CO_2 capture, model was used to find operating windows that will allow the CaL system to be applied on a large scale
2012, Romano et al [13]	The model is based on the Kunii–Levenspiel theory for circulating fluidized bed taking into account the effects of coal ash and sulfur species
2009, 2013, Romano et al [79], [80]	Simulation of a coal fired retrofit power plant, simulation of oxy-fuel CFB fitted with calcium looping to reach ultrahigh CO_2 capture efficiencies
2009, Hawthorne et al [11]	Simulation involving the coupling of the carbonate looping reactor model from ASPEN Plus™ with the steam cycle in EBSILON Professional code
2013, Vorias et al [81]	Process simulation based on thermodynamic approach to analyze a large scale calcium looping unit retrofitted to a lignite fired boiler using ASPEN Plus™ and IPSEPro
2009, Ströhle et al [82]	ASPEN Plus™ process simulation to study the feasibility of a calcium looping unit applied at existing coal-fired power plant
2015, Atsonios et al [134]	Process modeling of the CaL implementation on a typical cement plant as a retrofit option, process simulations using ASPEN Plus™ in conjunction with house-built models for the CaL process itself

Table 3: Summary of models incorporating spatial discretization

Reference	Model main characteristics
2011, Lasheras et al [83]	1D fluidized bed carbonator model based on an approach of Kunii and Levenspiel, submodels predict the solid distribution along the reactor height and the core wall layer effect, the model is integrated to a process model to determine the CaL process efficiency
2011, Myohänen [84]	Three-dimensional, semi-empirical, steady state model for simulating the combustion, gasification, and formation of emissions in circulating fluidized bed (CFB) processes
2014, Ylätalo et al [85]	Application of a 1D dynamic model to a large scale calcium looping concept capturing CO_2 from a 250 MW_{th} power plant
2013, Ylätalo et al [86]	1D describing the carbonator, regenerator and solid return system, 3D model which describes the calciner reactor, modeling work includes energy balance solution and simulates interconnected reactors in dynamic state

Table 4: CFD modeling work on Calcium looping process

Reference	Model main characteristics
2013, Nikolopoulos et al [87]	3D full-loop CFD isothermal simulation of the carbonator of the calcium looping process, the state of the art TFM approach is coupled with the advanced EMMS scheme for the calculation of drag coefficient exerted in the solid phase by the gas one, simulation of the flow characteristics of the re-circulation system of the unit, i.e. cyclone, downcomer and the pneumatic valve type of loop seal working as a flow regulator
2015, Atsonios et al [88]	A new methodology for the simulation of calcium looping process based on coupling of CFD and advance thermodynamic models
2015, Zeneli et al [140]	Application of an advanced coupled EMMS-TFM model to a pilot scale CFB carbonator

To conclude, although all these models as well as the experimental work performed are based on assumptions and simplifications, they proved the feasibility of the process and increase the possibilities of such a prototype technology to be realized industrially with a minimized financial risk.

2.5.4   Theoretical background

2.5.4.1   Basic carbon molar balance

The basic carbon molar balance of the calcium looping system is described as per equation (5). It indicates that the CO_2 captured in the carbonator (left side of the equation) is absorbed by the solids circulating between the two reactors and subsequently released by the solid phase in the regenerator (right side of the equation).

$$\dot{N}_{CO_2,in,CR}\,\eta_{CR} = \dot{N}_{Ca,rec}\,(X_{out,CR} - X_{out,RR}) \tag{5}$$

Based on the kinetic model of Alonso et al [80] as applied by Charitos et al [56] and Martinez et al [141] the carbon molar balance is further formulated as per equation (6). It is considered that only a fraction of the amount of the sorbent at the carbonator, $N_{bed,CR}\,f_{Act,CR}$ and regenerator, $N_{bed,RR}\,f_{Act,RR}$ is available for carbonation and calcination respectively. Due to the fact that after a critical time, $t_{crit,Carb}$ and $t_{crit,Calc}$ the carbonation and calcination reaction rate, $\dot{R}_{Carb}$ and $\dot{R}_{Calc}$ respectively becomes insignificant, only that fraction of the particles is able to react with residence time at the reactor less than this critical time.
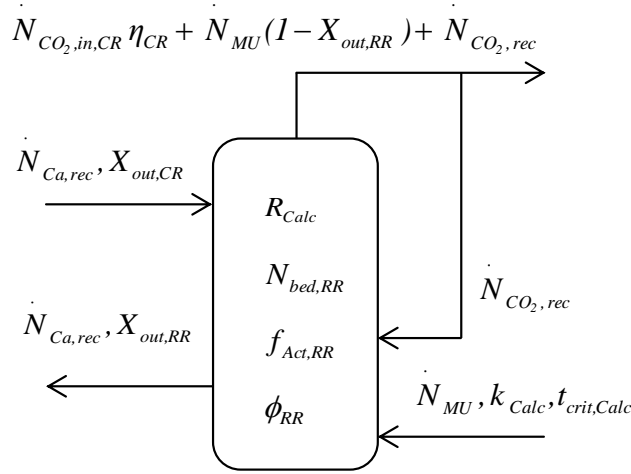
$$N_{bed,CR}\,f_{Act,CR}\,\dot{R}_{Carb} = N_{bed,RR}\,f_{Act,RR}\,\dot{R}_{Calc} \tag{6}$$

2.5.4.2   Correlations of regenerator efficiency

The operation of the regenerator (Figure 8) is characterized through the ability to fully calcine the solid flow coming from the carbonator, $\dot{N}_{Ca,rec}$ with a carbonate content, $X_{out,CR}$ as well as the fresh limestone fed, $\dot{N}_{MU}$ so as to provide to the

carbonator CaO in high quantity and quality. As per equation (5) the lower the carbonate content calculated over all the particles exiting the regenerator, $X_{out,RR}$ the less looping ratio, $\xi_{CaL} = \dot{N}_{Ca,rec} / \dot{N}_{CO_2,in,CR}$ is required for the same CO_2 capture efficiency, η_{CR}. Thus, regenerator efficiency in terms of sorbent calcination conversion degree, as proposed by [56], is a crucial reactor design parameter. It is defined as follows:

$$\eta_{RR} = 1 - \dot{N}_{Ca,rec} \, X_{out,RR} \, (\, \dot{N}_{Ca,rec} \, X_{out,CR} + \dot{N}_{MU} \,)^{-1} \tag{7}$$

$$\dot{N}_{CO_2,in,CR} \, \eta_{CR} + \dot{N}_{MU}(1 - X_{out,RR}) + \dot{N}_{CO_2,rec}$$

$\dot{N}_{Ca,rec}, X_{out,CR}$

R_{Calc}

$N_{bed,RR}$

$\dot{N}_{CO_2,rec}$

$\dot{N}_{Ca,rec}, X_{out,RR}$

$f_{Act,RR}$

ϕ_{RR}

$\dot{N}_{MU}, k_{Calc}, t_{crit,Calc}$

Figure 8: Basic measures of the regenerator reactor

Charitos et al [56] showed experimentally a dependence of regenerator efficiency on space time expressed as: $\tau_{RR} = t_{res,RR} / X_{out,CR}$, where $t_{res,RR}$ is the particle residence time in the reactor and can be calculated as $t_{res,RR} = N_{bed,RR} / \dot{N}_{Ca,rec}$.

Duelli et al [90] used the parameter to interpret the data from dual fluidized bed experiments under high CO_2 partial pressure at dry regenerator conditions. Based on Martinez et al [141], the following equation (8) is proposed for the regenerator efficiency [112]:

$$\eta_{RR} = k_{Calc} \, \phi_{RR} \, \tau_{Act,RR} \, (\overline{y_{CO_2,eq} - y_{CO_2}}) \tag{8}$$

where the regenerator active space time, $\tau_{Act,RR}$ is a variable comparable to the active space time already successfully applied to the carbonator reactor [56] and is expressed as:

$$\tau_{Act,RR} = N_{Ca,RR} \, f_{Act,RR} \, / (\, \dot{N}_{Ca,rec} \, X_{out,CR} + \dot{N}_{MU}) \tag{9}$$

These equations indicate the effect of the limestone, through the calcination kinetic constant, k_{Calc} and the carbonate content of the sorbent entering the regenerator, $X_{out,CR}$ on the efficiency. Moreover, it shows the dependency of the efficiency on process parameters namely the $y_{CO_2,eq}$ influenced by the temperature, the y_{CO_2} as per combustion characteristics and flue gas recycle, solids recirculation rate, $\dot{N}_{Ca,rec}$ and makeup flow, $\dot{N}_{MU}$. Finally, the efficiency is influenced by the basic reactor design characteristic of the inventory, $N_{Ca,RR}$. The parameter ϕ_{RR} comprises (i) specific facility related effects on sorbent calcination i.e. fluidization conditions, heat transfer as well as (ii) measurement errors that cannot be quantified i.e. sampling and TGA analysis, measurement of the solids flow (iii) the difference between the theoretical sorbent kinetic constant as measured by TGA studies compared to the real value in a DFB system. Finally, the active fraction of the reactor inventory is defined as per equation (10) [141].

$$f_{Act,RR} = 1 - exp(-t_{crit,calc} / t_{res,RR}) \tag{10}$$

2.5.4.3   Correlations of CO_2 capture

The carbonator efficiency is defined as the moles of CO_2 captured by the solids with respect to the moles introduced in the reactor as per equation (11). The efficiency is dependent on the space time, τ_{CR} and the Ca looping ratio, ξ_{CaL} [91]. The

first one is defined as the ratio of Ca mols present in the carbonator and the molar flow of CO_2 contained in the flue gas entering the reactor as per equation (12). The second one is the ratio of the incoming Ca molar flow from the regenerator and the molar flow of CO_2 contained in the flue gas entering the carbonator reactor as per equation (13).

$$\eta_{CR} = 1 - \dot{N}_{CO_2,out,CR} / \dot{N}_{CO_2,in,CR} \tag{11}$$

$$\tau_{CR} = N_{bed,CR} / \dot{N}_{CO_2,in,CR} \tag{12}$$

$$\xi_{CaL} = \dot{N}_{Ca,rec} / \dot{N}_{CO_2,in,CR} \tag{13}$$

Following the same approach as for the regenerator, the carbonator operation (Figure 9) is characterized by CO_2 capture efficiency while the carbonator active space time is a parameter that can be used for design purposes [56], [71], [76]. The simple empirical model is described by the following equations:

$$\eta_{CR} = k_{Carb} \; \phi_{CR} \; \tau_{CR} \; f_{Act,CR} \; X_{max,Ave} \; (\overline{y_{CO_2} - y_{CO_2,eq}}) \tag{14}$$

$$f_{Act,CR} = 1 - exp(-t_{crit,Carb} / t_{res,CR}) \tag{15}$$

$$t_{crit,Carb} = (X_{max,Ave} - X_{out,RR}) / (k_{Carb} \; \phi_{CR} \; X_{max,Ave} \; (\overline{y_{CO_2} - y_{CO_2,eq}})) \tag{16}$$

The model is based on the carbon molar balance of equation (5) and on the assumption that only a fraction of the CaO particles, $f_{Act,CR}$, with a sufficient residence time (less than $t_{crit,Carb}$) is active in the carbonator bed, meaning that it can react with CO_2 in the fast reaction regime up to the average maximum carbonation conversion $X_{max,Ave}$ [76]. Considering equation (14), the active space time defined as the space time of the active particles, $\tau_{CR} \, f_{Act,CR} \, X_{max,Ave}$ is the carbonator characteristic design parameter [56], [71]. The gas-solid effectiveness factor, ϕ_{CR} is included in the expression of the carbonator efficiency in order to consider the fluidization conditions affecting the reaction.
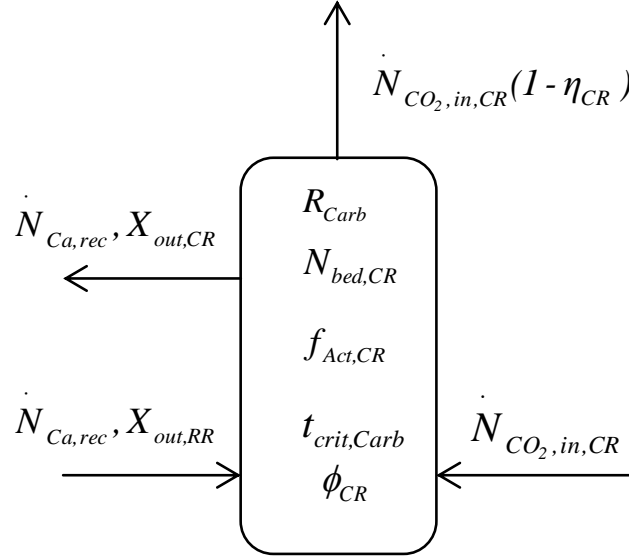
Figure 9: Basic metrics of the carbonator reactor

Equation (14) indicates that in addition to the carbonator space time, the average maximum carbonation conversion is a key parameter influencing the carbonator CO_2 capture efficiency. In order to study the evolution of $X_{max,Ave}$ during the experiments in the course of time, the theoretical cycle number, N_{theo} as per equation (17) is used [56], which represents the number of times that a particle has been carbonated up to its maximum CO_2 carrying capacity, $X_{max,Ave}$ and then calcined.

$$N_{theo} = \int_{0}^{t} \frac{\dot{N}_{CO_2,in,CR} \eta_{CR(t)}}{N_{Ca} X_{max,Ave}} dt \tag{17}$$

2.5.4.4 Particle size reduction and material loss

In the circulating fluidized bed of the calcium looping system most of the elutriated mass, which is defined to be the attrition product [142], is captured and returned to the riser and only the very fine particles are lost. In this work, the attrition rate as per [130] is used to express the rate of fines generation. Nevertheless, this

equation can not be applied for pilot or full scale applications operating on a continuous base [94]. The attrition rate might be calculated as percentage of the elutriated fines referred to the mass of the sorbent initially loaded in the reactor [130]:

$$R_{Attr} = -\frac{1}{M_0}\frac{\Delta M}{\Delta t}100\%$$

(18)

where M_0 is the initial total system inventory and ΔM is the material lost over a period of time Δt.

It is well known that attrition contributes not only to the material loss but on the reduction of the particle size of the remaining particles in the system thus the amount of particles in the system increases [69], [92], [93], [94], [95], [96]. The particle size diameter that is studied in this work refers to the mean sauter particle size using the mass fraction of the particles x_{Pi} with diameter D_{Pi} expressed as [93]:

$$D_P = \frac{1}{\sum (x_{Pi}/D_{Pi})}$$

(19)

An empirical approach on the particle size reduction is based on the model proposed by Cook et al [95]. After evaluating different attrition models, they proposed the second order model by introducing M_{min} as the minimum mass of solids after which attrition becomes negligible and using the attrition rate constant, k_{Attr} as per equation (20).

$$-\frac{\Delta M}{\Delta t} = k_{Attr}(M^2 - M_{min}^2)$$

(20)

After integration, using the suitable boundary conditions as well as an overall attrition rate constant K_{Attr} proportional to both attrition rate constant and the square of the excess velocity the following equation is obtained [95]:

$$K_{Attr}\,t = \frac{(U - U_{mf})^2}{2M_{min}}\left[ln\left(\frac{M_0 - M_{min}}{M_0 + M_{min}}\right) - ln\left(\frac{M - M_{min}}{M + M_{min}}\right)\right] \tag{21}$$

After substituting the mass as a function of the diameter, assuming that the particles are spherical and the density remains constant, the mean particle diameter D_P is expressed as follows [93]:

$$D_P = D_{Pmin}\left[\frac{1 + \dfrac{D_{P0}^3 - D_{Pmin}^3}{D_{P0}^3 + D_{Pmin}^3} - exp(\dfrac{2D_{Pmin}^3}{D_{P0}^3(u - u_{mf})^2}K_{Attr}\,t)}{1 - \dfrac{D_{P0}^3 - D_{Pmin}^3}{D_{P0}^3 + D_{Pmin}^3} + exp(\dfrac{2D_{Pmin}^3}{D_{P0}^3(u - u_{mf})^2}K_{Attr}\,t)}\right]^{1/3} \tag{22}$$

where D_{Pmin} is the minimum mean particle diameter, D_{P0} the initial mean particle diameter, u is gas velocity and u_{mf} is the minimum fluidization velocity.

2.6   Objectives of this work

Although a lot of research is performed and the currently ongoing work promotes the technological maturity of the process, literature review indicates the necessity of further experimentation on continuous dual fluidized bed facilities.

Experimental investigations are necessary for parameters or aspects that have been up to now studied with TGA and batch reactors. One of these parameters is the water vapor presence in the carbonator and the regenerator as well as the high CO_2 concentration in the regenerator. Water vapor as product of the coal combustion is present in the flue gas entering the carbonator as well as in the oxy-fired regenerator for both the cases of dry and wet flue gas recycle. Moreover, as mentioned above the oxy-fuel combustion in the regenerator implies high CO_2 concentration in the off-gas and requires a flue gas recycle thus the calcination takes place in an atmosphere of high CO_2 concentration. Additionally, the carbonation/ calcination reaction is temperature and CO_2 concentration dependent and a change

in one of the two parameters will affect the reaction, moving it towards the carbonation or the calcination step as established by the equilibrium. Numerous studies have been performed up to now [54], [61], [68], [69], [97], [98], [99], [100], [101], [102], [103], [104]. Nevertheless, these studies have restrictions and cannot be fully applied to the calcium looping system. As far as TG studies are concerned, the high residence times, low heating rates and fresh highly active limestone are far from the ones applicable for the process. On the other hand, batch mode cyclic BFB experimentation may overpredict the sintering effects possibly due to the full carbonation/calcination taking place. This is opposed to the highly cycled and partly carbonated particles characteristic of calcium looping applications [105].

Moreover, testing at pilot facilities was focused on the carbonator behavior while the regenerator operated at appropriate conditions as to deliver a sufficient flow of CaO particles to the carbonator [23], [36]. However, most of the parametric studies have been performed under dry carbonator and air-fired conditions in the regenerator. Nonetheless, there is lack of data from a pilot scale facility where both reactors are operating under realistic process conditions. Finally, there is very few information on elutriation rates as well as quantification of the material loss from both bench scale facilities and pilot plants.

From a theoretical point of view, up to now the model that predicts the CO_2 capture level for the carbonator as proposed by Alonso et al [76] is successfully applied for the process characterisation. The data used for the carbonator reactor derive from both the 10 kW_{th} facility at University of Stuttgart and the 30 kW_{th} facility at INCAR-CSIC. For the regenerator reactor, the model proposed by Martinez et al [141] predicts the regenerator efficiency in terms of sorbent calcination. The model is based on the previous one for the carbonator. This model has not yet been applied to the calcium looping process realised at a dual fluidized bed in continuous operation. Both models are semi-predictive based on a simple fluid dynamics combined with a kinetic model for the carbonation and the calcination reaction. In addition, both models utilize the average conversion of the sorbent and residence time distribution functions. The main disadvantage of the models is the fact that they do not consider

ash accumulation and sulfation. However, the average carbonation conversion can be adapted to account for the sorbent sulfation as well as the inert mass accumulation in the regenerator. Lastly, the main advantage of these two models is that together they can represent the calcium looping performance in terms of carbonator and regenerator efficiency as determined by Charitos et al [8].

Finally, the model of Cook et al [95] is profitably applied for calculating the attrition constant of limestone used at experiments performed at INCAR-CSIC [97]. It is a simple model that relates the velocity of the particles in the fluidized bed, the time the particles spend in the system and the particle diameter. All these parameters are easily calculated or measured thus can be utilized for interpretation of results and calculation of limestone attrition constant from data resulting from pilot scale experimentation.

In this frame, the scope of this work is to extend the knowledge on the calcium looping systems. The study presents experiments performed at University of Stuttgart, in the 10 kW$_{th}$ dual fluidized bed calcium looping facility under conditions close to those expected industrially: wet flue gas in the carbonator reactor and atmospheres rich in CO_2 and H_2O_{st} in the regenerator reactor. The analysis of the system is performed through evaluating the carbonator and regenerator efficiency as well as the decay of the sorbent carbonation conversion and the particle size reduction as recorded, calculated or measured. By validating the above mentioned models, tools that may be applied for design purposes as well as for interpretation of experimental results from other facilities are offered.
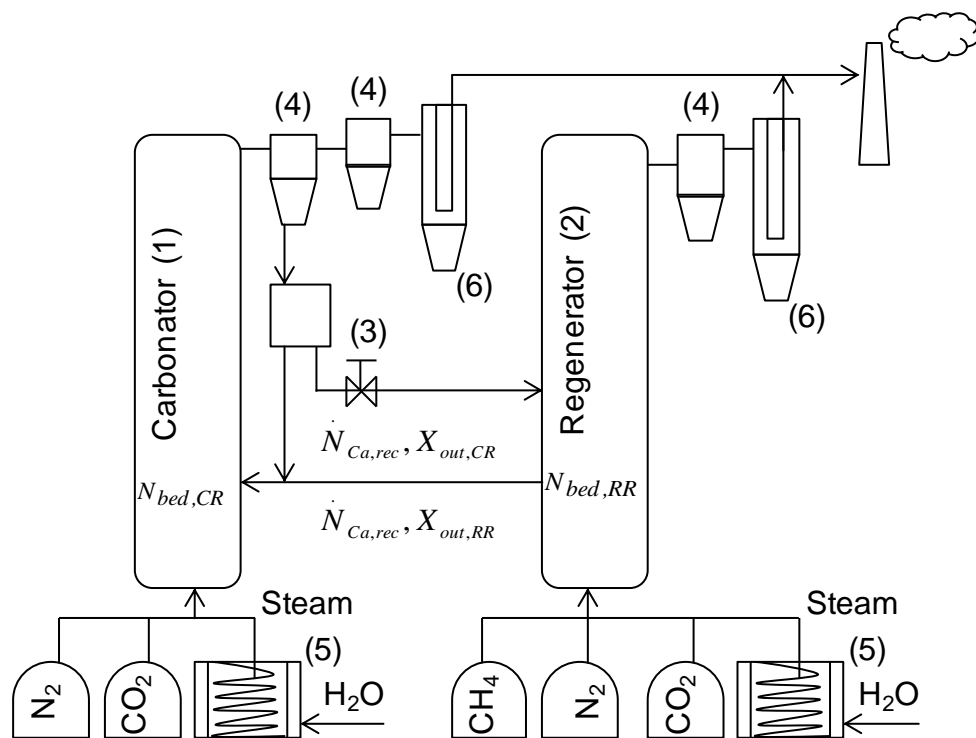
3 Experimental

3.1 Materials and experimental methodology

For the investigation of the calcium looping system performance the process has been realized at the 10 kW$_{th}$ continuously operating dual fluidized calcium looping facility at University of Stuttgart, which is in detail described elsewhere [91], [90] and briefly summarized here.

The facility consists of two fluidized beds, a circulating (H: 12.4 m, D: 0.071 m) and a bubbling one (H: 0.5 m, D: 0.15 m). Figure 10 depicts the general schematic representation of the facility as it is used in the frame of this work. The circulating fluidized bed is the carbonator (1), whereas the bubbling/turbulent bed acts as the regenerator (2). A cone valve (3) regulates the flow of solids entering the regenerator while solids enter the carbonator from the regenerator through an overflow or a loop seal at the bottom of the reactor. The bottom loop seal was necessary to partly increase the flexibility in the reactor mass load and thus, the solids residence time. The facility is electrically heated with CH$_4$ combustion as a supplementary heating source when necessary in the regenerator. A system of cyclones (4) separates the solid from the gas flow at the outlet of each reactor. Gases are introduced in the reactors from tanks/bottles of liquefied gases.

The temperatures are measured with N type thermocouples while BURKER mass flow controllers are used to set up the desired gas inlet flows. The gas outlet concentrations are continuously measured by an ABB Easy Line 3020 and an ABB Advance Optima 2020 analyzer. In various positions along the facility, digital pressure transducers provide on-line measurements, which are critical for the control of the hydrodynamics. Finally, the LabView software program is chosen to control the facility and acquire the respective data. The solid circulation rate is measured at the outlet of the cone valve before entering the regenerator as described in detail in [94].

Figure 10: Schematic representation of the experimental set up [105]

For the present study, two steam generators (5) have been adapted to the system. The steam generators are made from a stainless steel coil surrounded by ceramic electrical heaters and a pump for the water supply. The water supply is continuously recorded on a computer.

The experimental procedure under continuous dual mode of operation was carried out in the following manner: pre-calcined sorbent was introduced in the system while both reactors were fluidized with N_2 and heated up to the required temperatures. In addition to the electrical heaters CH_4 combustion was used when necessary i.e. to achieve temperatures as high as 1203K. When CH_4 combustion was necessary the regeneration took place in an atmosphere containing $5\%_{vol}$ water vapor. After coupling the reactors by opening the cone valve and when hydrodynamic stability was achieved, CO_2 diluted with N_2 and/or steam was introduced in the regenerator and/or the carbonator. The regenerator was operating with a superficial velocity between 0.3 and 2 m/s in the bubbling/turbulent regime and the carbonator

between 4.5 and 5.5 m/s in the fast fluidization regime. A gas bag filled with carbonator and/or regenerator inlet gas was connected to the analyzer in the beginning and after some steady states in order to verify the values set. The O_2 concentration was measured in order to quantify any air streams (e.g. from purge gases) entering the carbonator.

When the temperature, pressure, solids circulation rate, inlet and outlet volumetric concentration of gases were constant for a period of at least 10min a steady state was recorded. Afterwards, the parameters were varied as per the experimental plan and a new steady state was recorded. After every steady state, samples were collected from the outlet of the carbonator and the regenerator for further laboratory analysis. Moreover, the loss of fines was calculated through collecting and weighing the material found at the cyclones (4) and the candle filters (6). The solid samples underwent thermogravimetric analysis in a TGA 701 by LECO at University of Stuttgart to determine the carbonate content, X . Besides, the average maximum carbonation conversion in the fast reaction regime, $X_{max,Ave}$ was calculated using a thermogravimetric analyzer (RITA-TGA) developed by University of Stuttgart in cooperation with Linseis Thermal Analysis GmbH [109]. Annex A includes a description of the RITA-TGA.

The variation of the parameters as included in Table 5 are chosen considering the findings from the studies performed up to now, equilibrium limitations, facility technical oriented restrictions and operational safety.

The studied simulated gas concentrations are based on the fact that flue gas emitted from typical coal fired power plants with combustion air contain ~78%$_{vol}$ N_2 from the atmosphere, ~15%$_{vol}$ CO_2 from the oxidation of the carbon in the hydrocarbon, and around ~7%$_{vol}$ water from both the oxidation of hydrogen in the coal and the vaporization of water that was adsorbed on the coal [45].

While typical flue gas from elementary combustion calculation for the oxy-fuel combustor contains ~25%$_{vol}$ water and ~75%$_{vol}$ CO_2 [45].

No continuous makeup was fed to the system. However, batchwise material was added to compensate for the loss due to attrition. The process has been realized in absence of sulfur, ash, or other combustion species either for simplification reasons, due to technical restrictions as well as for operational safety reasons.

Table 5: Basic experimental and operational conditions

Parameter	Unit	Carbonator	Regenerator
Temperature	K	873-953	1153-1203
Velocity	m/s	4.5-5.5	0.3-2.0
Fluidization regime	-	Fast	Bubbling/ turbulent
Inlet CO_2	%$_{vol,dry}$	10-16	0-75
Inlet H_2O_{st}	%$_{vol}$	0-10	0-35
Space time	h	0.44-0.66	0.3-1.2
Ca looping ratio	-	2-15	
Max carbonation conversion	mol$_{CaCO3}$/mol$_{CaO}$	0.085-0.215	
Carbonate content	mol$_{CaCO3}$/mol$_{CaO}$	0.08-0.219	0.007-0.032
Efficiency	-	0.4-0.85	0.82-0.98

For the investigations two natural limestone forms (LS-1 and LS-2) originating from south Germany have been used. The criteria to select the limes was the ability to capture CO_2 and the performance in terms of material loss determined from lab scale fluidized bed experiments [69], [106]. Limestone was pre-calcined in bubbling fluidized bed conditions at around 1173K in N_2 resulting in a particle size D_P of around 0.413 µm and 0.442 µm for LS-1 and LS-2 respectively. Details of the experimental works can be found in [107], [126], [127], [131].

Table 6: Characteristics of the tested limestone forms [69,106]

Parameter	Unit	LS-1	LS-2
Mass fraction of CaO	kg/kg	0.5364	0.5601
Mass fraction of impurities (SiO_2)	kg/kg	0.351	0.003
Porosity	m^3/m^3	0.2416	0.1345
Mean pore diameter	nm	160	71.0
Capture capacity	g_{CO2}/g_{Ca}	0.08[i]	0.20[i]
Capture capacity	g_{CO2}/g_{Ca}	0.09[ii]	0.14[ii]
Average elutriation rate	g/min	0.015[i]	0.001[i]

(i) The value is obtained at the first Carb-Calc cycle at BFB tests. Experimental conditions: Carb: 1min, 923K, 15%$_{vol,dry}$ CO_2, Calc: 20min, 1213K, 70%$_{vol,dry}$ CO_2

(ii) The value is obtained at the first Carb-Calc cycle at BFB tests. Experimental conditions: Carb: 15min, 923K, 15%$_{vol,dry}$ CO_2, 75 ppmvol SO_2 Calc: 20min, 1213K, 70%$_{vol,dry}$ CO_2, 750 ppmvol SO_2

3.2   Example of process realization

In Figure 11, a general view of an experimental day is depicted. The progress of work is time consuming and includes six steps. Firstly, the preparation consists of the calibration of the analyzers, the material fill in the reactors and the loop seals, as well as the control of the measurement equipment and the gas analyzers. Afterwards, the system must be heated up. The sorbent is fed to the arrangement, around 10 kg CaO in the regenerator, 7 kg in the upper loop seal and 3 kg in the lower loop seals. The next step is the circulation of the material that includes first the achievement of stable operation of the carbonator in a single loop and afterwards the additional feed of material to obtain the desired pressure drop in the carbonator. The coupling of the two reactors includes the opening of the cone valve and the lower loop seal aeration so as the material circulates between the two reactors in a stable operation. The process realization is performed by setting the parameters as per the experimental plan and accomplishing steady state operation. Finally, the facility shutdown comprises the very careful removal of all the material for the balance of the mass but also to avoid blockages in the reactor when cooled down.

For the shown case, the facility was ready to perform the planned experimental set ups at 13:30. At that point, CO_2 was introduced to the carbonator and steady states were obtained. The facility was in operation for around 14 hours in total and for around 6 hours the calcium looping process was demonstrated.
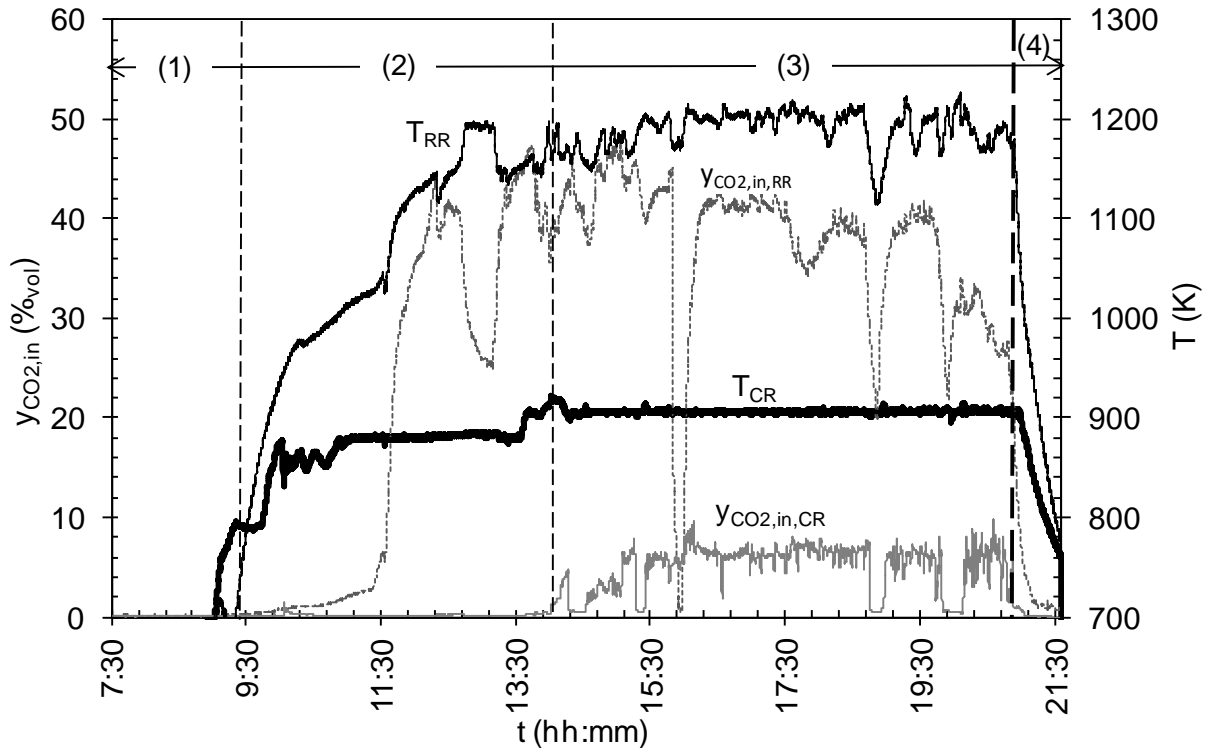

Figure 11: Example of the process realization in four phases: (1) preparation works, (2) heating up, material circulation and reactor coupling, (3) process realization/CO_2 feed, (4) facility shutdown [107].

For the same day, the CO_2 capture efficiency, as it is calculated through the inlet and outlet CO_2 flow in the carbonator, is depicted in Figure 12. Efficiencies between 20 and around 90% were recorded.
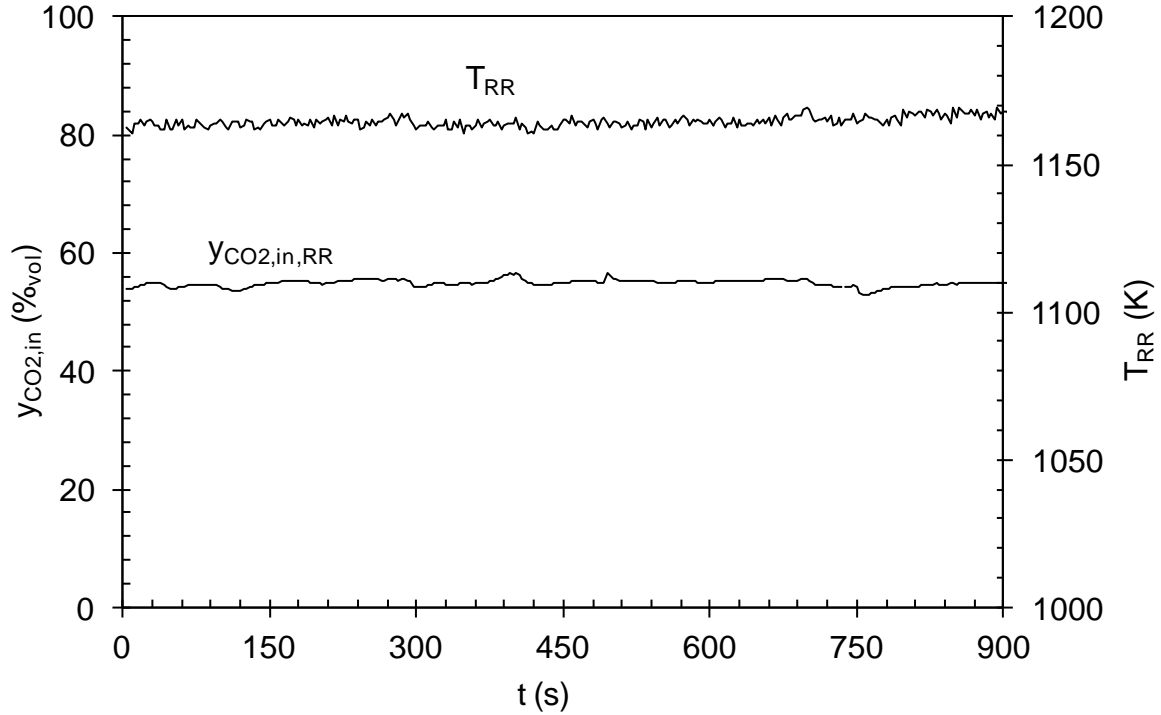
In Figure 13 and Figure 14 an example of a steady state operation is shown for the carbonator and the regenerator respectively. The temperature, the carbonator CO_2 capture efficiency as well as the inlet and outlet CO_2 concentration is plotted versus the time. A good performance and stable operation is achieved.
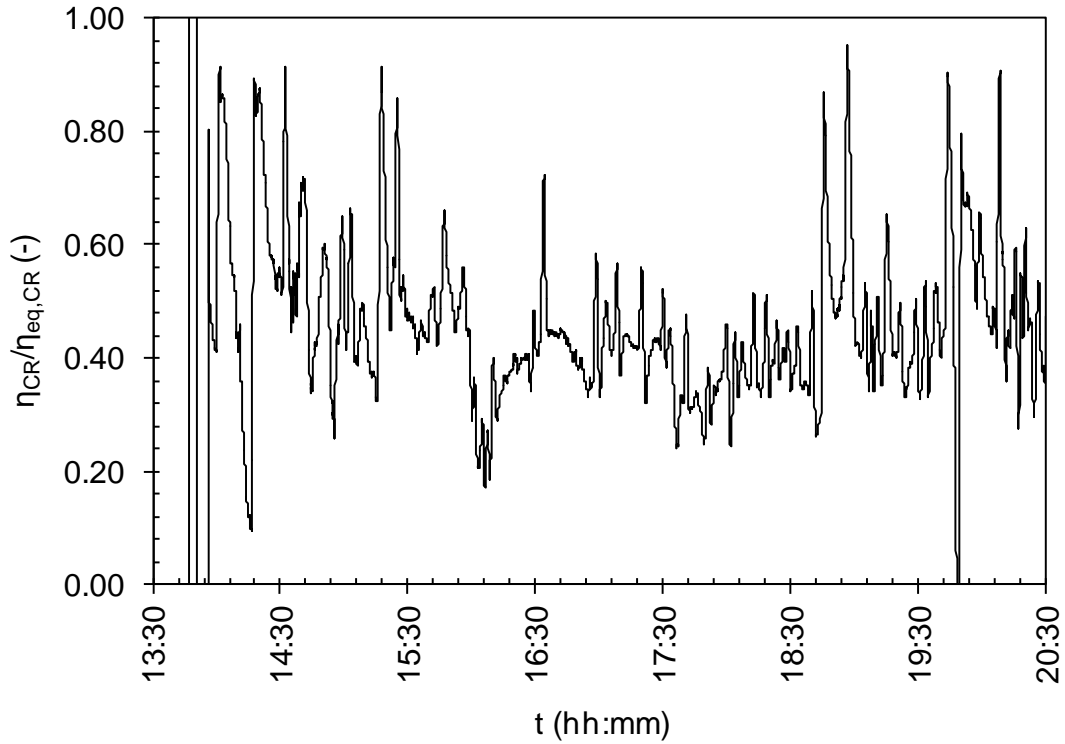
Figure 12: Example of evolution of the CO_2 capture efficiency at an experimental day [107]
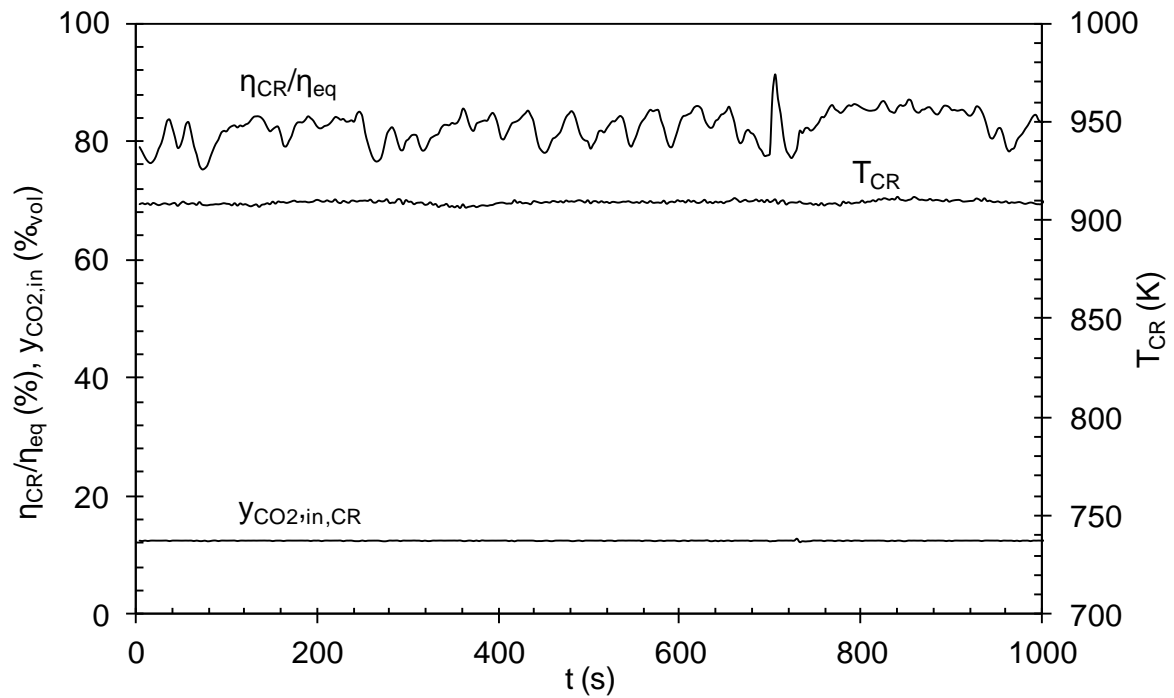

Figure 13: Example of a steady state with reference to the carbonator reactor in dry conditions [107]

Figure 14: Example of a steady state with reference to the regenerator reactor in dry conditions [107]

3.3   Data evaluation

The data attained during steady state operation has been validated through the closure of the basic molar balance of equation (5) for the carbonator and the regenerator. Figure 15 depicts the equality between the CO_2 removed in the gas phase as derived from gas measurements and that absorbed in the solid phase as calculated from measurements of the solids circulation rate and carbonate content after the carbonator and regenerator. Additionally, Figure 16 represents the equality between the CO_2 released in the regenerator as per gas-analyzer computations and the CO_2 released from the solid phase as calculated through the measurements of the solids flow rate and carbonate content leaving the reactor. The good closure, as shown in the following figures, is a strong indication of the correctness of the experimental procedure and the measurement/ analysis techniques applied.
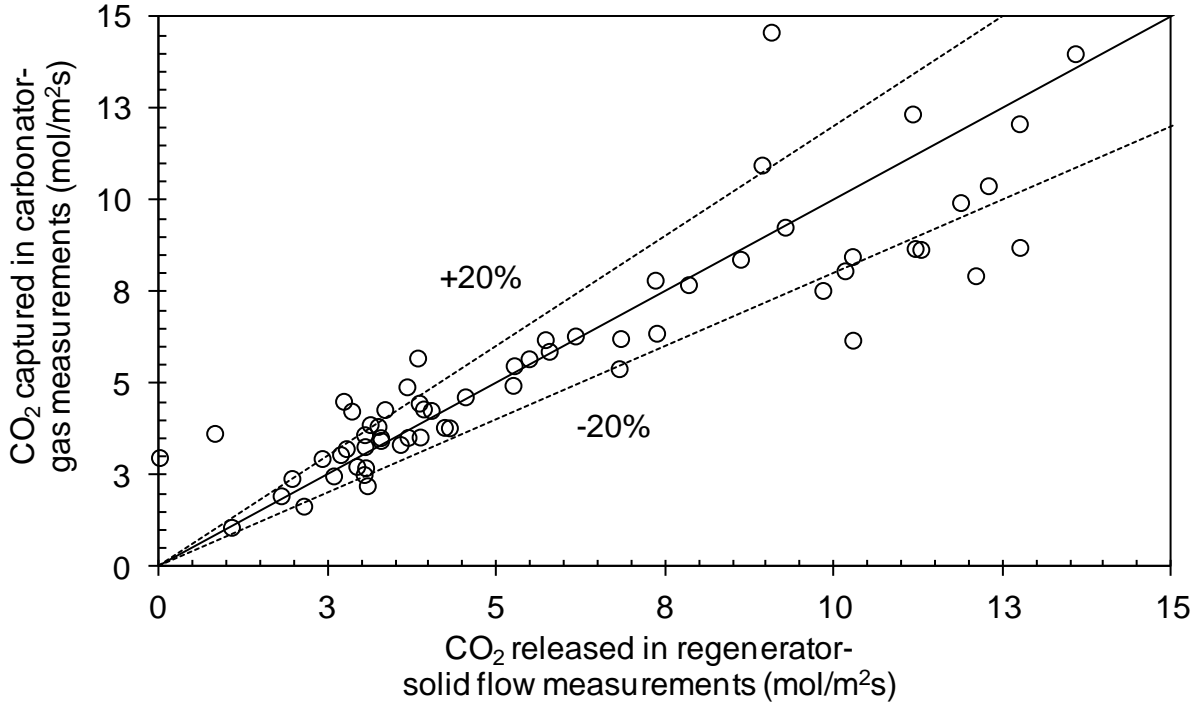
Figure 15: Closure of the carbon molar balance as far as concerns the carbonator [105]
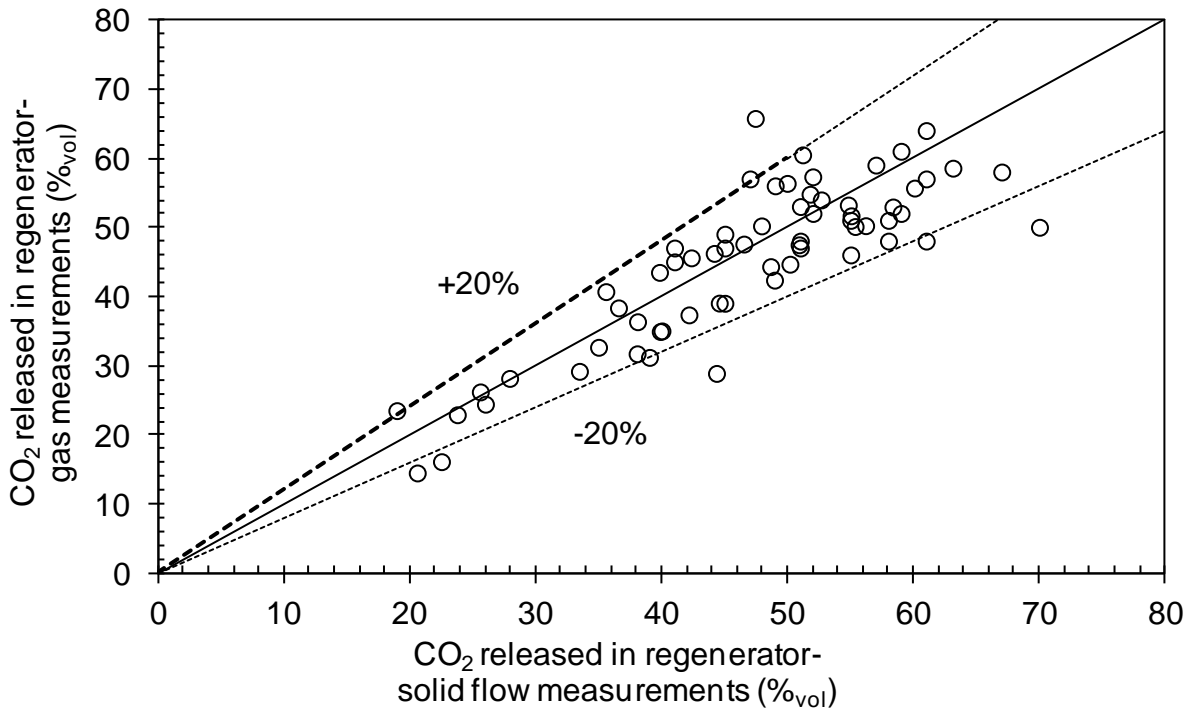
Figure 16: Closure of the carbon molar balance as far as concerns the regenerator [105]

4   Results and Discussion

4.1   General

The optimal operating temperature, CO_2 partial pressure and water vapor are a tradeoff between the reaction kinetics, the equilibrium forces as well as the sorbent sintering and attrition. Nevertheless, the selection of the operating temperatures, flue gas recycle, mass flows, sorbent purge and makeup is a design optimization problem in which the CO_2 capture or release level is restricted, process performance must be maximised while the unit size must be minimized [23], [36]. The following subsections address a parametric study of these main operational parameters focusing on their effect mainly on the carbonator and regenerator efficiency as well as the sorbent average maximum carbonation conversion and the sorbent behavior towards attrition as defined in section 2.

4.2   Effect of temperature on CO_2 capture and carbonation conversion

Figure 17 presents the effect of temperature on carbonator CO_2 capture efficiency for both the air-combustion reference case (AComb) as well as the oxy-combustion case (OComb) inside the regenerator. For both cases, the CO_2 inlet concentration was kept constant at the carbonator and was varied at the regenerator: around 30%$_{vol}$ for the AComb case and 55%$_{vol}$ for the OComb. The limestone used is the LS-1. Moreover, CH_4 combustion took place, supplementary to the electrical heaters, in order to achieve the required temperatures, when necessary. It is shown that CO_2 capture efficiency is a decreasing function of the carbonator temperature because the equilibrium CO_2 concentration increases (see Figure 6). On the other hand, as observed from Figure 18 the CO_2 capture efficiency increases with increasing regenerator temperature, since: (i) the equilibrium CO_2 concentration in

the regenerator increases, thereby (ii) the calcination reaction rate increases resulting to lower $X_{out,RR}$ values (see Figure 19) and thus (iii) a higher flow of active Ca, expressed by the product $\dot{N}_{Ca,rec}(X_{max,Ave} - X_{out,RR})$ is delivered to the carbonator. The findings are in agreement with previous investigations [95].
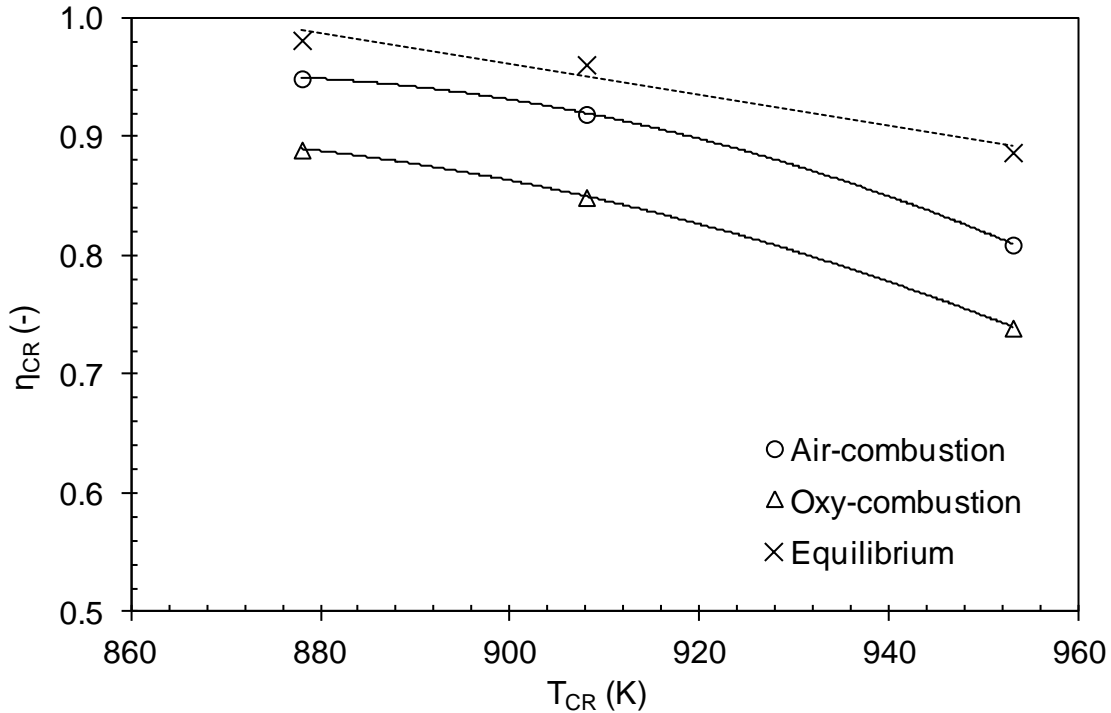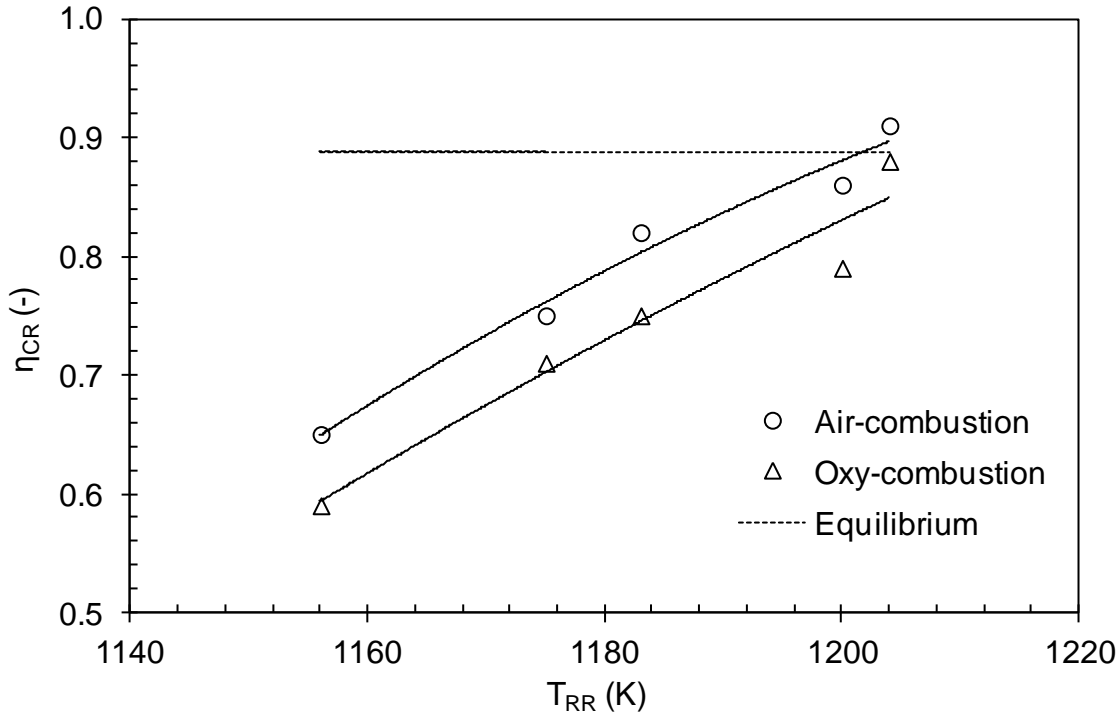

Figure 17: Carbonator CO_2 capture efficiency versus carbonator temperature for LS-1 and T_{RR}=1178K, TURB RR, CFB CR, $y_{CO_2,RR}$=30(AComb)/55(OComb)%$_{vol}$ bal N_2, no H_2O_{st}, ξ_{CaL} =15 mol$_{Ca}$/mol$_{CO2}$, τ =0.65h(CR)/0.75h(RR), $X_{max,Ave}$=0.07-0.09 [105]

When comparing the AComb with the OComb cases, slightly higher regenerator temperatures are required in the second case for the same CO_2 capture efficiency. This can be explained as follows: At the OComb regenerator the difference between actual and equilibrium CO_2 concentration becomes smaller (related to the AComb case) for a given temperature and thus calcination reaction rate decreases. Hence, for the same residence time and temperature in the regenerator the fraction of non calcined $CaCO_3$ ($X_{out,RR}$) increases. Consequently,

less active Ca is delivered to the carbonator to react with CO_2 resulting in a lower CO_2 capture efficiency for the same looping ratio (ξ_{CaL}).

Figure 18: Carbonator CO_2 capture efficiency versus regenerator temperature for LS-1 and T_{CR}=898K, TURB RR, CFB CR, $y_{CO_2,RR}$=30(AComb), 55(OComb)%$_{vol}$ bal N_2, no H_2O_{st}, ξ_{CaL} =15 mol$_{Ca}$/mol$_{CO2}$, τ =0.65h(CR)/ 0.75h(RR), $X_{max,Ave}$=0.07-0.09 [105]

The temperature influence on the $X_{out,RR}$ for the AComb and OComb case is anticipated in Figure 19. It can be seen that the $X_{out,RR}$ is higher for the oxy-combustion case compared to the air-fired one. On the other hand, it can be observed from Figure 19, that (1) the sorbent, based on its maximum average carbonation conversion, is highly cycled and that (2) its residual activity is not affected by the CO_2 concentration. The latter is a further proof that the downturn of the CO_2 capture efficiency for the oxy-combustion case is due to the elevated $X_{out,RR}$ values.
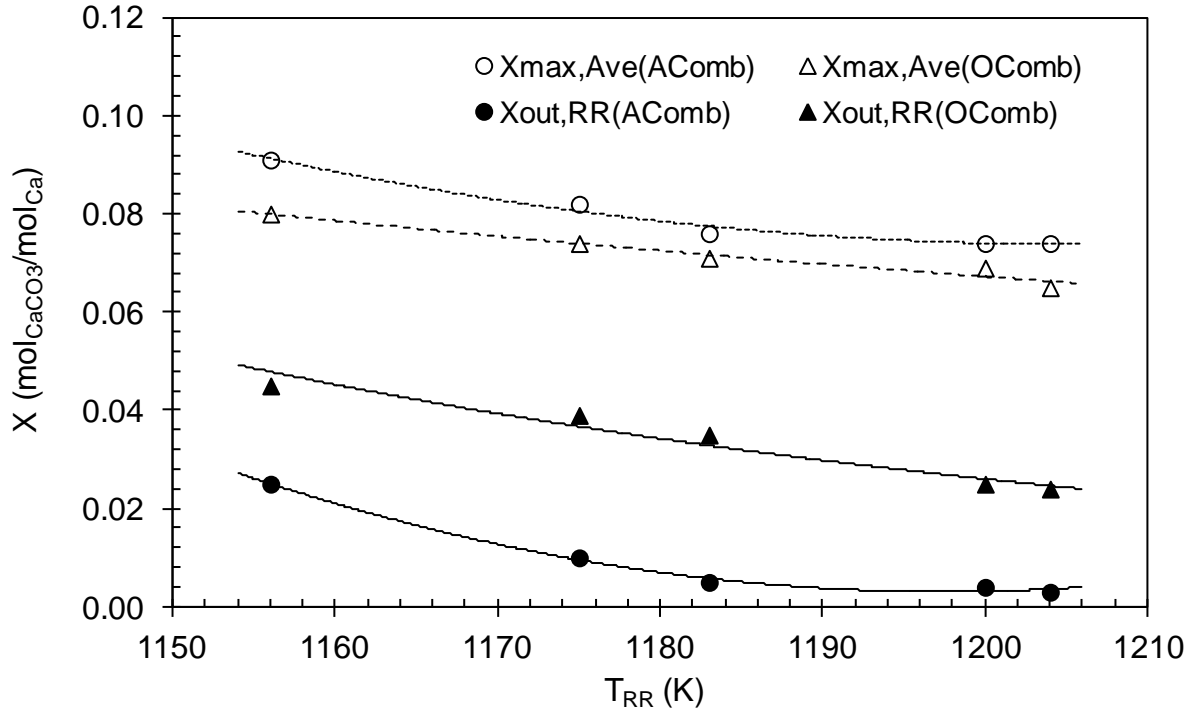
Figure 19: Sorbent carbonate content vs. regenerator temperature for LS-1, TURB RR, CFB

CR, $y_{CO_2,RR}$ =30(AComb)/55(OComb)%$_{vol}$ bal N$_2$, no H$_2$O$_{st}$, ξ_{CaL} =15 mol$_{Ca}$/mol$_{CO2}$, τ_{CR} =0.65h,

τ_{RR} =0.75h, $X_{max,Ave}$ =0.07-0.09 [105]

## 4.3   Effect of CO$_2$ presence during calcination on CO$_2$ capture

Figure 20 depicts the carbonator efficiency for various space time values and looping ratios in OComb dry conditions. The increasing trend of the CO$_2$ capture efficiency by increasing the looping ratio and the space time is the same as the one observed and discussed by Charitos et al [91] for the air-fired case using a different limestone. As per Charitos et al [91], the higher looping ratios result in higher active fraction of bed inventory in the carbonator thus higher CO$_2$ capture efficiencies.
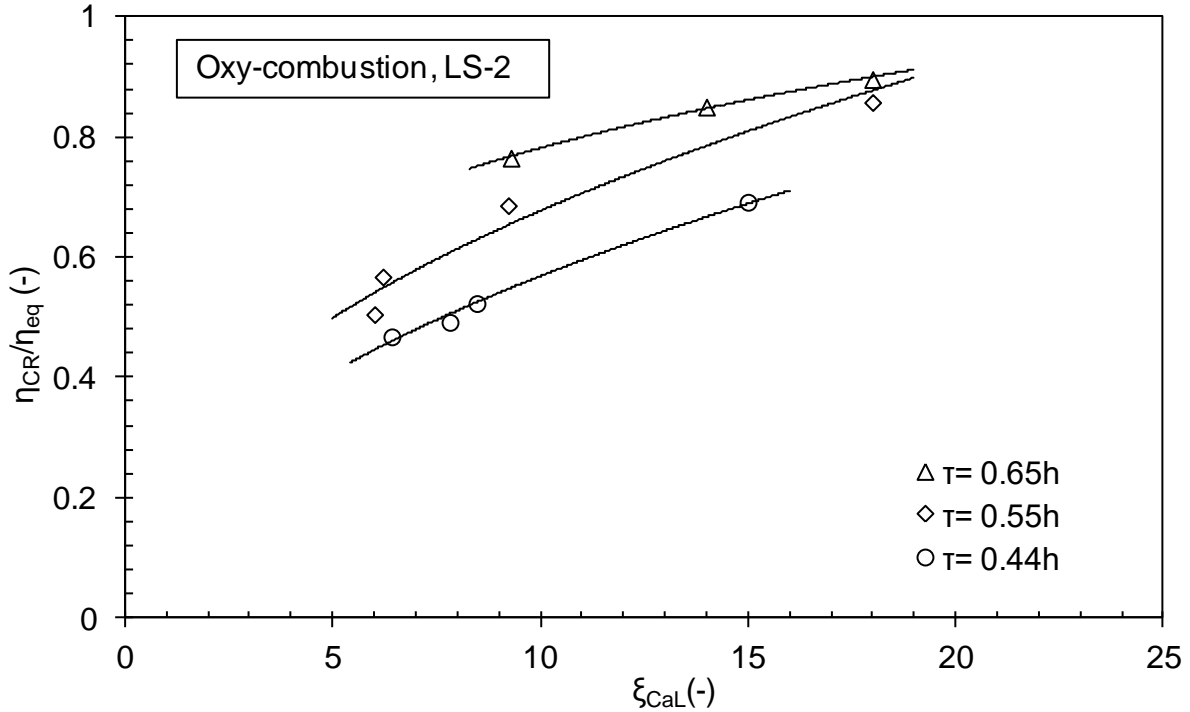
Figure 20: CO_2 capture efficiency vs Ca looping ratio in dry conditions for various CR space times. Experimental conditions: CFB CR, T_{CR}=903K, $y_{CO_2,CR}$=10-16%vol, BFB RR, T_{RR} =1178K, $y_{CO_2,RR}$=55%vol, $X_{out,RR}$=0.05, $X_{max,Ave}$=0.12-0.15, τ_{RR}=0.94h [105]

For the air-combustion case of Figure 21 an equilibrium normalized CO_2 capture efficiency of almost 100% is attained for the CFB carbonator operating at a looping ratio of around 16, at a space time of 0.65h and at an $X_{max,Ave}$ value of around 0.13. For the OComb case, a looping ratio of around 16 results to an equilibrium normalized CO_2 capture efficiency of more than 80% (for a space time more than 0.55h and an $X_{max,Ave}$ of around 0.13).

Figure 21 represents a rise of around 40% of the looping ratio necessary to achieve CO_2 capture efficiencies of more than 90%, for the case of oxy-fired calcination environment in comparison to the air-fired one and same limestone, space time and temperature inside the regenerator.
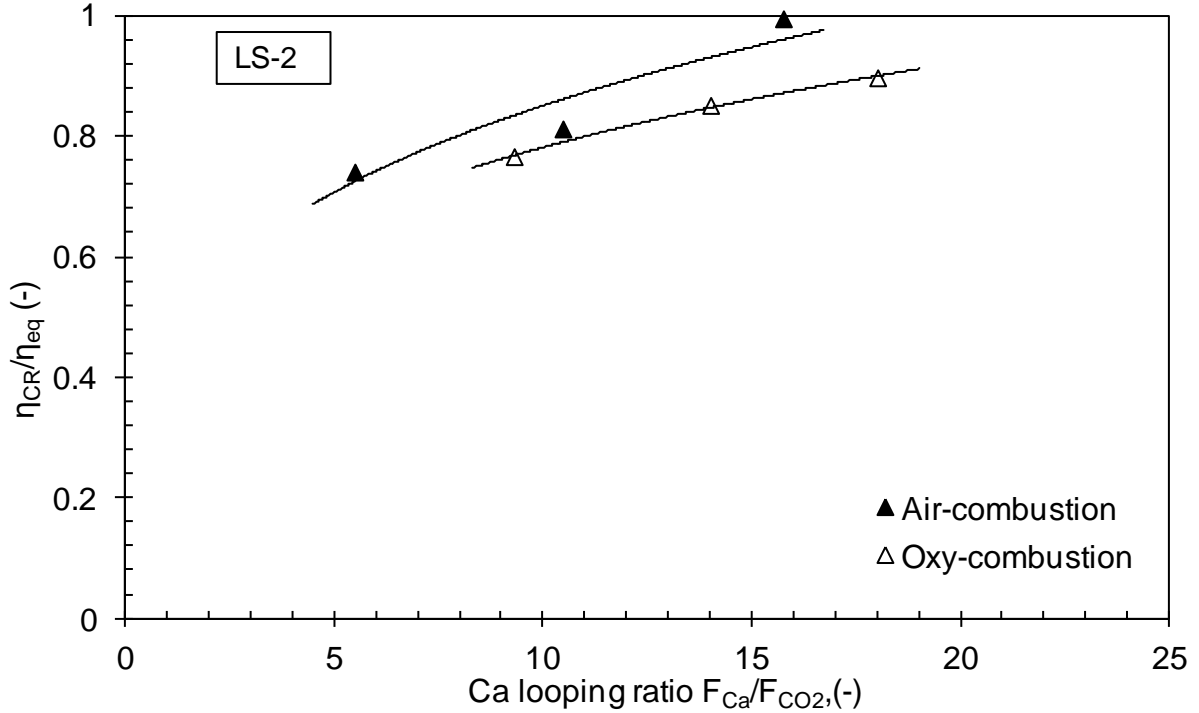
Figure 21: CO_2 capture efficiency vs Ca looping ratio in dry conditions: CFB CR, T_{CR}=903K, $y_{CO_2,CR}$=10-16%$_{vol}$, τ_{CR}=0.65h, BFB RR T_{RR}=1178K, $y_{CO_2,RR}$ =30(AComb)/55(OComb)%$_{vol}$, $X_{out,RR}$=0.02(AComb)/0.05(OComb), $X_{max,Ave}$=0.12-0.15, τ_{RR} =0.94h [105]

The same trends can be disclosed for the limestone LS-1 as reported in Figure 22 and Figure 23. Even if this lime presents worst residual activity (0.08 mol$_{CO2}$/mol$_{Ca}$) similar looping ratios and space times as for the LS-2 lime are required for efficiencies of around 90%. This finding is associated to the specific facility and experimental set up and is not expected in a large scale facility. The main reason is that the regeneration of the sorbent is restricted due to the source of heat supply (electrical heaters) as well as the fluidization regime. Local temperature difference as well as gas bypassing phenomena reduce the sorbent calcination degree. Thus, low fluidization velocities (bubbling fluidization regimes) should be avoided in process design works.
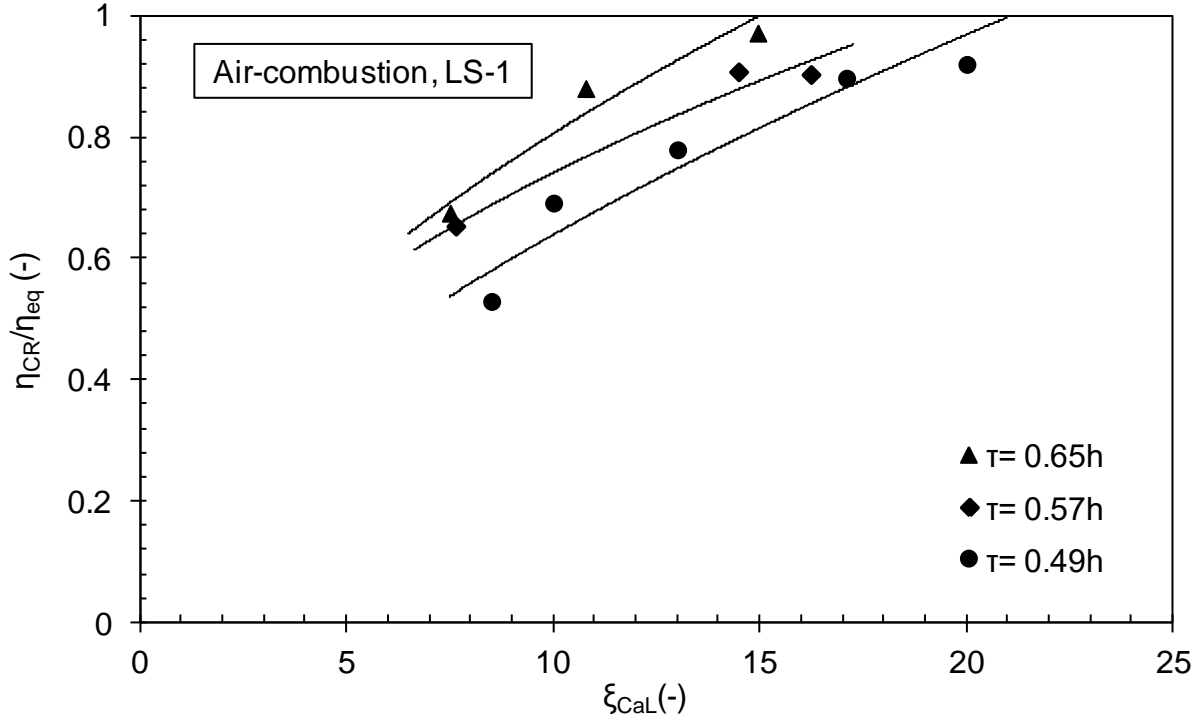
Figure 22: CO_2 capture efficiency vs looping ratio in air-combustion dry conditions and various carbonator space times. Experimental conditions: CFB CR, T_{CR}=903K, $y_{CO_2,CR}$=10-16%$_{vol}$, BFB RR, T_{RR}=1178K, $y_{CO_2,RR}$=30%$_{vol}$ [107]

Based on the diagrams and the previous discussion, it can be concluded that the CO_2 capture efficiency decreases when calcination takes place at high CO_2 concentrations. It has been noted that incomplete calcination results from the high pressure of CO_2 which reduces the calcination reaction rate. A rise of the amount of $CaCO_3$, $X_{out,RR}$ delivered to the carbonator lowers the CO_2 capture in agreement with equation (5).

Moreover, the data indicates that, in accordance with the literature [61], the presence of CO_2 in the regenerator may cause pronounced sintering phenomena. The subsequent pore blockages favor the diffusion resistances in the carbonator during the carbonation reaction which becomes slower and thus less CO_2 can be captured.
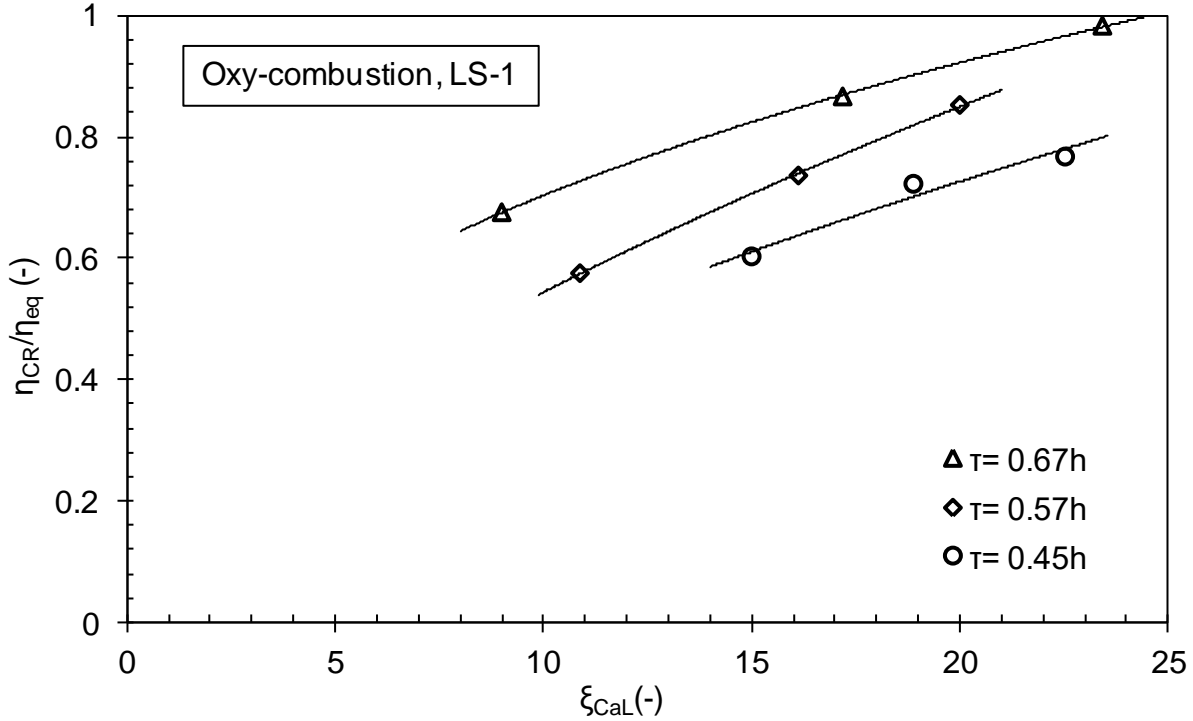
Figure 23: CO_2 capture efficiency vs looping ratio in dry conditions and various carbonator space times: CFB CR, T_{CR}=903K, $y_{CO_2,CR}$=10-16%vol, BFB RR, T_{RR}=1178K, $y_{CO_2,RR}$=55%vol [107]

4.4 Effect of CO_2 presence during calcination on regenerator efficiency

Figure 24 discloses the impact of CO_2 presence on the regenerator efficiency. A clear trend pointing out a strong decay of the efficiency is revealed when raising the CO_2 concentration. Charitos et al [8] reported complete sorbent calcination for low CO_2 concentrations at space time of around 0.5h (BFB regenerator). As depicted in Figure 24, 80% sorbent calcination is attained while a space time value of 0.94h is requisite. However, the outcome should be treated qualitatively since that high space time values are attributed to restrictions imposed by the facility. This issue is explained in detail in Duelli et al [94] and summarized as follows: i) the indirect heat transfer through electrical heaters from the walls to the particles result in lower heat transfer rate correlated to the one aquired by direct heat transfer through combustion

ii) the bubbling fluidization regime results in local zones with higher partial pressure of CO_2 than the one measured at the outlet of the reactor. Nevertheless, based on the findings of Grasa and Abanades [54] and considering the fact that in this study the calcination times are not more than 10min as well as that the pilot performs in continuous mode, the increased space times required here are not expected to add any additional impact on sorbent performance that could be neglected at higher scale.
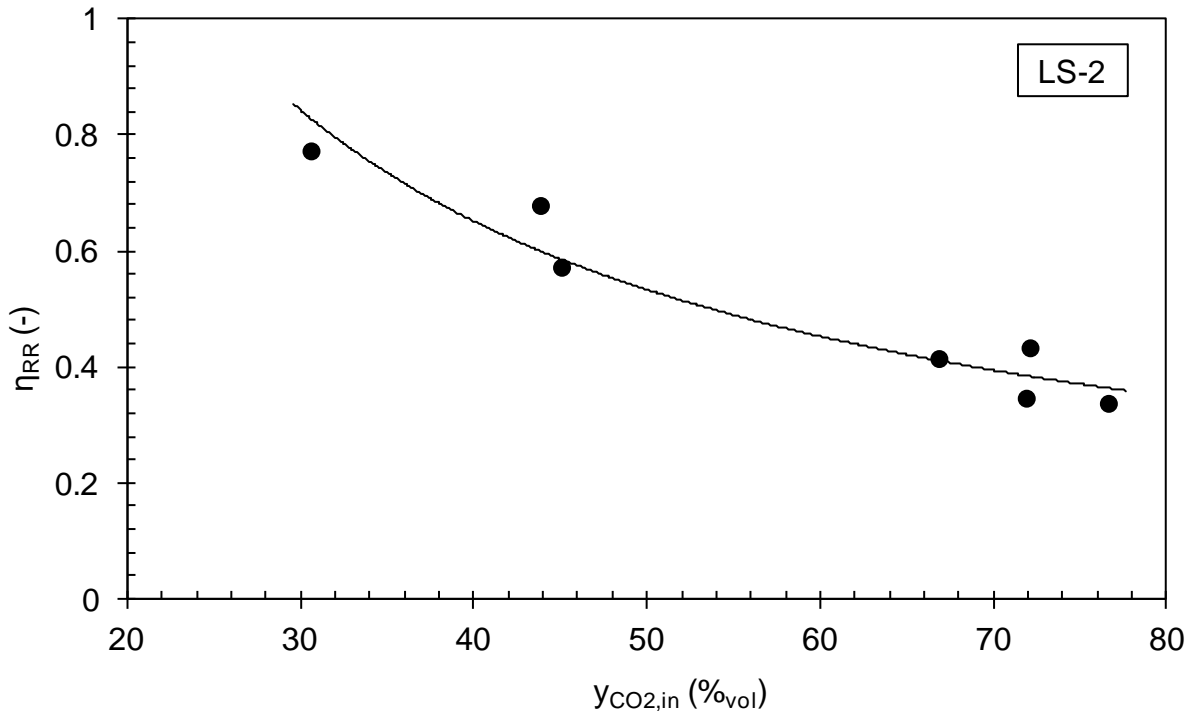
Figure 24: The effect of CO_2 presence on regenerator efficiency without water vapor presence, τ_{RR}=0.94h, T_{RR}=1183K [105]

Figure 25 and Figure 26 depict the effect of regenerator space time on the regenerator efficiency for the two limestones tested: for both limestones the higher the residence time of the particles and the lower their carbonate content the higher the amount of calcined particles will be. For full sorbent regeneration a space time of more than 1h is required when elevated CO_2 concentrations are present in the reactor while for the same facility in case of low CO_2 concentrations space time of less than 1h is needed. These space times for a typical sorbent carbonate content of

0.1 would necessitate a residence time of the average particle in the regenerator of around 6min.

From a commercial point of view, this residence time is not realistic for a fluidized bed reactor and the results reported should be treated only qualitatively since facility design and operation restraints-related to electrical heating and associated heat transfer phenomena noted above-impose such high residence times.
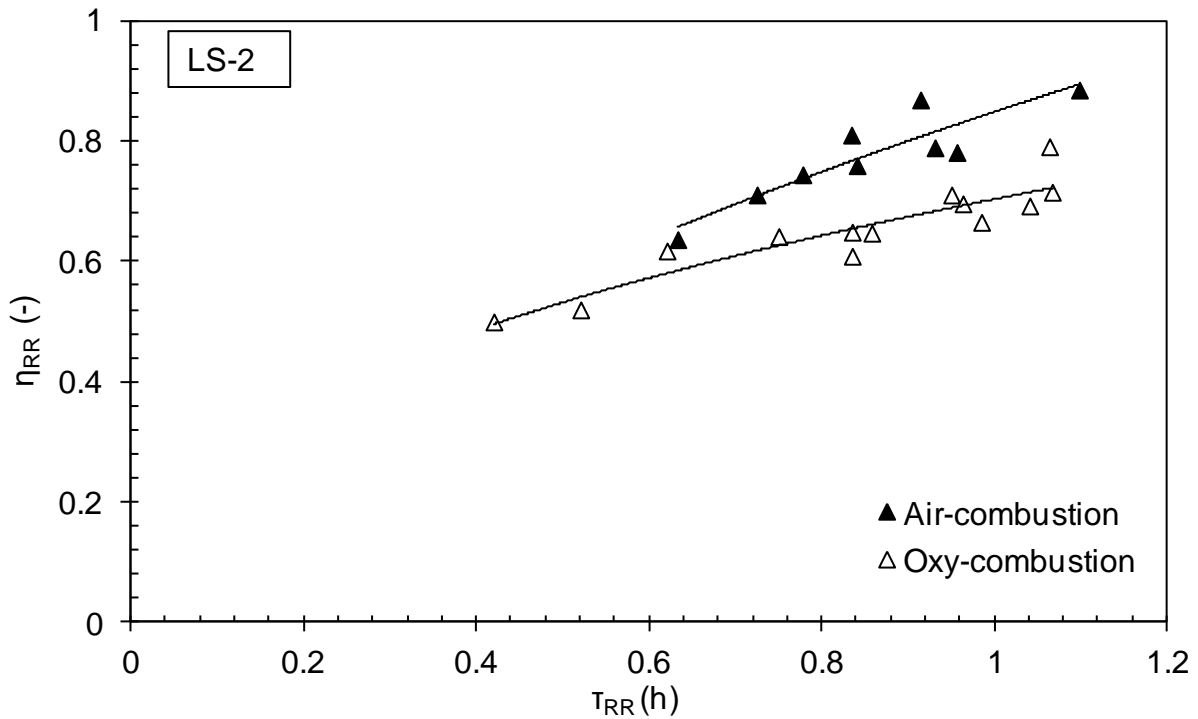
Figure 25: Regenerator efficiency vs regenerator space time in dry conditions and CFB CR, T_{CR}=903K, $y_{CO_2,CR}$=10-16%$_{vol}$, BFB RR, T_{RR}=1178K, $y_{CO_2,RR}$=30(AComb)/55(OComb)%$_{vol}$ [105]
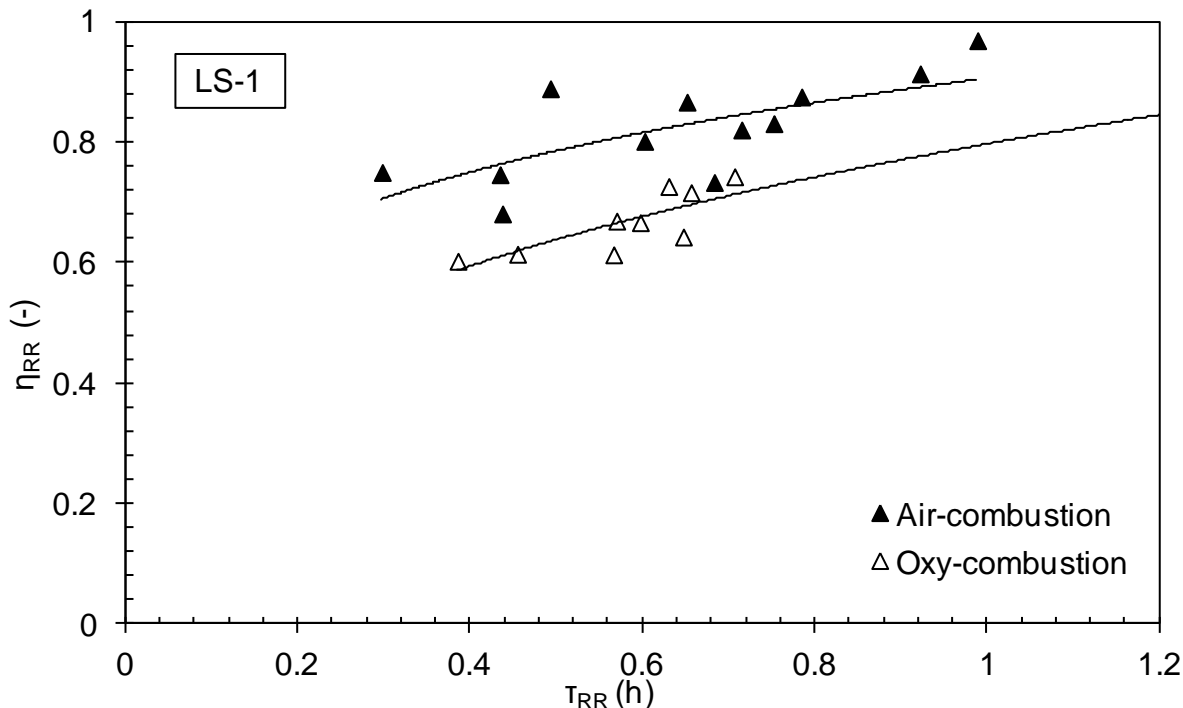
Figure 26: The effect of regenerator space time on regenerator efficiency in dry conditions as per Fig. 25 [107]

4.5   Effect of CO₂ presence during calcination on carbonation conversion

In Figure 27 the evolution of the decay of $X_{max,Ave}$ along the experimental hours (in continuous mode) is depicted for two different levels of CO_2 concentration for the limestone LS-2. The residual activity decays rapidly in the first three hours of continuous operation and after 12 hours it stabilizes at approximately 10% independently of the amount of CO_2 present during calcination.

The same behavior is perceived for the limestone LS-1 and is illustrated in Figure 28. For this limestone the carrying capacity achieves a residual activity of approximately 8.5%. Literature report residual activities in this range for low CO_2 partial pressures [95]. For low sorbent theoretical cycles, the theoretical $X_{max,Ave}$ decay curve as per TG test deviates from the values obtained in the fluidized bed, which is

reasonable taking into consideration the fluidizing phenomena in the bed. In the fluidized bed, the sorbent is imposed to severe thermal and mechanical stresses that change the surface and the pore structure and thus the maximum carbonation conversion. Both limestones achieve their residual activity and this is independent of the partial pressure of CO_2 during calcination. However, the presence of CO_2 seems to accelerate the decay of the carbonation conversion which is in agreement with the literature [28]
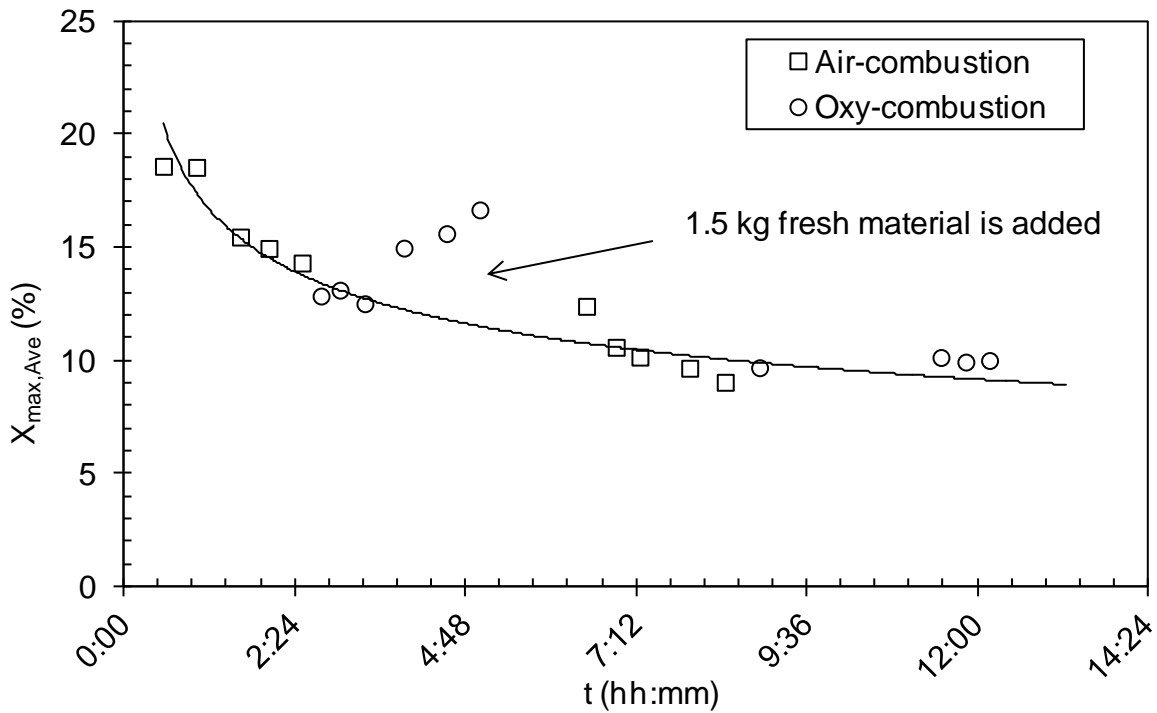
Figure 27: The decay of the maximum average sorbent carbonation conversion vs the actual hours of DFB system operation for LS-2, $y_{CO_2,RR}$=27(AComb)/53(OComb)%$_{vol}$ and no water vapor presence [90]

Microstructural analysis of the sorbent i.e calculation of the surface area and the pore volume is not included in this work. However, results from literature [95] refer to a limestone that was pre-calcined for many hours and afterwards was used for the simulated air-fired case experiments without water vapor presence. For this material, it was shown that the particles were highly sintered and this was observed through a

loss in the BET surface area and a decrease in the pore volume compared to the original limestone.
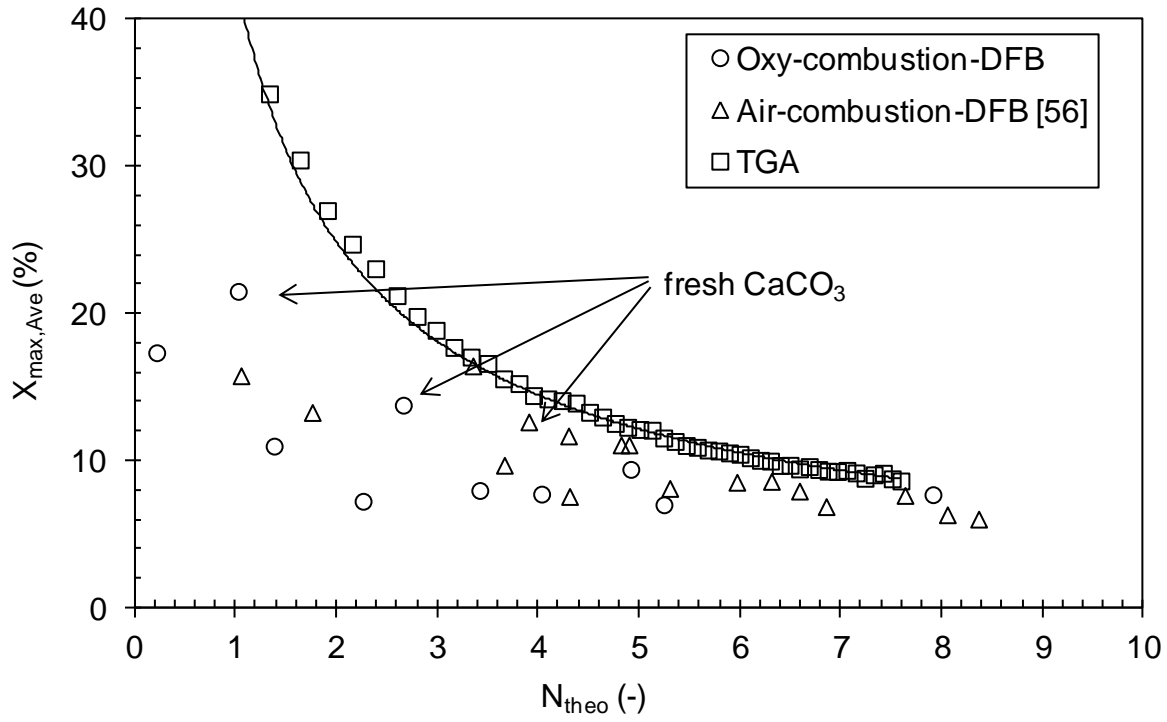
Figure 28: The decay of the maximum average carbonation conversion of LS-1 vs the theoretical cycle number as measured in dry conditions: (i) $y_{CO_2,RR}$ ≥45(OComb)/30(AComb)%vol, T_{RR}=1173K, T_{CR}=903K (DFB experimentation), (ii) T_{Calc} =1123K, T_{Carb}=903K, $y_{CO_2,Calc}$=10%vol (TG tests) [133]

Moreover, the influence of the batchwise inclusion of fresh limestone makeup is depicted as an instant rise of the sorbent carrying capacity for the two limestones in both Figure 27 and Figure 28. Additionally, correlated to the lime performance in TG tests [135], the $X_{max,Ave}$ drop is quicker in DFB experiments by cause of the relatively higher heating rates. Nevertheless, in both instances the residual activity is comparable. However, the regeneration under high CO_2 concentration does not step up or worsen the deterioration of the CO_2 sorption capacity. This may be associated with the fact that in the DFB system the uncompleted calcination and subsequently the partly carbonated particles as well as the short residence times may decline the

sintering effects. Finally, the residual activity may be adjusted to values higher than those reported here through continuous addition of makeup of unused limestone, which in our case was batchwise fed to counteract for the mass displaced due to attrition and likely cyclone inefficient operation.

4.6 Effect of water vapor presence on CO_2 capture

Figure 29 delineates conspicuous increase of carbonator performance when water vapor is simultaneous in both carbonator and regenerator opposed to the respective when water vapor is omitted. This is convenient to process realization at industrial scale.
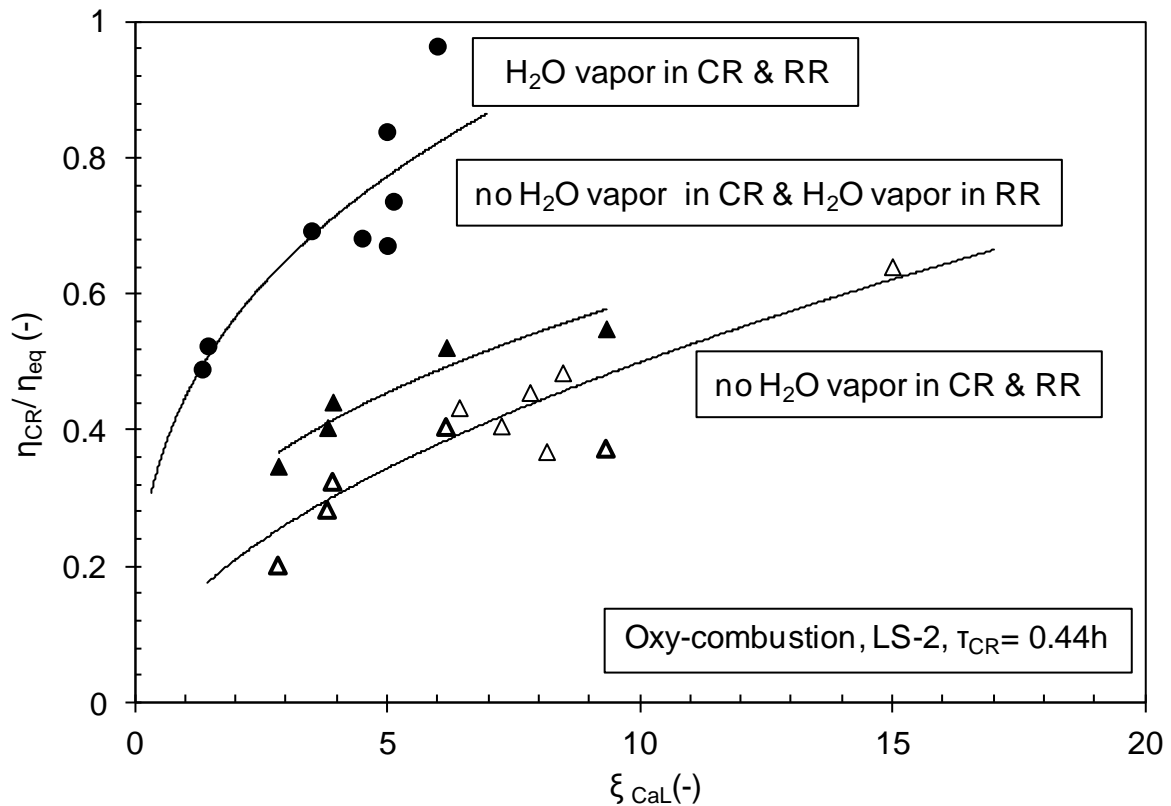
Figure 29: CO_2 capture efficiency vs looping ratio. Experimental conditions: CFB CR, T_{CR} =903K, $y_{CO_2,CR}$ =10-16%$_{vol}$, $y_{st,CR}$ =0-10%$_{vol}$, BFB RR, T_{RR} =1178-1193K, $y_{CO_2,RR}$ =55%$_{vol}$, $y_{st,RR}$ =0 or 25-35%$_{vol}$, $X_{max,Ave}$ =0.12-0.25 [105]

It can be seen that for a looping ratio of around 8, CO_2 capture efficiencies of around 90% can be achieved. For the case without water vapor very high looping ratios of more than 15 are required when operating with a highly cycled sorbent with an $X_{max,Ave}$ close to the residual activity (Figure 31). This significant improvement is related to the enhancement of the limestone reactivity. This behavior has been already reported by [98], [102] as well as [108] and [143], who performed TG and bench scale experiments. According to their argumentation, the improvement is a result of the changes of sorbent morphology: water vapor presence enhances sintering and thus a shift from smaller to larger pores with a more stable structure and a BET surface area greater than the one without water vapor presence. For their experimentation, most of the pore volume was associated with slightly larger pores (50nm) when water vapor was present compared to about 30nm pores when water vapor was absent. The larger pores are less susceptible to pore blockage thus allowing for the higher conversion. Besides, literature reports that reduction in the particle surface area (compared to the original lime), would adversely affect CO_2 absorption at the surface, but larger pores would allow lower diffusional resistance caused by carbonate formation at the surface, allowing higher overall conversion thus larger pores can be better exploited [108].

Additionally when considering the twofold nature of CO_2 diffusion and reaction within sorbent particles the favourable effect of steam can be explained as follows: Carbonation results from multiple processes in series: intraparticle diffusion of CO_2 in the pore space between the "grains"; diffusion of CO_2 across the $CaCO_3$ product layer; reaction of CO_2 with unreacted CaO. The latter two processes are actually a non-trivial combination of ion solid state diffusion and reaction, which is strongly influenced by the presence of steam. In this general framework, literature [143], reports that the favourable effect of exposure to steam, and the much more pronounced effect when exposure takes place during the carbonation stage as compared to the calcination stage, has not much to do with pore opening or widening, related to the "intraparticle" and "intergrain" diffusion of CO_2, but rather by

steam acting as a "catalyst" of CO_2 "intragrain" diffusion within and across the sorbent $CaCO_3$-based product layer.

Moreover, a slight improvement of the reactor performance is observed when water vapor is present only during regeneration in comparison to the dry case (less looping ratios are needed for the same CO_2 capture efficiency). As per recent literature [143] this improvement should be ascribed to the pronounced effect of steam on microstructure enhancement during calcination, which improves CO_2 capture in the subsequent carbonation. However this gain is not as large as for the wet regenerator-carbonator case compared to the dry case. Based on this observation, it can be concluded that this notable improvement results mainly from presence of water vapor during carbonation. It seems that water vapor presence during carbonation enhances the reaction rate due to lower diffusion resistances and thus more CO_2 is captured. This is in agreement with literature reporting that steam addition produces a larger impact on sorbent reactivity for carbonation than for calcination [108], [143]. It should be noted that the values of the equilibrium normalized CO_2 capture efficiency without presence of water vapor in the carbonator are slightly lower than those presented in Figure 20 for the same space time (0.44h). This variation is due to differences in the activity of limestone, as in the curve of the $X_{max,Ave}$ is between 0.12-0.15 (Figure 20), and around 0.10 (Figure 29).

4.7   Effect of water vapor presence on regenerator efficiency

Figure 30 reflects the increase of the calcination conversion of the sorbent when experiments were realized in presence of water vapor in both carbonator and regenerator reactors. This is in agreement with the basic process equation (5) indicating that increase of sorbent calcination conversion benefits the sorbent carbonation conversion. Furthermore, this aligns with the findings of the trends as observed in Figure 29.

It is shown that almost all the incoming flow of lime is calcined for a regenerator space time of around 0.5h thus the $X_{out,RR}$ is close to 0 and the active Ca flow for capturing CO_2, $\dot{N}_{Ca,rec}(X_{max,Ave} - X_{out,RR})$ is maximized. The results are in accordance with those reported by Charitos et al [56]. In that work, the same facility (with the BFB as the regenerator) was used, while natural gas in combination with electrical heating was utilized to cover the regenerator heat requirements. The regenerator space time reported in that work was 0.4h in order to achieve almost full calcination. The similar values between the current work and that of Charitos et al [56] may be attributed to the presence of water vapor in both cases (in the latter case water vapor is generated through natural gas combustion).

It can generally be concluded that space times of 0.4-0.5h are viable for industrial applications and would lead to regenerators having an average solid residence time of 2.4-3min.
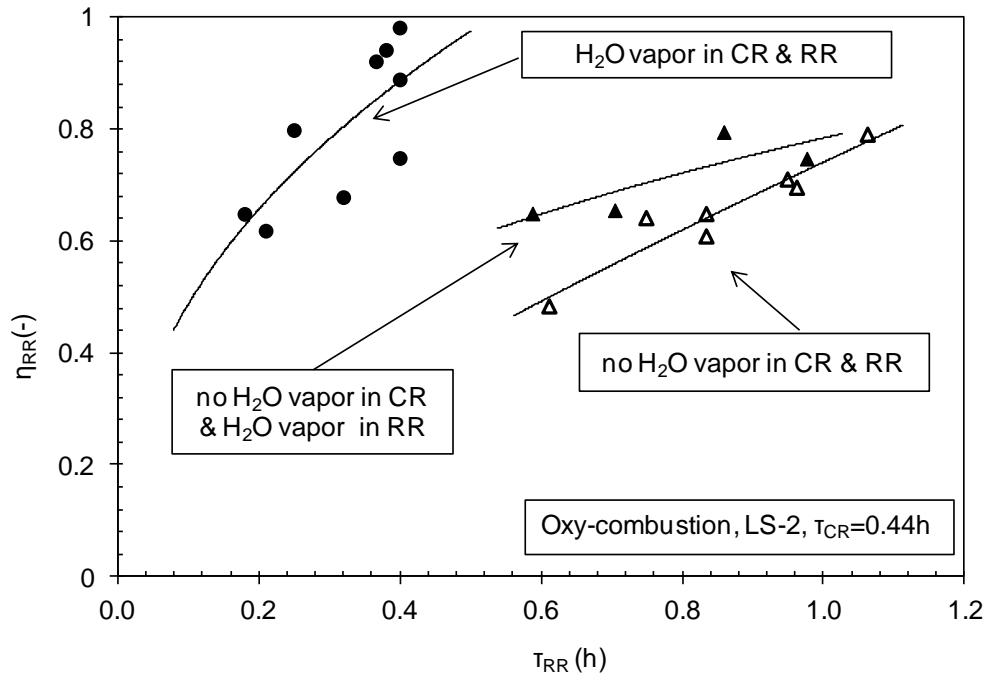
Figure 30: Regenerator efficiency vs space time for LS-2, Exp. conditions: CFB CR, T_{CR}=903K, $y_{CO_2,CR}$=10-16%$_{vol}$, $y_{st,CR}$=0 or 10%$_{vol}$, BFB RR, T_{RR}=1178-1193K, $y_{CO_2,RR}$=55%$_{vol}$, $y_{st,RR}$=0 or 25-35%$_{vol}$, $X_{max,Ave}$=0.12-0.25 [105]

4.8   Effect of water vapor presence on carbonation conversion

Figure 31 illustrates the evolution of chemical activity of the sorbent measured with a TG test and expressed as maximum CO_2 that can be captured at the end of the fast carbonation reaction regime. The metric used to interpret the results is the cycle number as per equation (17). The N_{theo} expresses the amount of times that the moles of CO_2 captured could carbonate the bed inventory $N_{bed,CR}$ up to its CO_2 carrying capacity, $X_{max,Ave}$ [56].
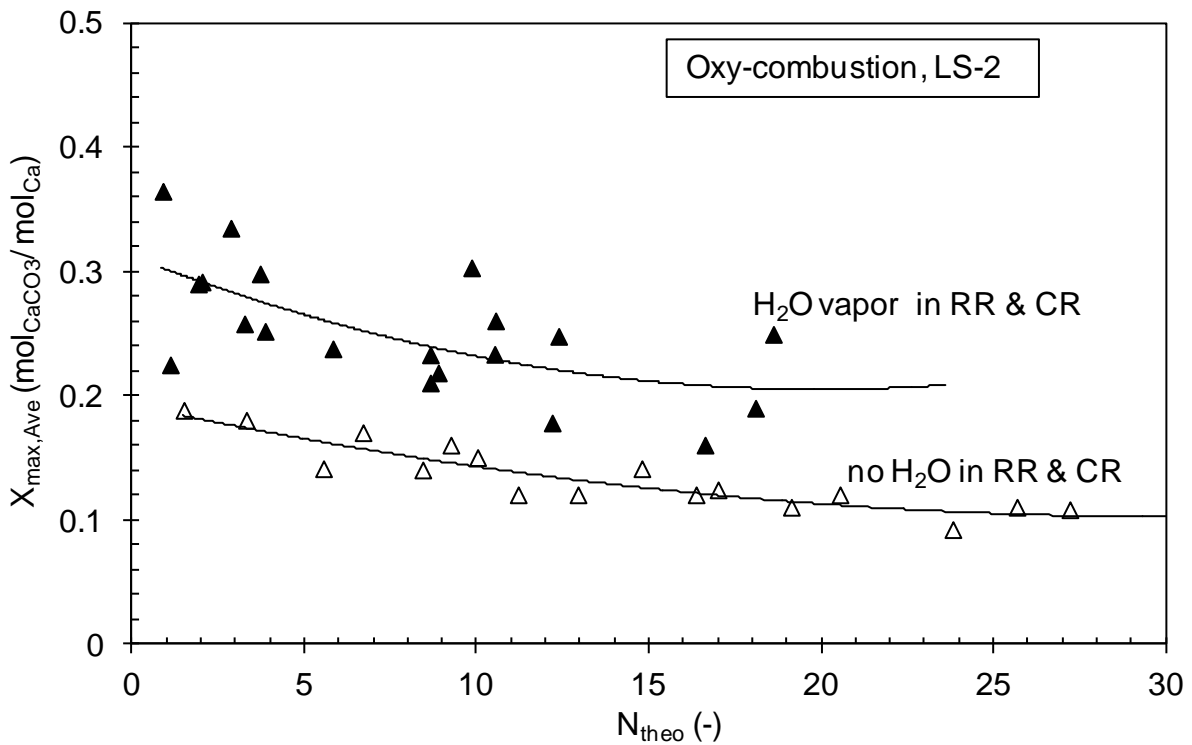
Figure 31: The evolution of the average maximum carbonation conversion vs the theoretical cycle number. Experimental conditions: CFB CR, T_{CR}=903K, $y_{CO_2,CR}$=10-16%$_{vol}$, $y_{st,CR}$=0 or 10%$_{vol}$, BFB RR, T_{RR}=1178-1193K, $y_{CO_2,RR}$=55%$_{vol}$, $y_{st,RR}$=0 or 25-35%$_{vol}$, $X_{max,Ave}$=0.12-0.25 [105]

As can be seen by Figure 31 the $X_{max,Ave}$ is a decreasing function of the number of cycles and a residual activity is achieved after more than 15 cycles. A clear improvement of the limestone activity is recorded when water vapor is present in both reactors. After 20 cycles with calcination taking place between 1178 and 1193K the activity of the limestone was measured to be more than 0.2 mol_{CaCO3}/mol_{Ca}, almost twice the value measured when water vapor is absent in both reactors. The results indicate that a change in the microstructure of the particles may have occurred, with a shift from smaller to larger pores with a more stable structure in agreement with the findings of [98], [108] and [102] as discussed in section 4.6. This would indicate that the particle pore size rather than the surface area, could be more influential in assisting the diffusion of CO_2 deeper inside the particle where there are still active CaO sites, thus increasing sorbent conversion [108]. Moreover, the results indicate that when steam is present in both calcination and carbonation stage a "synergistic" effect is established which is in accordance to the literature [143] that reports: (1) the positive role of microporosity in dictating sorbent accessibility and reactivity (due to water vapor presence in regenerator) and (2) the pronounced catalytic role of the water vapor presence in carbonator in enhancing CO_2 diffusion and capture regardless of the effects on the development of the pore structure. Unfortunately, these explanations cannot be confirmed for the experimental results presented in this study since no BET analysis of the relative samples is available.

Moreover, when water vapor is present less diffusion resistances are taking place thus more CO_2 is captured: this is depicted in the ($X_{out,CR} - X_{out,RR}$) values of the respective experiments which are measured to be around 0.35 for the case of wet carbonator and regenerator conditions (T_{RR}=1178K), while for the case where no water vapor was present in the carbonator and either was or was not present in regenerator (T_{RR}=1193K) the values were found between 0.07 and 0.12.

The previously stated finding is very important and justifies the significantly lower space times (0.44h) as well as low looping ratios (around 8) necessary for CO_2

capture of more than 90% at regenerator temperatures below 1193K and regenerator space times of around 0.5h.

Finally, it must be noticed that the $X_{max,Ave}$ values measured during these experiments are not higher than 0.4 mol_{CaCO3}/mol_{Ca} while theoretically using the expression of Grasa and Abanades [54] the highest value of $X_{max,Ave}$ should be around 0.7 mol_{CaCO3}/mol_{Ca}. This observation is in agreement with previous findings for both the 10 kW_{th} and the 30 kW_{th} facilities of University of Stuttgart and INCAR-CSIC [56]. These authors attributed this to the long pre-calcination stage of the limestone which was approximately the same for both facilities and in the range of several hours. During this work, the pre-calcination stage was also in the range of some hours. The sorbent was as well imposed for some hours in high temperatures until the facility was hydrodynamically coupled and the desired parameters were reached. The $X_{max,Ave}$ after pre-calcination was measured around 0.3 mol_{CaCO3}/mol_{Ca}.

4.9 Study of attrition phenomena

In a fluidized bed reactor limestone particles are subjected to attrition phenomena which are already investigated [68], [69], [92], [109], [110], [111]. In the context of the calcium looping process, particle attrition determines a net calcium loss from the circulating loop, as elutriate fines leave the cyclone with the gas stream. This loss of material adds to sorbent deactivation and contributes to the required makeup of fresh sorbent. Moreover, attrition adds to the change of the particle size distribution in comparison to the one considered for the design of the plant. This may cause operational problems since main operational parameters may need to be adjusted i.e. the velocity or the heat requirements. Even worse, equipment such as cyclones and filters may not be able to operate in design conditions. Thus, it is important to study the mechanical behavior of the sorbent in terms of particle size evolution as well as in terms of material loss.

4.9.1   Particle size evolution

In Figure 32 and Figure 33 the evolution of the initial particle size after 3 and 10 hours of operation is depicted for experiments performed in dry conditions for both reactors. The sorbents are collected from the carbonator and the regenerator outlet. It is generally found that the particles became smaller in the course of the experiment. In this experimental set up no difference was noticed between the particle size of the material entering and exiting the regenerator. This may occur because the regeneration takes place in a bubbling mode and the collision between the particles and/or the walls are less pronounced than in a turbulent fast fluidizing bed.

Moreover, as shown in Figure 32 after 10 hours of continuous operation the D10 of the particles is 125 µm. The D50 of the particles is around 275 µm and has proven to be adequate for a very stable and long-time continuous operation of the system. The particle shrinkage is confirmed through: (i) the material collected at the solids exit at the cyclones that are designed to keep particles larger than 75 µm (ii) the pressure drop of the reactors and (iii) the closure of the mass balance at the end of the experiments. This loss was measured around $0.8\%_{wt}$/h. This material loss would impose a makeup requirement of 0.024 mol/h fresh limestone for each mol/h CO_2 entering the carbonator.
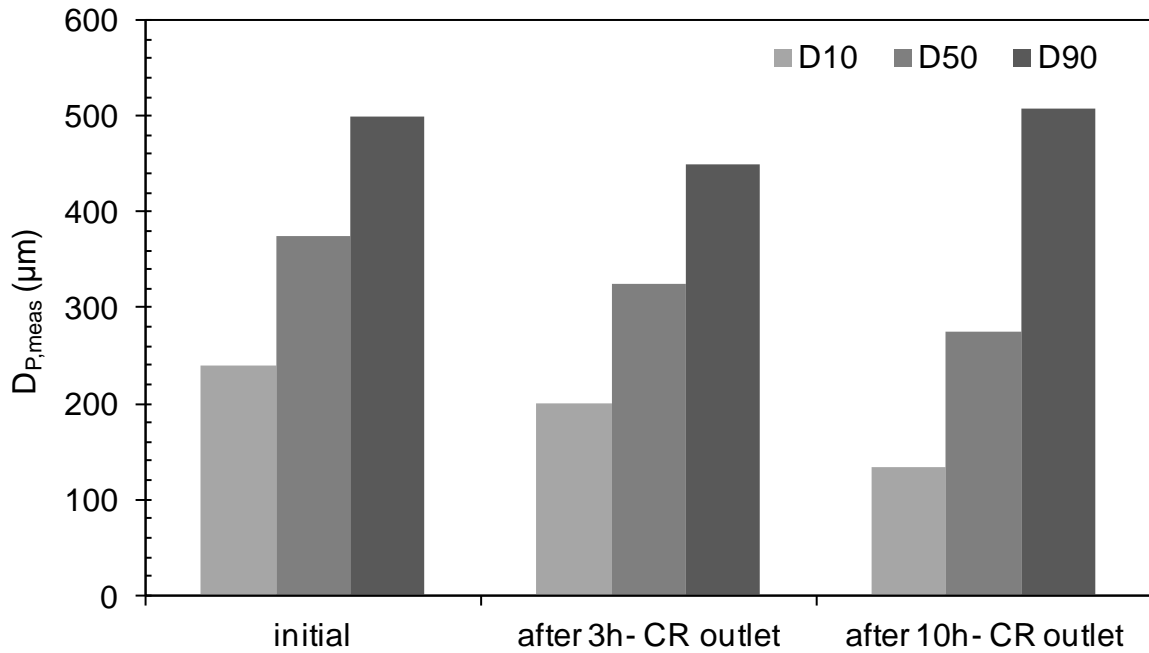
Figure 32: Particle size evolution for raw and carbonated LS-2 under dry conditions, and samples taken from CR outlet. Exp. conditions: CFB CR, T_{CR}=903K, $y_{CO_2,CR}$=14%$_{vol}$, BFB RR, T_{RR}=1178-1193K, $y_{CO_2,RR}$=53%$_{vol}$ [94]
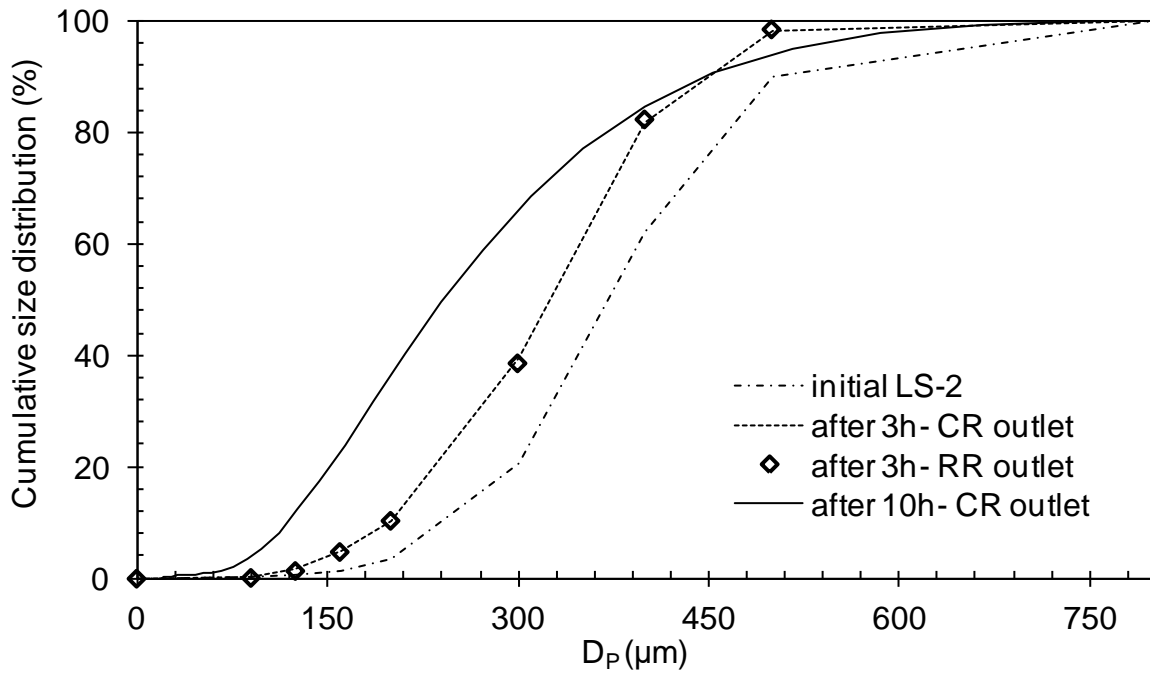
Figure 33: Cumulative size distribution for raw LS-2 as well as for carbonated and calcined samples taken from RR outlet and CR outlet under dry experimental conditions as per figure 32 [94]

4.9.2 Material loss and makeup demands

The material loss that is mentioned in this section is calculated on a mass basis of the total inventory of the DFB system.

In the presence of water vapor results show a significant increase of material loss in comparison to the loss under dry conditions. As depicted in Figure 34 this loss has been calculated around 4.78%$_{wt}$/h for experimentation under water vapor presence during both carbonation and calcination reaction (Case C). The same loss in terms of makeup needed to compensate the sorbent losses per mol introduced CO_2 to be captured, $\dot{N}_{MU} / \dot{N}_{CO_2,in}$ around 0.095 mol$_{Ca}$/mol$_{CO2}$ is depicted in Figure 35. This result indicates pronounced material softening thus particle breakage and fines production.
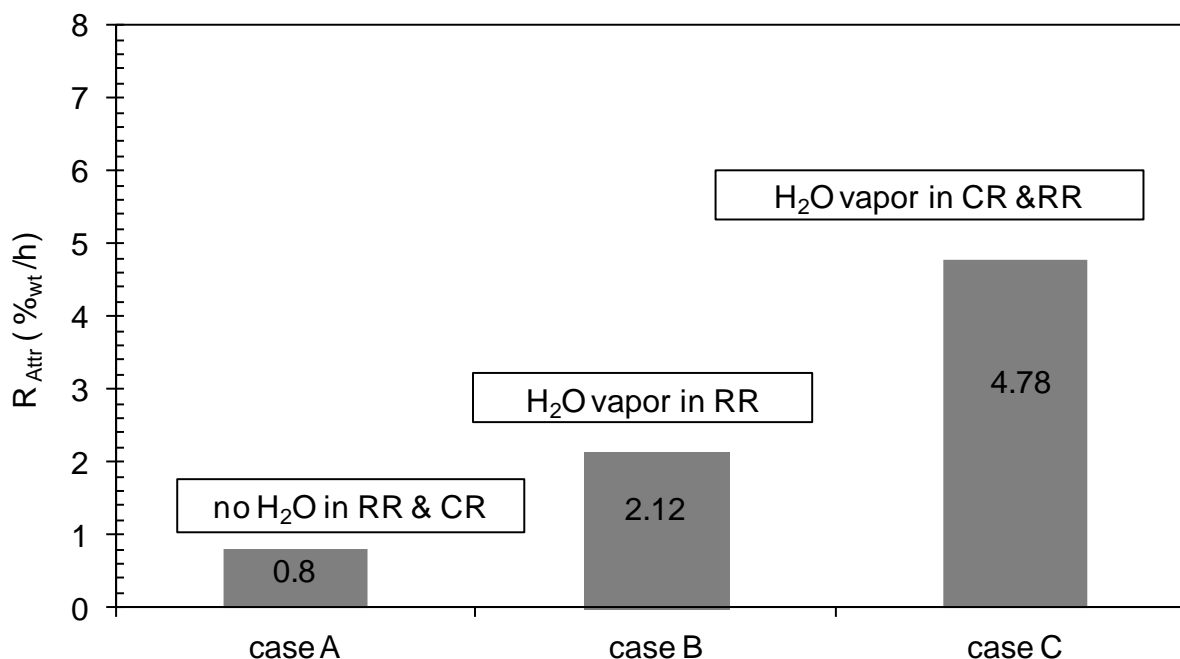
Figure 34: Comparison of material loss for LS-2 due to attrition for the dry conditions (Case A), wet conditions only in regenerator (case B) and wet conditions in both carbonator and regenerator (case C). Experimental conditions as per Fig 29. [107]

When water vapor is present only during regeneration (Case B) this amount was recorded to be around $2\%_{wt}$/h or 0.075 mol_{Ca}/mol_{CO2}. This behavior may have been caused by the presence of cold spots in the facility that could have led to $Ca(OH)_2$ formation. These cold spots may have taken place in the pipeline at the exit of the carbonator or in its first cyclone, although, no temperature measurements are possible in these regions to check if hydration conditions were met. On the other hand, oxy-fired conditions may favor mechanical stresses. These stresses may be pronounced by the fast CO_2 release during the calcination reaction. The structure of the particles becomes weak by the cracks caused by the calcination. Moreover, carbonation takes place in the riser operating under the fast fluidizing regime while calcination occurs at the bubbling fluidized bed reactor with low velocities around 8 times u_{mf}. The already weak structure is further mechanically stressed under the high velocities of 5 m/s in the riser and more than 20 m/s at the inlet of the cyclone thus causing such high material loss. These argumentations becomes stronger when considering the material loss with no water vapor presence. In that case, the amount

was very small and around $0.8\%_{wt}$/h or 0.024 mol_{Ca}/mol_{CO2} indicating the hardening mechanism of the particles as an outcome of sintering.

These losses are lower compared to the numbers reported in the literature, around $5\%_{wt}$/h and $2\%_{wt}$/h for previous lab and pilot scale DFB experiments respectively [8]. Literature mentions that the fines elutriation rate is relatively large after the first calcination and is decreased with the number of carbonation-calcination cycles, since the combined chemical-thermal treatment influences the particle structure making it increasingly hard [63], [131]. The presence of a high CO_2 concentration during calcination may have led to this low value of fines generation primarily due to the fact that the sintering hardens the particle surface [113] as well as the low calcination reaction rates, leading to lower internal particle pressures due to lower CO_2 diffusion rate. Another reason may be the pre-calcination of the material as well as the regeneration under low fluidization velocities.

Finally, it must be remarked that in this facility occasional blockages appeared which sometimes led to a facility shutdown. Most of the blockages happened at the 1st cyclone after the outlet from the riser. The phenomenon was less pronounced when water vapor was absent. Noted issues where encountered when water vapor was present especially during carbonation (CFB reactor). Facility shutdown was imposed when agglomerate build-ups that formed on the walls, were detached and caused closure of the exit of the cyclone and interruption of the facility operation. However, such a phenomenon can only occur in such small units (the cyclone exit diameter is 45 mm).
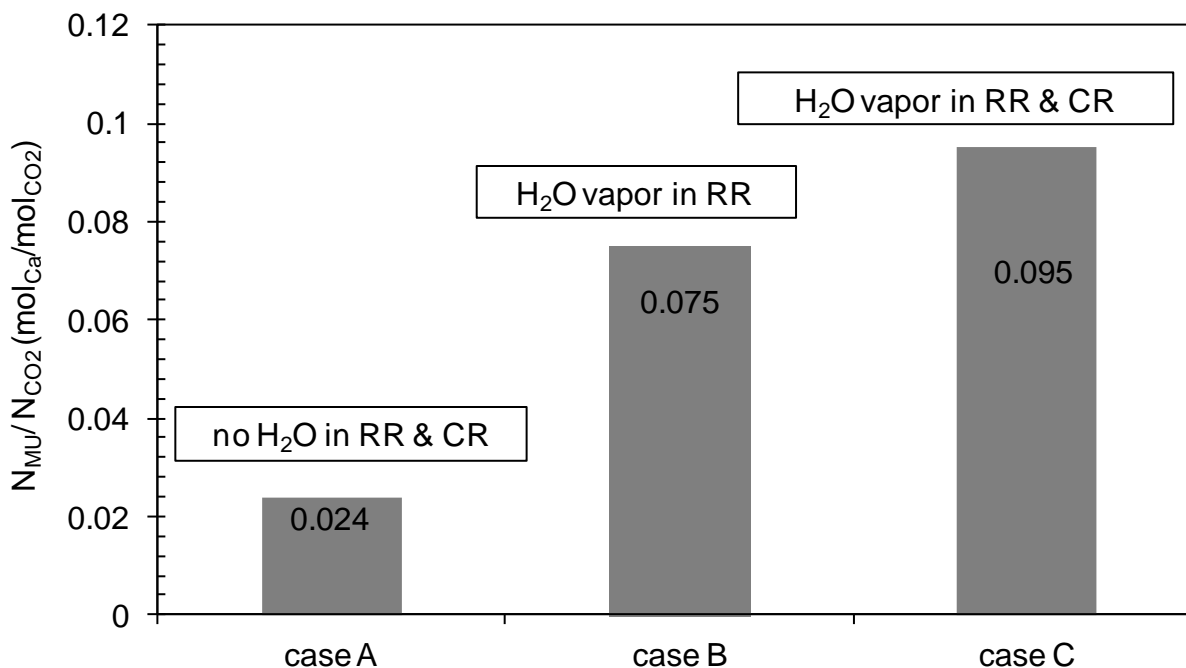
Figure 35: Makeup demands for dry conditions (Case A) and wet conditions only in regenerator (case B) and wet conditions in both carbonator and regenerator (case C), LS-2 [107]

4.10 System analysis by means of semi-empirical simplified models

4.10.1 General system carbon molar balance

The characterization of the reactors of the 10 kW$_{th}$ dual fluidized bed facility is based on the kinetic model of Alonso et al [76]. This model was utilised by Charitos et al [56] and Martinez et al [141] for the analysis of the carbonator and the regenerator respectively.

4.10.2 Regenerator reactor analysis

The efficiency of the regenerator is expressed by means of active space time and calcination reaction [81] as per equation (8). The definition for the efficiency (left side of the equation (23) is as per Charitos et al [56]. The equation results by combining equations 5-8. Moreover, the equation is valuable under the consideration that no continuous makeup is fed to the system which is true for the type of experiments that are used in this work.

$$1 - \frac{X_{out,RR}}{X_{out,CR}} = k_{Calc}\, \phi_{RR}\, \frac{N_{bed,RR}\, f_{Act,RR}}{\dot{N}_{Ca,res}\, X_{out,CR}} \left(\overline{y_{CO_2,eq} - y_{CO_2}} \right) \tag{23}$$

The left side of the equation expresses the CO_2 released from solids circulating between the reactors and is experimentally determined through thermogravimetric analysis of the samples. The right side of the equation expresses the calcination conversion of the inventory of the regenerator. It is calculated by using experimental data. The equality between the two sides of the equation (23) is met by applying a fitting constant, ϕ_{RR} and is depicted in Figure 36.

For case 1, with wet conditions in carbonator and regenerator, the apparent rate regenerator constant, $k_{calc}\, \phi_{RR}$ is 0.017s^{-1} (a fitting factor, ϕ_{RR} of 1.036 is applied). For case 2, with dry conditions in both reactors, the $k_{calc}\, \phi_{RR}$ is 0.011s^{-1} (a fitting factor ϕ_{RR} of 0.67 is applied). Since neither microstructural nor any kinetic analyses were performed a proved justification of the fitting factors cannot be provided. Nevertheless, this improvement may be related to water vapor presence that enhances heat transfer [118]. Moreover, water vapor may favor changes of the pore structure and specifically the shift from smaller to larger pores that are less accessible to pore blockages [98], [108]. However, more detailed investigations need to be performed for a better understanding of the mechanism. Lastly, an apparent kinetic constant of 0.012s^{-1} (fitting factor ϕ_{RR} of 0.78) is found for the case of wet

regenerator and dry carbonator conditions (case 3). This indicates an improvement of the performance due to the water vapor presence as derived by examining the other two cases.
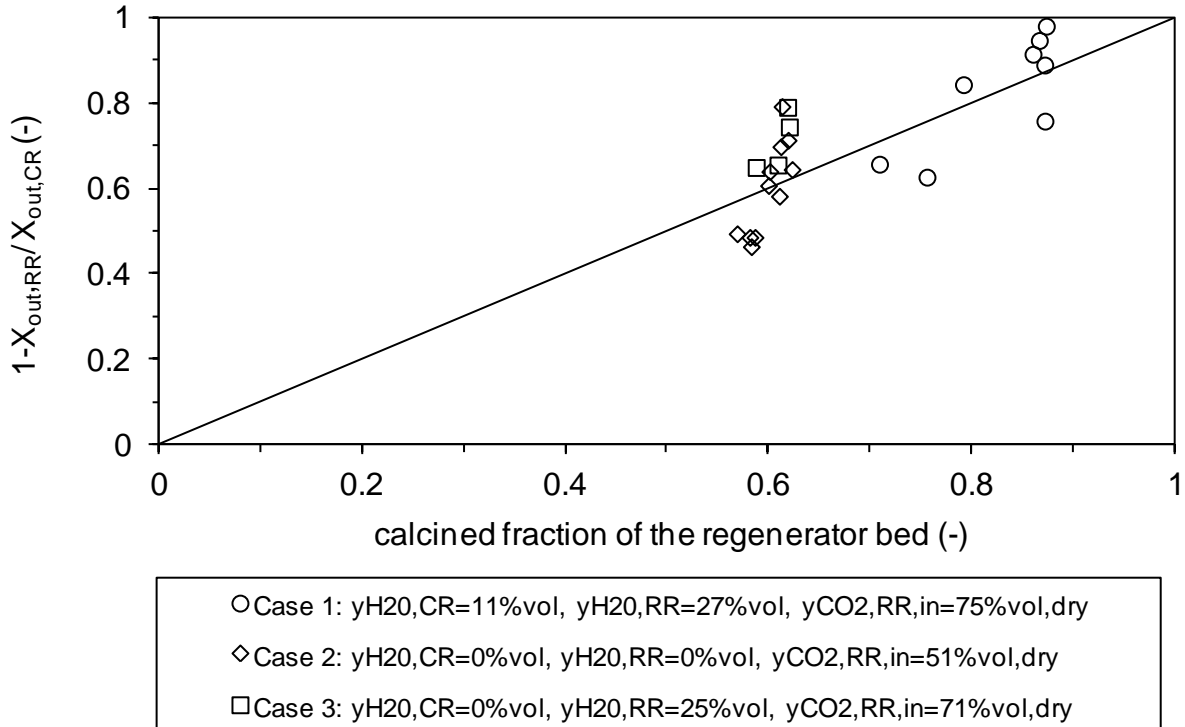
Figure 36: The calcined sorbent mass in the regenerator (x-axis) vs the calcination conversion of the solid flow circulating between the carbonator and the regenerator (y-axis) as per eq. 23 [112]

Figure 37 presents the regenerator efficiency in terms of calcination conversion versus the regenerator active space time. It can be seen that the experimental data lay very close to the applied model line. Besides, as expected, regenerator efficiency is an increasing function of active space time while reactor performance is optimized when water vapor is present in both carbonator and regenerator. For the specific experimental set up a regenerator active space time of around 0.11h is enough for complete sorbent calcination for the realistic case of water vapor presence in both carbonator and regenerator at a temperature of around 1178K and CO_2 average concentration of around 75% in the reactor. However, it should be noticed that this value is a viable one as it corresponds to solids residence

times in the reactor of not more than 3 minutes. These findings confirm the results from the La-Pereda Hunosa 1.2 MW$_{th}$ Ca-L pilot plant operation, where full sorbent calcination at temperature below 1223K is recorded [73], [25].
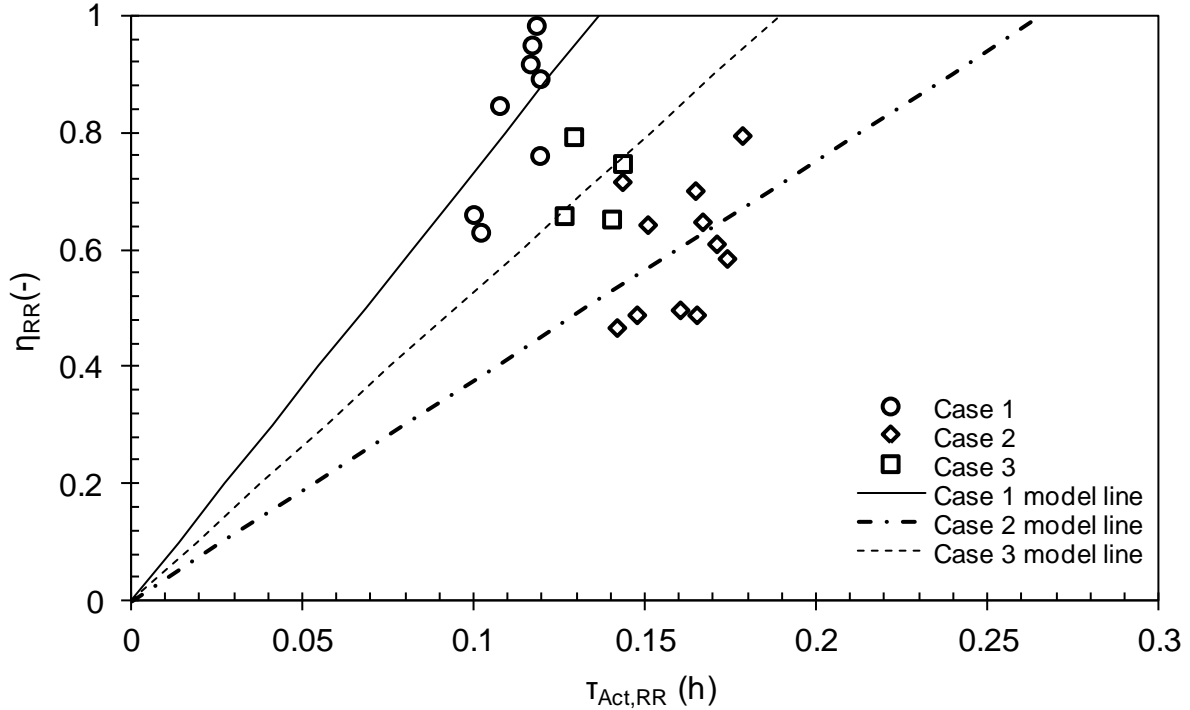
Figure 37: The regenerator efficiency vs. the regenerator active space time for the cases as per Fig. 35 and τ_{CR}=0.44-0.66h. Model lines as per equation (8) and T_{RR}=1178K, $y_{CO_2,RR}$ =51-75%$_{vol,dry}$ [112]

4.10.3 Regenerator efficiency characterization by means of active space time

In Figure 38, the regenerator efficiency is plotted vs. the active space time for a mean CO_2 volumetric concentration of 50%, for two different values of temperature. It is obvious that in this environment with high partial pressure of CO_2 concentration the regenerator efficiency is an increasing function of the active space time and the temperature. For this bubbling electrically heated regenerator a minimum active

space time of approximately 1.2h (average solids residence time of around 7min) is required to achieve a regenerator efficiency of more than 70%, while the efficiency is not drastically increased at 1193K. This indicates that for a specific type of lime by changing the carbonate content of the solids and the residence time the optimum point can be set for high regenerator efficiencies, which reveals that the particles delivered to the carbonator have little to none carbonate content so the available CaO to capture CO_2 is maximized.
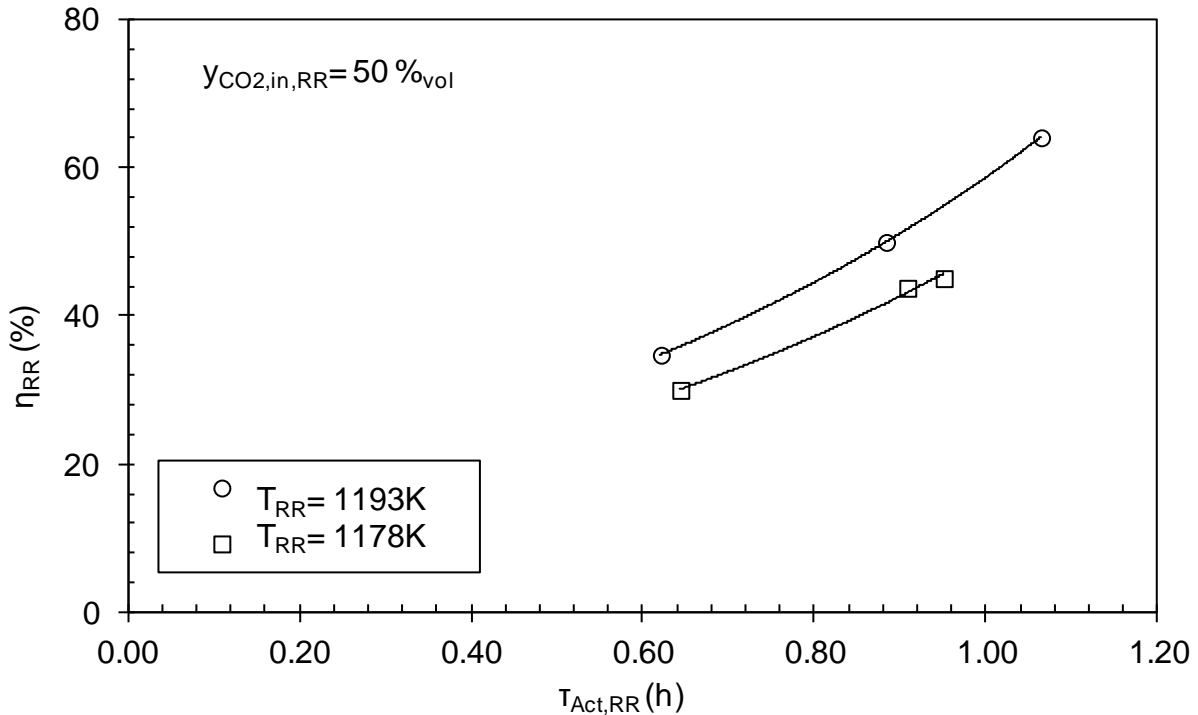
Figure 38: The effect of active space time and temperature on regenerator efficiency in absence of water vapor [90]

In Figure 39, the effect of the CO_2 concentration on the regenerator efficiency is depicted for a temperature of 1193K, for two different active space time values. As expected, the higher the partial pressure of CO_2 during sorbent regeneration is, the lower the regenerator efficiency will be. For this reactor there is a critical active space time of 1.35h (respective solids residence time of around 8min) for which the partial pressure influence appears to be minimized and the efficiency achieved is more than 80%. This finding is important as it indicates the optimum operational conditions for this facility in order to reach almost full calcination. Nevertheless, these values should

be treated only qualitatively because of the specific facility design that imposes limitations on the calcination reaction (see section 4.10.4 and Figure 40).
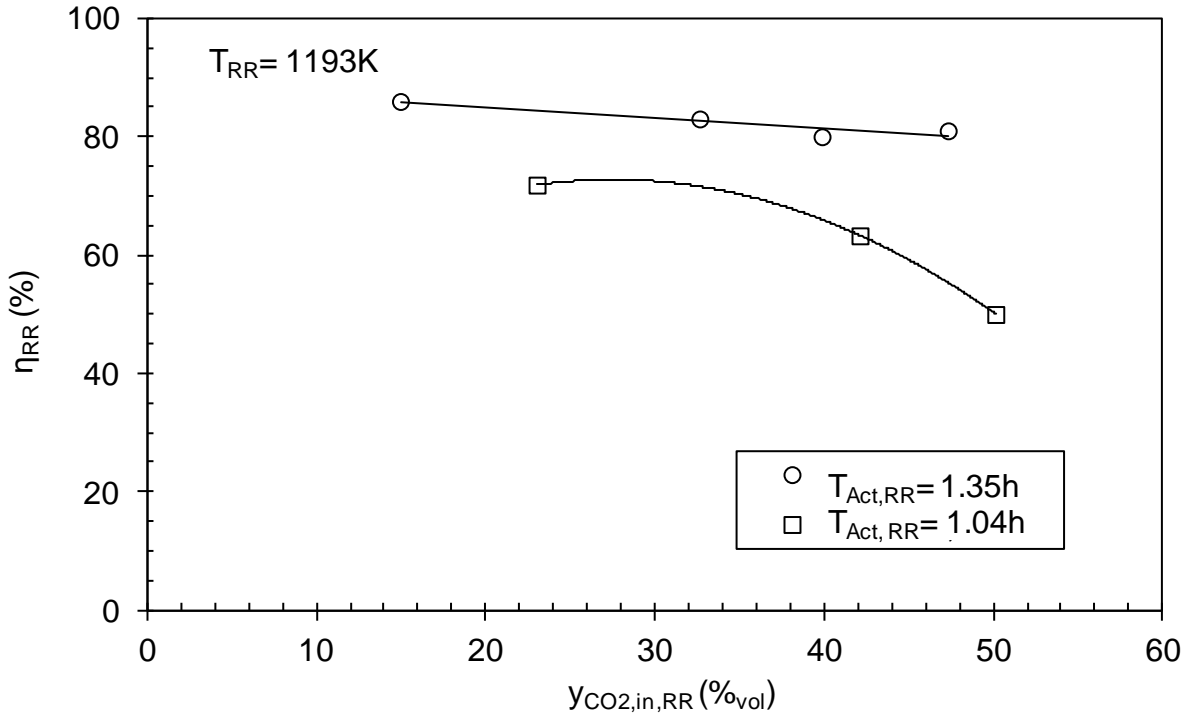
Figure 39: The effect of CO_2 volumetric concentration on regenerator efficiency under dry conditions [90]

4.10.4   Limitations of the maximum regenerator efficiency

Figure 40 indicates that the maximum efficiency achieved in the DFB facility was not more than 90% regardless of the reactor load. In this figure, the efficiency is plotted vs. the active space time. It is observed that high residence times in the range of minutes (5-8min) thus resulting in high active space times in the range of h are required to calcine the solid flow entering the regenerator. This calcination time is much higher when compared to the literature where calcination is completed within some seconds i.e. in TG experiments [61], [77], [100]. This phenomenon may be relevant to the fluidization of the bed mass. It seems that the bubbling bed with low velocities results in low heat and mass transfer coefficient as well as gas-bypassing through the bubbles allowing higher local partial pressures of CO_2 in the emulsion phase where actual calcination takes place. This explains the fact that even with low

measured mean CO_2 concentrations around 25%$_{vol,dry}$ and temperatures as high as 1193K the calcination is not completed independent of the active space time. Another reason can be the quality of heat provided through the electrical heaters where the heat is transferred from the outside source inside the bed and not generated in the bed as when combustion takes place. In this case, the heat transfer rate is low enough allowing for temperature differences in the different areas of the bed as well as in the particle itself. A justification for this assumption can be seen in Figure 40, where by increasing the overall temperature, the efficiency increases. An additional explanation is related to the particle size, since literature reports resistances on the reaction that can be imposed with increasing the particle size [100] which for the used lime in these experiments was between 150 and 450 μm (D50=325 μm). To conclude, the above mentioned factors control the calcination reaction in our test rig which justifies the high solids average residence time (5-8min).
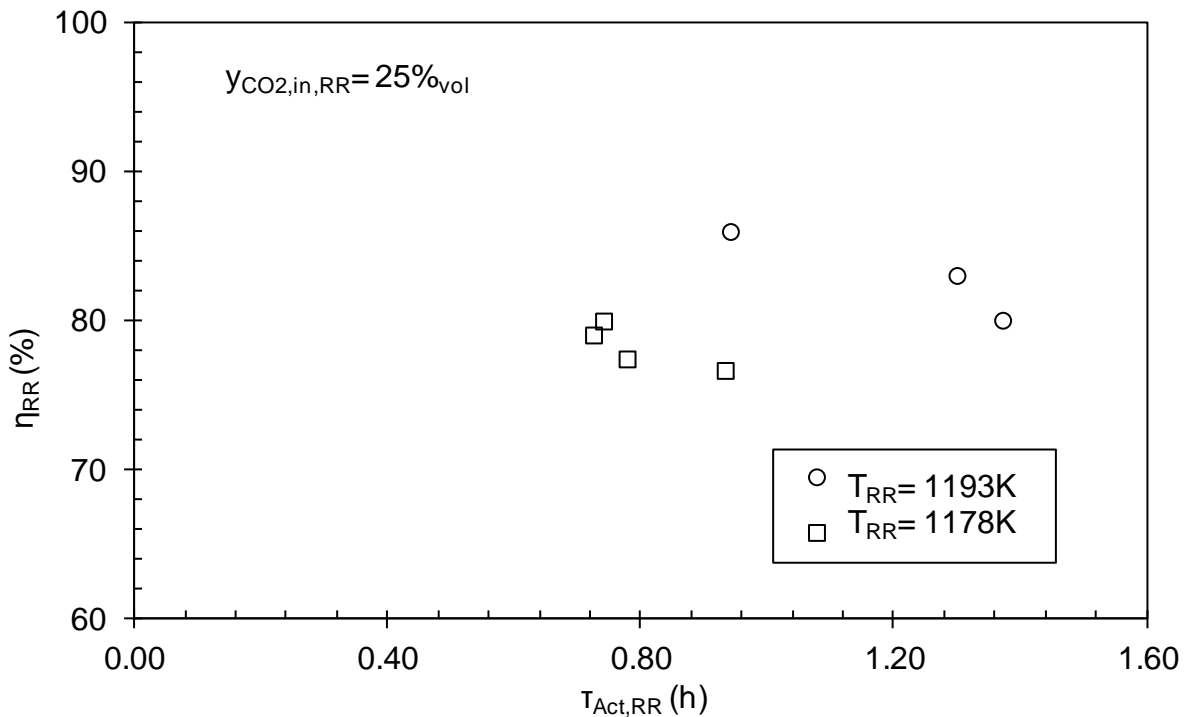
Figure 40: Limitations of the facility related to the achievable regeneration efficiency under dry conditions [90]

4.10.5 Carbonator reactor analysis

The carbonator analysis will be performed following the same approach as for the regenerator. Combining equation (2) (with the simplification that no continuous makeup is fed to the system, as per our experiments) and equation (9) the equality between carbonated inventory of the carbonator and CO_2 in the solid phase circulating between the carbonator and the regenerator is expressed by equation (24).

$$\xi_{CaL} \left(X_{out,CR} - X_{out,RR} \right) = k_{Carb} \ \phi_{CR} \ \tau_{CR} \ f_{Act,CR} \ X_{max,Ave} \ \left(\overline{y_{CO_2} - y_{CO_2,eq}} \right) \tag{24}$$
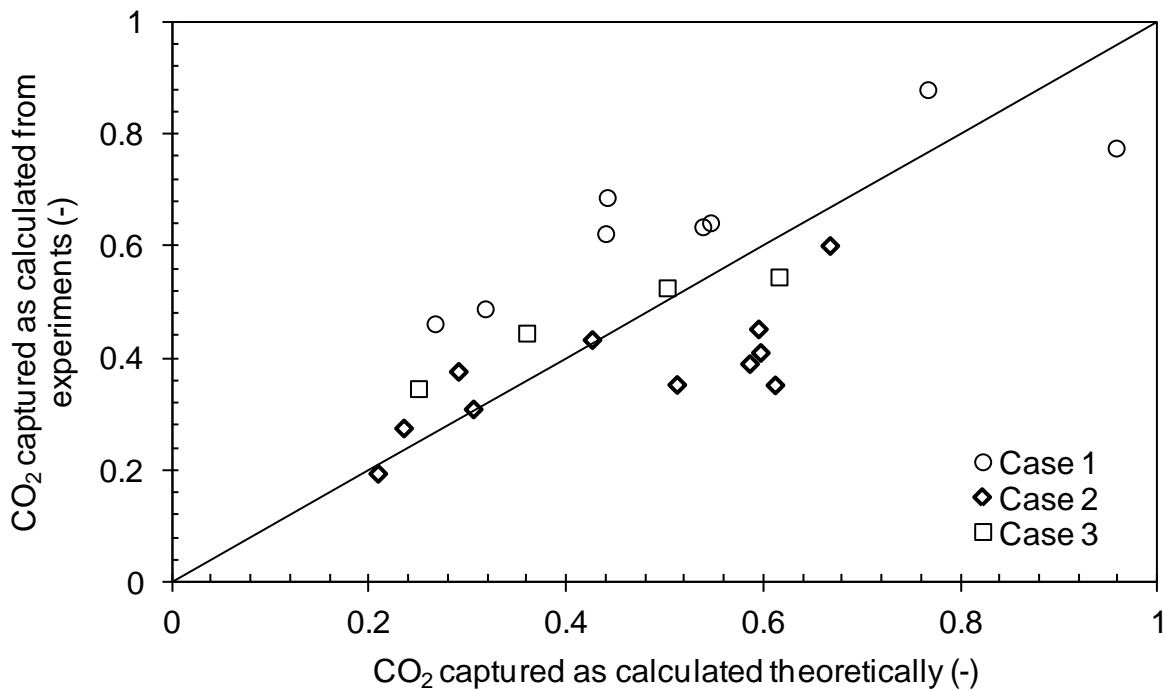
Figure 41: The CO_2 captured/ disappeared from the gas phase (y-axis) (left side of eq. 24) versus CO_2 captured by the carbonator inventory (x-axis) (right side of eq. 24) (cases as per Figure 36) [112]

Figure 41 depicts the carbonated inventory of the carbonator reactor (right side of equation (24)) on the x-axis and the carbonate content of the solids

circulating between the reactors as per left side of equation (24), on the y-axis. The data result by applying a fitting factor as per the methodology used by Charitos et al [56], Rodriquez et al [89], Diego et al [115] and Arias et al [25]. It can be seen that all data are close to the 45° line showing a good agreement between the two expressions of the CO_2 captured. The kinetic constant, k_{Carb} of the used limestone is calculated by thermogravimetric analysis and is around 0.33s^{-1}.

Using equation (24) and in order to fit the data, significant differences of the fitting factors are found between the studied cases. For the case of water vapor presence in both reactors (case 1), the apparent reaction constant, $k_{Carb}\phi_{CR}$ is found to be 0.68 s^{-1}, which is much higher than the respective 0.22s^{-1} at dry case 2. The fitting factor, ϕ_{CR} for the first case is 1.71 indicating a very good gas solid contact and an enhanced conversion. According to the literature this improved conversion may be due to the enhanced diffusion in the product layer [105]. The reaction rate constant at the kinetically controlled regime is not influenced by steam presence [54] and thus the enhanced conversion cannot be attributed to such a phenomenon. Additionally, Arias et al [116] showed that the carrying capacity of the sorbent depends on the experimental conditions if the sorbent is allowed to react under the slow diffusion controlled regime. Moreover, they proposed for the CO_2 carrying capacity of the sorbent, the expression of equation (25), where N is the carbonation-calcination cycle number, k_{Deac} is the limestone deactivation constant and X_{Resi} is the residual conversion after an infinite number of cycles, refer to Grasa and Abanades [54].

$$X_N = (\frac{1}{\frac{1}{1-X_{Resi}} + k_{Deac}N} + X_{Resi})(1 + k_{diff}) \tag{25}$$

Following this argumentation and considering the simplistic consideration that the diffusion regime enhances the CO_2 capture by a factor of ($1 + k_{diff}$), equation (27) can be formulated as follows:

$$\eta_{CR} = \phi_{CR} \; \tau_{CR} \; k_{Carb} \; f_{Act,CR} \; (1 + k_{diff}) \; X_{max,Ave} \; (\overline{y_{CO_2} - y_{CO_2,eq}})$$ (26)

$$\tau_{CR,kin,diff} = \tau_{CR} \; k_{Carb} \; f_{Act,CR} \; (1 + k_{diff}) \; X_{max,Ave}$$ (27)

By using equation (26), actual experimental data and predicted ones fit well by applying fitting factors. These constants include the various sources of experimental and measurement errors as well as the effect of the diffusion regime.

When examining the case where no water vapor is present in both carbonator and regenerator, a fitting factor ϕ_{CR} characteristic of the gas-solid phase contact of 0.68 is applied. This experimental data indicates no influence of the diffusion regime on the CO_2 capture, which is in agreement with the literature reporting under the same conditions no improvement of the CO_2 carrying capacity in absence of water vapor. In contrast, when water vapor is present during regeneration the fitting factor ϕ_{CR} is slightly raised to 0.80. Since the conditions in the carbonator are the same as for the dry case, it is assumed that the increase is a result of the ability of the lime to capture more CO_2. This is reported in the literature and is attributed to the fact that the lime calcined under water vapor and high CO_2 partial pressure is characterized by a shift towards the larger pores and thus a more stable pore structure and a greater surface area is available for CO_2 capture [108]. Nevertheless, the difference between the apparent kinetic constant of these two cases is not significant and can be attributed to the various sources of the experimental inaccuracy. Thus no conclusion can be derived with regard to the positive effect of the water vapor presence in the regenerator on the CO_2 capture in the carbonator.

Figure 42 depicts the plot of the carbonator efficiency versus the active space time both as predicted by equation (15) (line) as well as from the experimental data (single points). This diagram also includes a line (ref case) predicting the CO_2 capture efficiency as reported by the literature for an air-fired regenerator with CH_4 combustion and under dry conditions at the carbonator [56]. For cases 2 & 3 one model line is depicted since the difference in the apparent reaction constant is not

significant. It can be seen that under conditions more close to the industrial ones, with water vapor presence in both carbonator and regenerator, for a CO_2 capture of more than 90% a carbonator active space time of around 30s is required (case 1).

In order to evaluate the effect of limestone, a comparison can be performed with the one of the reference case [56]. Besides, a relatively high impurity limestone used for the reference case would require almost 40% more active space time as the one of high purity, used under the same conditions (case 2). Nonetheless, it should be considered that this difference is also attributed to the different CO_2 inlet concentrations since it is known that the carbonation as a first order reaction, with respect to the CO_2 partial pressure, influences the carbonation reaction rates [117].
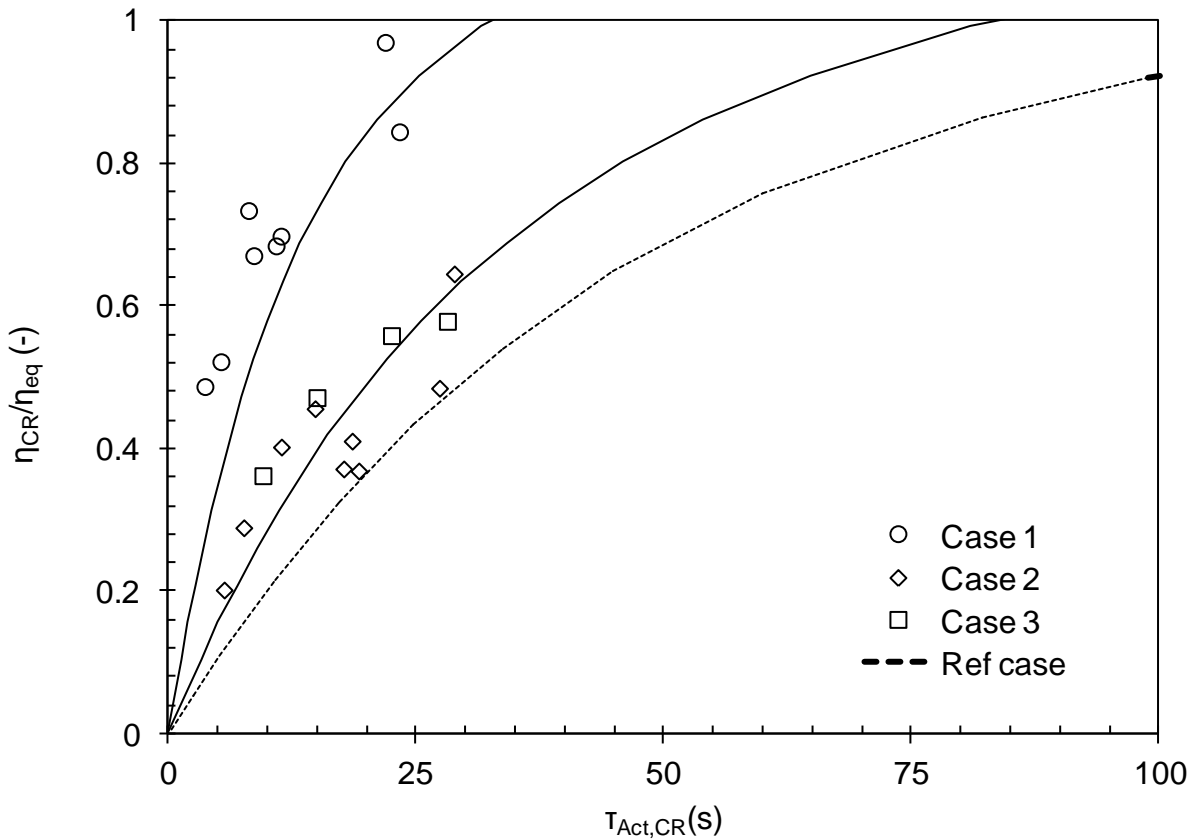
Figure 42: The equilibrium normalized CO_2 capture as measured and as predicted versus the active space time. Model lines: T_{CR}=903K, $y_{CO_2,in,CR}$=15.6(Case1,2&3)-11.4(Ref case)%$_{vol,dry}$ (cases as per Figure 36) [112]

4.10.6 Evolution of particle size by using the model of Cook et al

By solving equation (22) and using the experimental data, the overall attrition rate constant is found to be $3.4×10^{-4}$ $m^2/(kgs^3)$ for case 1 (wet carbonator and regenerator conditions) and case 3 (dry carbonator and wet regenerator conditions) and for case 2 (dry carbonator and regenerator conditions) $4.4×10^{-4}$ $m^2/(kgs^3)$. It must be considered that Figure 34 reports higher attrition rate for case 1 and 3 compared to the attrition rate for case 2. This is not consistent with these attrition rate constants and may be contributed to possible errors during sampling related to the sampling position. For cases 1 and 3 no major differences were observed for the particle size measured after the carbonator and the regenerator (particle size measurements of case 2 for the regenerator are not available). In comparison to the overall attrition rate constants mentioned in the literature, $1.26×10^{-4}$ $m^2/(kgs^3)$ and $4.53×10^{-4}$ $m^2/(kgs^3)$ [93] and $5.27×10^{-4}$ $m^2/(kgs^3)$ [95], the limestone LS-2 used in these experiments seems to be a relatively hard one.

This is a result considering following differences in the experimental conditions, as well as in the limestone itself: (i) the limestone used has a much bigger initial mean particle size (around 400 µm) than the one used in the mentioned literature (178 µm-133 µm) [93], (ii) literature refers to velocities of 2 m/s [93], which is much lower than the 4.5-5.5 m/s implemented in the carbonator of this work. On the other hand there was a much lower velocity, around 0.3 m/s, in the regenerator.

Figure 43 depicts the good agreement between the particle size as predicted by using equation (22) and the particle size measured by samples taken from the facility, for both the carbonator and the regenerator. It should be noticed that the samples are taken after exit of the reactors at the upper and lower loop seal (see position 4 and 7) [90]. For technical reasons, this is the only possibility at the facility to extract the samples. Undesired effects such as additional mechanical stresses due to the velocity imposed by the cyclone geometry as well as possible sorbent hydration,

may have changed the particle size after the exit of the reactors. These phenomena are reported and discussed in detail in [105].
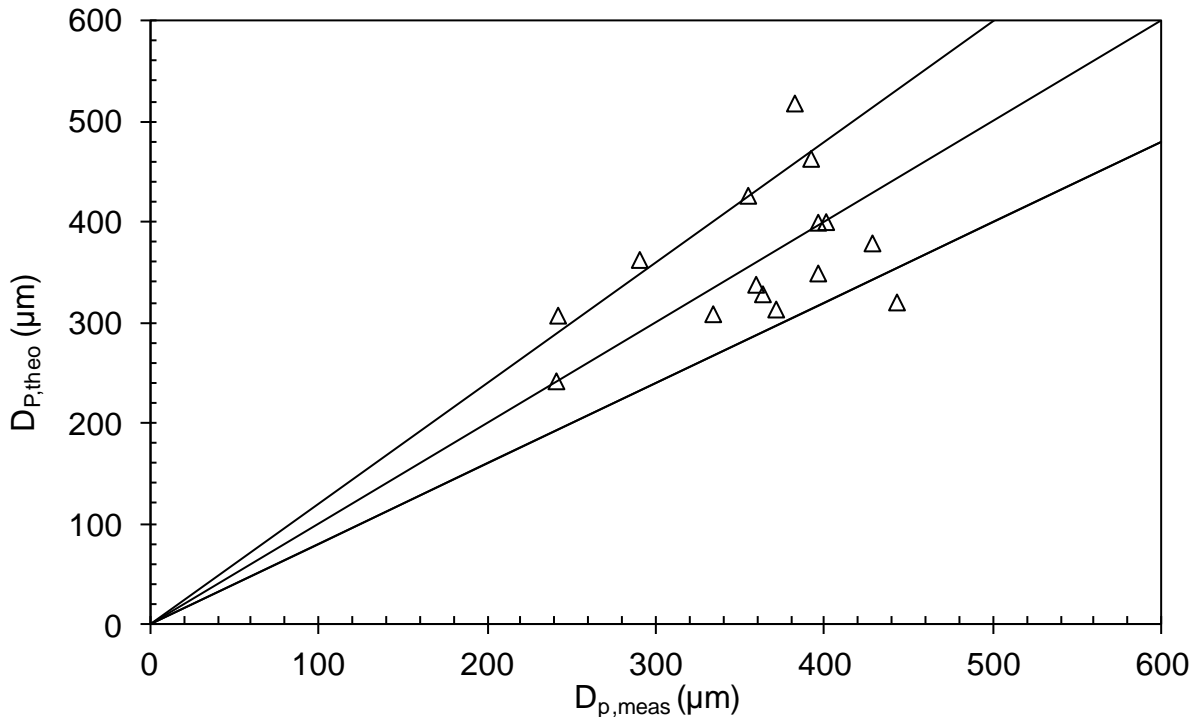
Figure 43: The mean particle size as predicted by applying equation (22) on the experimental data (y-axis) and as measured (x-axis), for LS-2 and for all cases as per Fig 35 [112]

Figure 44 shows for both carbonator and regenerator the evolution of the particle size over the course of the process as measured during experimentation. The predicted size evolution as per equation (22) is also given for the circulating fluidized bed operating under the kinetically controlled carbonation reaction regime. In line with equation (22) the decrease of the attrition rate with time indicates rounding of the sorbent particles whose surface is irregular as they enter the system. This results in a relative high rate of initial particle degradation during which the particles break and their edges and asperities are knocked off. With progressing time particles become smaller, rounder and smoother and the number of their weak points decreases. The elutriation rate, therefore, decreases continuously with time and

tends to a more or less constant value which can be interpreted as some kind of a steady-state level where only abrasion takes place [67], [68].
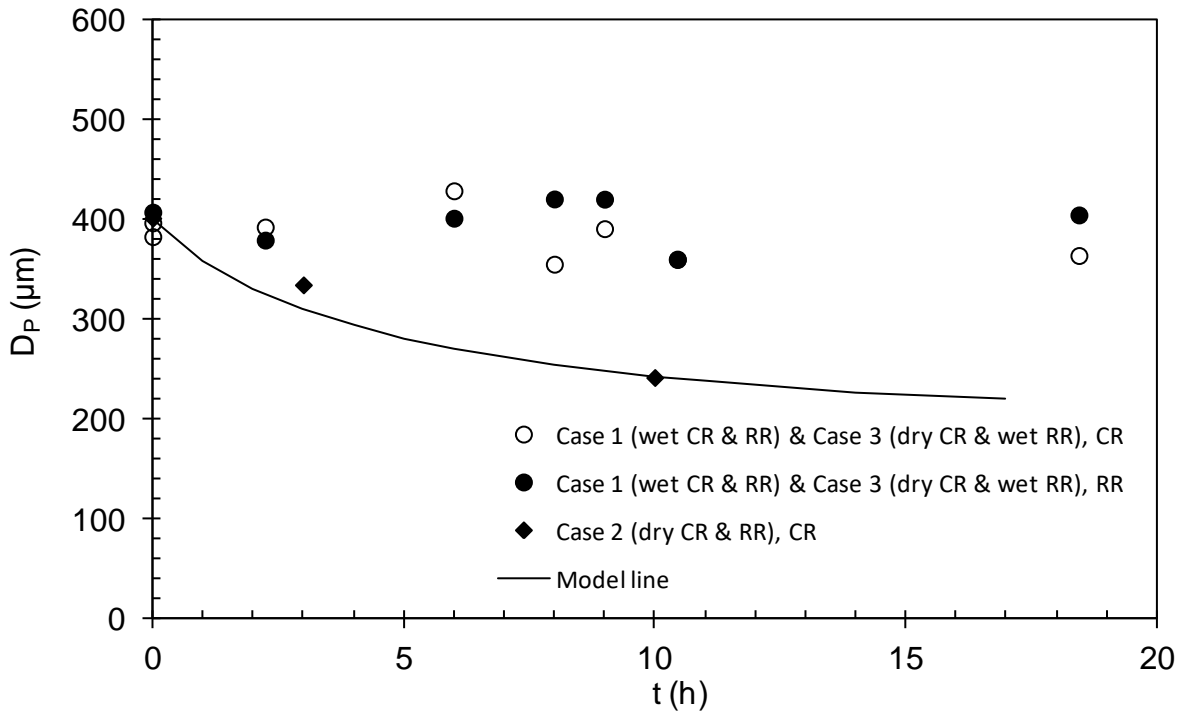
Figure 44: The evolution of the mean particle size for both carbonator and regenerator for cases as per Fig 35. (as per Fig 34: case 1=case C, case 2=case A, case 3=case B) Model line as per equation (22): D_{P0} =401 µm, D_{Pmin} =200 µm, $u-u_{mf}$ =5.35 m/s [112]

This behavior is also presented by Gonzalez et al who conducted experiments with continuous dual fluidized bed operation under similar experimental conditions [93]. Nevertheless, from our experiments this behavior can be only seen in the data of case 2. For the other two cases 1 and 3 the mean particle size is remaining unchanged for almost 20 hours of operation as depicted in Figure 44. It is fact that during the experiments most of the fines were created just when steam or fresh material was introduced in the system. However, when comparing the results reported in Figure 34 and 44 there is an indication that the particle size measured from the samples taken may not be representative of the particle size in the reactors.

For the specific set up of case 2, after 10 hours of operation, a mean particle size of around 241 µm is recorded, equivalent to a reduction of 39.9% of the initial

particle size. Gonzalez et al [93] mentioned a decrease of around 38.5% of the initial mean particle size after around 10h of operation and for velocities of 2 m/s for both reactors. It should be pointed out that during our experiments no fresh limestone was introduced in the reactor but after several hours of calcination under bubbling fluidization conditions CaO is added to the system. This fact may have caused absence of primary fragmentation [92] thus the rate of degradation is lower as the one reported by the literature [93]. On the other hand, the precalcined lime is relatively sintered thus harder while the fine particles are removed at the pre-calcination stage. Moreover, for cases 1 and 3, it has to be considered that the amount of fines collected by the cyclones was increased in comparison to case 2 and more intensive under wet carbonation. Additionally, 10% of the distribution of the particles were below 100 µm indicating that no fines were circulating in the facility under the consideration that the cyclone can keep particles greater than 50 µm.

Lastly, this subject should be further investigated in detail mainly in the already available pilot plant facilities. A great advantage of these facilities is their ability to operate in continuous mode for many days. Additionally, more reliable data for design purposes can be delivered since they can operate without simplifications such as absence of sulfur, char, ash accumulation, sorbent makeup.

5 Conclusions and Outlook

5.1 Conclusions

The calcium looping process has been realized at a 10 kW_{th} continuous dual fluidized bed facility at University of Stuttgart. The effect of main process parameters i.e. reactor temperature, mass and system circulation rates between the regenerator and the carbonator on CO_2 capture/ release efficiency was examined. The space time and the looping ratio were the metrics used for the interpretation of the results. For different cases the deactivation of the sorbent CO_2 capture capacity was measured with use of a thermogravimetric analyzer. Furthermore, the mass loss was recorded during the experiments and the evolution of particle size of samples was measured by a Malvern analyzer.

The results prove the feasibility of the calcium looping process with CO_2 capture efficiencies of more than 90% for process conditions closer to those expected industrially, i.e high CO_2 concentration, water vapor presence in both carbonator and regenerator, fluidization conditions, continuous operation and simultaneous carbonation/ calcination reaction. The data hereto presented, is of high quality as the trends observed are in good agreement with previous works reported by Charitos et al [8] and Rodríguez et al [89] performed under diverse conditions and in different facilities.

For the oxy-fired case, the carbonator CO_2 capture efficiency is found to be an increasing function of the sorbent flow entering the carbonator (looping ratio) and the bed inventory (space time). On the other hand, CO_2 capture efficiency is decreasing with increasing temperature, as expected from the equilibrium. The regenerator efficiency is revealed to be a decreasing function of the carbonate content of the incoming solids flow and an increasing function of the sorbents residence time and temperature.

The results also demonstrated that the water vapor presence enhances significantly both calcination and carbonation reaction. Thus for a certain bed inventory the necessary solids circulation rate is decreased. This is an important finding and a great advantage for the viability of the calcium looping process. Circulation rates expressed in terms of looping ratios of not more than 8 are proved enough for CO_2 capture efficiency of more than 90% while the required regenerator temperatures were not more than 1193K. In these terms, a great saving in energy demand results from lower circulation rates and bed inventory that need to be heated up and calcined. This improvement can be explained as a product of the changes that occur in particle morphology (likely shift from smaller to larger pores) when calcination takes place in presence of water vapor and high CO_2 partial pressure [98], [108]. The altered pore structure favors both CO_2 capture and release.

The limestone chemical activity decays and achieves a residual activity of around 10%. For the first time, it is shown that due to water vapor presence in the carbonator and the regenerator, the residual activity is maintained at higher levels of around 20%. This result is a further proof of the improvement of the process in presence of water vapor. The measurements and findings of attrition revealed significant material loss of up to 4.75%$_{wt}$/h related to the total system inventory and intensive system blockages due to water vapor presence in both reactors. Oxy-fired conditions enhanced mechanical stresses of the material which are mainly pronounced by the fast CO_2 release of the enhanced calcination reaction as well as the high velocities of the fast fluidization conditions during carbonation.

This study proves the feasibility of the basic process conceptual design. Even so, when considering process scale-up the results presented should be treated qualitatively since no combustion took place at this experimentation thus the calcination reaction as well as the sorbent chemical activity-structure may have been affected (electrical heaters were used and only for the high temperatures supplementary CH_4 combustion took place). Moreover, combustion may lead to faster calcination due to better heat transfer, however, local high temperature may cause pronounced sintering which may lead to further decay of the activity as

recorded here and hardening of the sorbent. Finally, additional stresses that are imposed by the dimensions of this facility (high values of diameter to surface area) are expected not to be present to the same extent at a pilot or full scale plant.This implies the elutriated mass may be lower as the one recorded here.

In addition, both reactors as well as limestone attrition behavior were analyzed by implementing already published semi-empirical simplified models. A good agreement between the predicted and the actual data is shown. The main design parameter of active space time is found to be around 30s and 0.11h for the carbonator and the regenerator respectively, with CO_2 capture and release efficiencies of more than 90% and for the realistic case of wet carbonator and regenerator conditions under high partial pressure of CO_2. An increased apparent kinetic constant was calculated for the case where water vapor is present in both carbonator and regenerator indicating a "catalytic" effect of the water vapor on CO_2 diffusion across the product layer. Besides, the evolution of the mean particle size of the limestone is found to remain almost unchanged which might result from limestone pre-calcination. The overall attrition rate constant was found to be around 4.4 $m^2/(kgs^3)$ for conditions more close to the real ones indicating a relatively hard limestone. However, the progress of attrition should be treated qualitatively and not quantitatively for the reasons discussed in section 4.9.2 and 4.10.6.

5.2   Outlook

Calcium looping may be beneficial for a sustainable development of the economies complying with a low carbon dioxide emission strategy. For studying the process, pilot plants are built up to the scale of 1.7 MW_{th} where CO_2 from either real or simulated flue gas is successfully captured up to more than 90%. Scientific groups worldwide identified most of the critical parameters and their values for a feasible design and a viable operation of a plant including a calcium looping unit. The work presented in this monograph adds further value in this direction.

First of all, the work presented here validates the results of previous works performed in the 10 kW$_{th}$ facility at University of Stuttgart. Trends found in this study are in agreement with previous research. This verifies the suitability of the chosen methodology for performing experiments, sampling and analysis as well as interpretation of the results. This work points out the need to optimize the tools and standarize the methods used for the sorbent chemical and mechanical characterization. Moreover, constraints of the current facility installations are revealed. These limitations should be taken into account in the planning, operation as well as when performing further experimentation in such scale facilities. This work may be used as a basis for further investigations focusing on the effect of sulphur, ash accumulation as well as the loss of sorbent and particle shrinkage due to attrition and fragmentation.

On the other hand, this work comprises the validation of simplified models used to predict the regenerator and carbonator efficiency in terms of sorbent conversion degree and the particle size evolution. A kinetic and attrition constant is calculated by fitting the data and a good agreement between the predicted and the actual data is shown. The models and the values of the main process data can be utilized for future simulation works as well as for economic models for equipment sizing, identification of the operating window, and process optimization.

# Annex A RITA-TGA basic data and operation principle

The TGA used in this work is a state of the art technology that was developed by the company Linseis Thermal Gmbh in cooperation with University of Stuttgart. Table 7 includes the main characteristics of the TGA. The heat is provided by induction with very high heating and cooling rates thus simulating conditions more close to the ones in fluidized beds. The weight difference as a result of the sorbent reaction under certain gas conditions and atmospheres is the basic principle of the TGA. The mass and the gas flows are set adequately so as to avoid differential conditions so as to reduce diffusion resistances. The analyzer was calibrated and tests were performed in conditions similar to the ones reported by the literature for reference reasons [118].

Table 7: TGA basic technical characteristics

Parameter	Unit	Value
Heating/ cooling rate	K/s	300/ 100
Sensitivity	µg	10
Response time	s	0.5
Max temperature	K	1373
Gas flow	cm^3/s	4
Reactive gas	-	CO_2, SO_2, CO, N_2, O_2, H_2O vapor
Sample mass	mg	10-100

Figure 45 includes cyclic carbonation calcination experimentation performed in the TGA. The mass change as a result of the CO_2 release during calcination at 1123K and CO_2 absorption at 923K is recorded in the y-axis left and the temperature in the y-axis right. The sorbent conversion is calculated by using the following formula:

$X = \dfrac{M_{N+1} - M_N}{M_N}$, where N is the number of the carbonation calcination cycle.
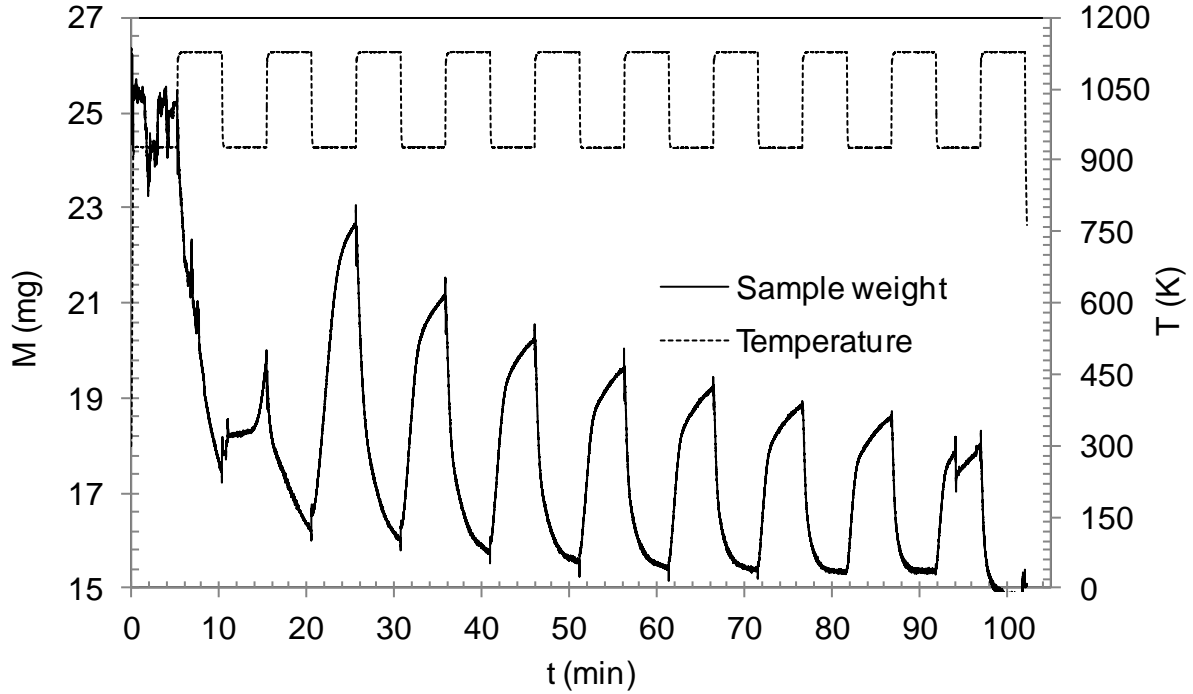
Figure 45: Measurement of the weight change under dry carbonation-calcination cyclic experimentation, $y_{CO_2,Carb}$=10%$_{vol}$ bal N$_2$, $y_{CO_2,Calc}$=0%$_{vol}$ bal N$_2$

Figure 46 presents the evolution of the X vs the time for 7 subsequent carbonation steps. Two reaction regimes can be clearly distinguished: the fast that is controlled by the kinetics and the slow controlled by the diffusion of CO$_2$ through the product layer. Moreover, the conversion decays rapidly with the cycle number and approaches only after 7 cycles around 20% of its maximum value.

Figure 47 indicates the calculation of the maximum carbonation conversion that is used in this work and is in agreement with the calculations as performed by Charitos et al [8].

The $X_{max,Ave}$ values that are recorded during the experimentation are plotted in Figure 48. It is shown a good agreement between the results as achieved by using this TGA and the ones reported in the literature for the same limestone as performed by the TGA in INCAR-CSIC. Moreover, the limestone follows the same trend in decay of the carbonation conversion as the typical one that is reported by the literature [118].
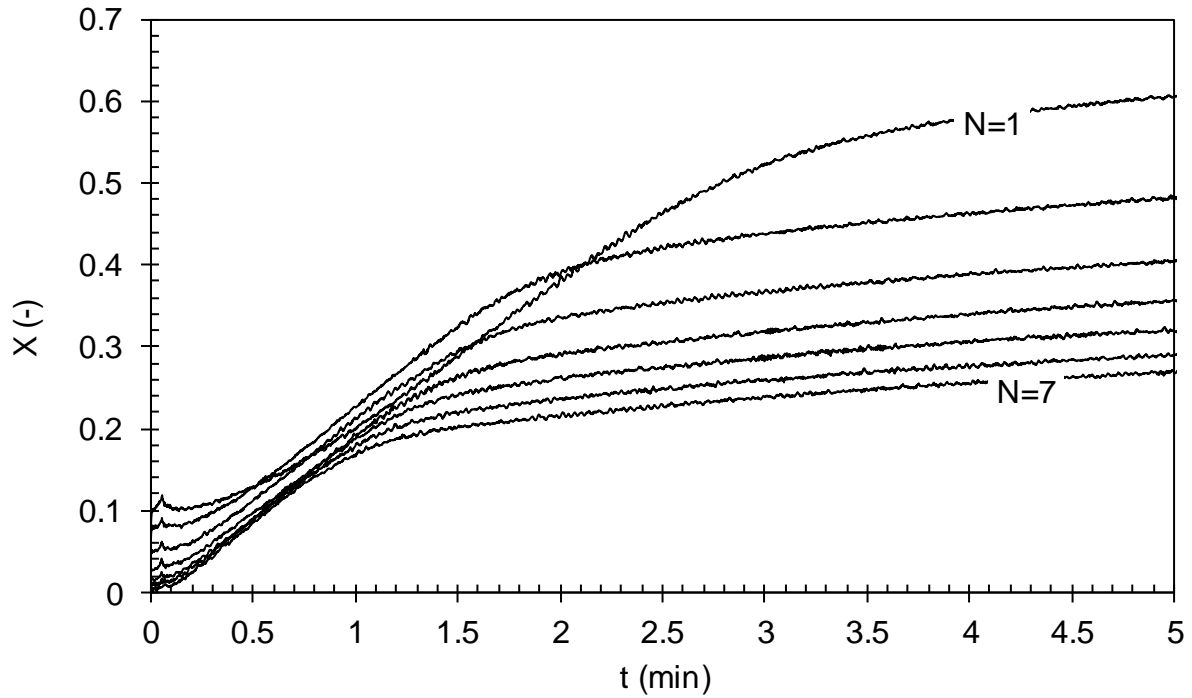
Figure 46: Carbonation conversion vs carbonation time for limestone LS-1 (0.3-0.6mm) calculated for 7 subsequent carbonation calcination cycles
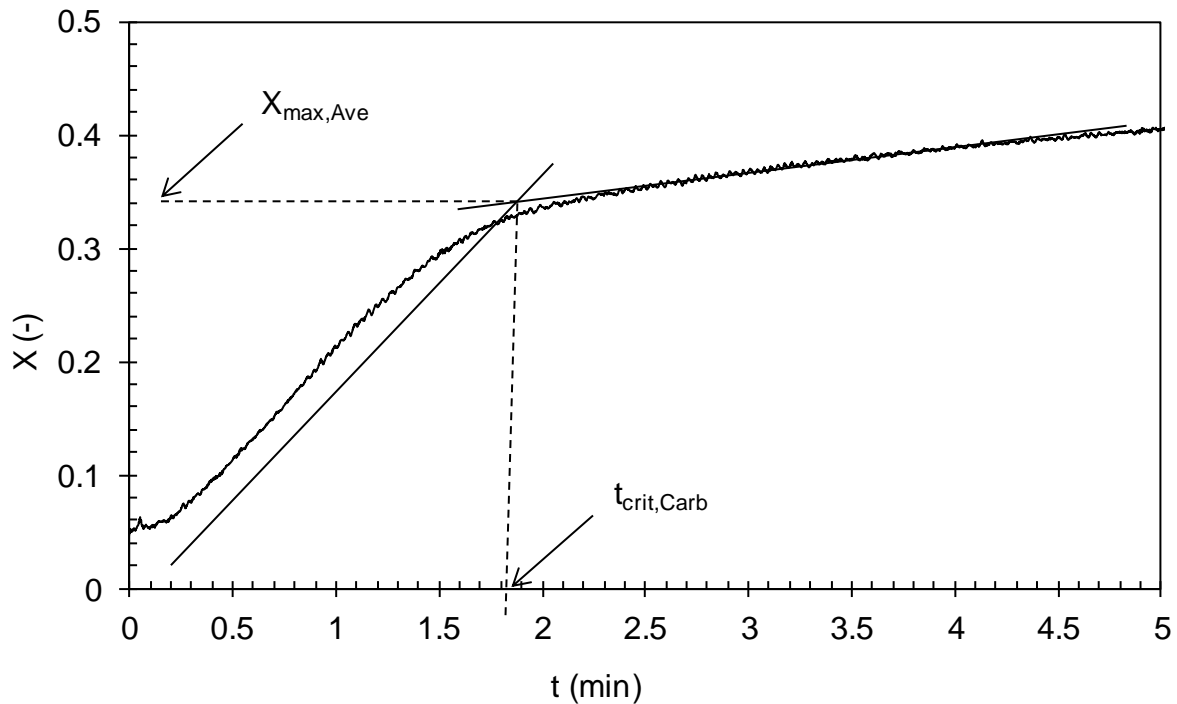
Figure 47: The maximum carbonation conversion $X_{max,Ave}$ and the critical time up to $X_{max,Ave}$
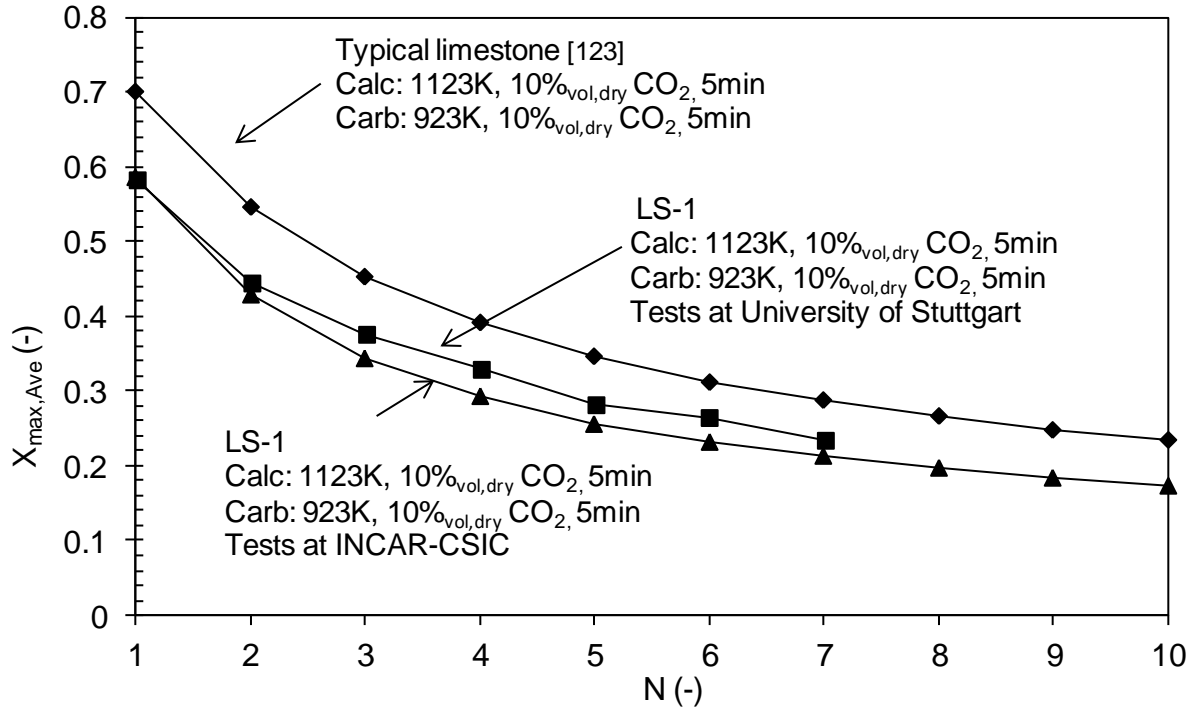
Figure 48: Comparison of the maximum average carbonation conversion as calculated after Rita TG tests with values reported in the literature for the typical limestone [118] and after tests with different TG analyzer at INCAR-CSIC.

Literature

[1] World energy outlook 2015 factsheet - Global energy trends to 2040, International Energy Agency, Paris, France 2015

[2] Climate change 2014: Synthesis report. Contribution of working groups I, II and III to the fifth assessment report of the Intergovernmental Panel on Climate Change. Core writing team, R.K. Pachauri and L.A. Meyer (eds.), Intergovernmental Panel on Climate Change, Geneva, Switzerland 2014

[3] International Energy Agency: World energy outlook 2015. Scenarios and projections. on line content (2016), website 2016. http://www.iea.org/publications/scenariosandprojections/

[4] Carbon capture and storage: the solution for deep emissions reductions, International Energy Agency, Paris, France 2015

[5] 2014:Technical summary. In: Climate change 2014: Mitigation of climate change. Contribution of working group III to the Fifth Assessment Report of the Intergovernmental Panel on Climate Change, Edenhofer, O., Pichs-Madruga, R., Sokona, Y., Kadner, S., Minx, J. C., Brunner, S., Agrawala, S., Baiocchi, G.,Bashmakov, I. A., Blanco, G., Broome, J., Bruckner, T., Bustamante, M., Clarke, L., Conte Grand, M., Creutzig, F., Cruz-Núñez, X., Dhakal, S., Dubash, P. Eickemeier, E. Farahani, M. Fischedick, M. Fleurbaey, R. Gerlagh, L. Gómez-Echeverri, N. K., Gupta, S., Harnisch, J., Jiang, K., Jotzo, F., Kartha, S., Klasen, S., Kolstad, C., Krey, V., Kunreuther, O. Lucon, O. Masera, Y. Mulugetta, R. B. Norgaard, A. Patt, N. H. Ravindranath, K. Riahi, H., Roy, J., Sagar, A., Schaeffer, R., Schlömer, S., Seto, K. C., Seyboth, K., Sims, R., Smith, P., Somanathan, E., Stavins, R., von Stechow, C., Sterner, T., Sugiyama, T., Suh, S., Ürge-Vorsatz, D., Urama, K., Venables, A., Victor, D. G., Weber, E., Zhou, D., Zou, J. and Zwickel, T., Cambridge University Press, Cambridge, UK, New York, USA 2014

[6] Heesink, A. B. M, Temmink, H.M. G.: Process for removing carbon dioxide regeneratively from gas streams: US Patent: W094/01203, 1994

[7] Manovic, V., Anthony, E. J.: Lime-based sorbents for high-temperature CO_2 capture. A review of sorbent modification methods. International Journal of Environmental Research and Public Health 7 (2010) 8, S. 3129–3140

[8] Charitos, A.: Experimental characterization of the calcium looping process for CO_2 capture., University of Stuttgart Dissertation. Stuttgart, Germany 2013

[9] Anthony, E. J.: Ca looping technology: current status, developments and future directions. 1 (2011) 1, S. 36–47

[10] Dean, C. C., Blamey, J., Florin, N. H., Al-Jeboori, M. J., Fennell, P. S.: The calcium looping cycle for CO_2 capture from power generation, cement manufacture and hydrogen production. 89 6, S. 836–855

[11] Hawthorne, C., Trossmann, M., Galindo Cifre, P., Schuster, A., Scheffknecht, G.: Simulation of the carbonate looping power cycle. Energy Procedia 1 (2009) 1, S. 1387–1394

[12] Martínez, I., Murillo, R., Grasa, G. S., Abanades García, Juan Carlos: Integration of a Ca looping system for CO_2 capture in existing power plants. AIChE Journal (2011) 57 (9), S. 2599–2607

[13] Romano, M. C.: Modeling the carbonator of a Ca-looping process for CO_2 capture from power plant flue gas. Chemical Engineering Science 69 (2012) 1, S. 257–269

[14] Abanades, J. C., Anthony, E. J., Wang, J., Oakey, J. E.: Fluidized bed combustion systems integrating CO_2 capture with CaO. Environmental Science & Technology 39 (2005) 8, S. 2861–2866

[15] Markusson, N.: The politics of FGD deployment in the UK (1980s - 2009). Final case study report as part of work package 2 of the UKERC project: „CCS – Releasing the potential?" University of Edinburg, England 2012

[16] Shimizu, T., Hirama, T:, Hosada, H., Kitano, K., Inagaki, M. , and Tejima K.: A twin fluidized bed reactor system for removal of CO_2 from combustion processes. Institution of Chemical Engineers (1999), S. 77 Pt A

[17] Abanades, J. C., Grasa, G., Alonso, M., Rodríguez, N., Anthony, E. J. , Romeo, L. M.: Cost structure of a postcombustion CO_2 capture system using CaO. Environmental Science & Technology 41 (2007) 15, S. 5523–5527

[18] Romeo, L. M., Abanades, J. C., Escosa, J. M., Paño, J., Giménez, A., Sánchez-Biezma, A. , Ballesteros, J. C.: Oxy-fuel carbonation/calcination cycle for low cost CO_2 capture in existing power plants. Energy Conversion and Management 49 (2008) 10, S. 2809–2814

[19] Zhao, M., Minett, A. I. , Harris, A. T.: A review of techno-economic models for the retrofitting of conventional pulverised-coal power plants for post-combustion capture (PCC) of CO_2. Energy Environ. Sci. 6 (2013) 1, S. 25–40

[20] Cormos, C.-C.: Economic evaluations of coal-based combustion and gasification power plants with post-combustion CO_2 capture using calcium looping cycle. Energy 78 (2014), S. 665–673

[21] Cormos, C.-C.: Assessment of chemical absorption/adsorption for post-combustion CO_2 capture from natural gas combined cycle (NGCC) power plants. Applied Thermal Engineering 82 (2015), S. 120–128

[22] Atsonios, K., Panopoulos, K., Grammelis, P., Kakaras, E.: Exergetic comparison of CO_2 capture techniques from solid fossil fuel power plants. International Journal of Greenhouse Gas Control 45 (2016) s, S. 106–117

[23] Hanak, D. P., Anthony, E. J., Manovic, V.: A review of developments in pilot-plant testing and modelling of calcium looping process for CO_2 capture from power generation systems. Energy Environ. Sci. 8 (2015) 8, S. 2199–2249

[24] Dieter, H., Hawthorne, C., Zieba, M., Scheffknecht, G.: Progress in calcium looping post combustion CO_2 capture: successful pilot scale demonstration. Energy Procedia (2013) 37, S. 48–56

[25] Arias, B., Diego, M., Abanades, J., Lorenzo, M., Diaz, L., Martínez, D., Alvarez, J., Sánchez-Biezma, A.: Demonstration of steady state CO_2 capture in a 1.7 MW_{th} calcium looping pilot. International Journal of Greenhouse Gas Control 18 (2013), S. 237–245

[26] Ströhle, J., Junk, M., Kremer, J., Galloy, A., Epple, B.: Carbonate looping experiments in a 1 MW_{th} pilot plant and model validation. Fuel 127 (2014), S. 13–22

[27] Stanmore, B., Gilot, P.: Review - calcination and carbonation of limestone during thermal cycling for CO_2 sequestration. Fuel Processing Technology 86 (2005) 16, S. 1707–1743

[28] Harrison, D. P.: Sorption-enhanced hydrogen production: a review. Industrial & Engineering Chemistry Research 47 (2008) 17, S. 6486–6501

[29] Florin, N. H., Harris, A. T.: Enhanced hydrogen production from biomass with in situ carbon dioxide capture using calcium oxide sorbents. Chemical Engineering Science 63 (2008) 2, S. 287–316

[30] Blamey, J., Anthony, E., Wang, J., Fennell, P.: The calcium looping cycle for large-scale CO_2 capture. Progress in Energy and Combustion Science 36 (2010) 2, S. 260–279

[31] Liu, W., An, H., Qin, C., Yin, J., Wang, G., Feng, B., Xu, M.: Performance enhancement of calcium oxide sorbents for cyclic CO_2 capture. A review. Energy & Fuels 26 (2012) 5, S. 2751–2767

[32] Kierzkowska, A. M., Pacciani, R., Müller, C. R.: CaO-based CO_2 sorbents: from fundamentals to the development of new, highly effective materials. ChemSusChem 6 (2013) 7, S. 1130–1148

[33] Romano, M. C., Martínez, I., Murillo, R., Arstad, B., Blom, R., Ozcan, D. C., Ahn, H., Brandani, S.: Process simulation of Ca-looping processes: review and guidelines. Energy Procedia 37 (2013), S. 142–150

[34] Boot-Handford, M. E., Abanades, J. C., Anthony, E. J., Blunt, M. J., Brandani, S., Mac Dowell, N., Fernandez, J. R., Ferrari, M.-C., Gross, R., Hallett, J. P., Haszeldine, R. S., Heptonstall, P., Lyngfelt, A., Makuch, Z., Mangano, E., Porter, Richard T. J., Pourkashanian, M., Rochelle, G. T., Shah, N., Yao, J. G., Fennell, P. S.: Carbon capture and storage update. Energy Environ. Sci. 7 (2014) 1, S. 130–189

[35] International Energy Agency: Key trends in CO_2 emissions. Excerpt from: CO_2 emissions from fuel combustion, Paris, France 2015

[36] Abanades, J. C., Arias, B., Lyngfelt, A., Mattisson, T., Wiley, D. E., Li, H., Ho, M. T., Mangano, E., Brandani, S.: Emerging CO_2 capture systems. International Journal of Greenhouse Gas Control 40 (2015), S. 126–166

[37] Key coal trends Excerpt from: Coal information (2015 edition), International Energy Agency, website, 2015. https://www.iea.org/publications/freepublications/publication/coal-information---2015-edition---excerpt.html

[38] A Roadmap for moving to a competitive low carbon economy in 2050, European Commission, website, 2011. http://eur-lex.europa.eu/legal-content/EN/ALL/?uri=CELEX:52011DC0112

[39] United States environmental protection agency: on line content (2016), website, 2016. http://www3.epa.gov/climatechange/ghgemissions/sources/electricity.html

[40] Leung, D. Y., Caramanna, G. , Maroto-Valer, M. Mercedes: An overview of current status of carbon dioxide capture and storage technologies. Renewable and Sustainable Energy Reviews 39 (2014), S. 426–443

[41] Koornneef, J., Ramírez, A., Turkenburg, W., Faaij, A.: The environmental impact and risk assessment of CO_2 capture, transport and storage – An evaluation of the knowledge base. Progress in Energy and Combustion Science 38 (2012) 1, S. 62–86

[42] Hoffmann, S., Bartlett, M., Finkenrath, M., Evulet, A. , Ursin, T.: Performance and cost analysis of advanced gas turbine cycles with precombustion CO_2 capture. ASME. J. Eng. Gas Turbines Power (2008) 131 (2), S. 021701-021701-7

[43] Buhre, B. J. P., Elliott, L. K., Sheng, C. D., Gupta, R. P., Wall, T. F.: Oxy-fuel combustion technology for coal-fired power generation. Progress in Energy and Combustion Science 31 (2005) 4, S. 283–307

[44] Toftegaard, M. B., Brix, J., Jensen, P. A., Glarborg, P. , Jensen, A. D.: Oxy-fuel combustion of solid fuels. Progress in Energy and Combustion Science 36 (2010) 5, S. 581–625

[45] Kather, A., Scheffknecht, G.: The oxy-coal process with cryogenic oxygen supply. Naturwissenschaften 96 (2009) 9, S. 993–1010

[46] Scheffknecht, G., Al-Makhadmeh, L., Schnell, U., Maier, J.: Oxy-fuel coal combustion - A review of the current state-of-the-art. International Journal of Greenhouse Gas Control 5 (2011), S. S16

[47] United States department of energy: On line content (2016): website, 2016. http://www.netl.doe.gov/research/coal/carbon-capture/post-combustion

[48] Douglas, A., Tsouris, C.: Separation of CO_2 from flue gas: A review. Separation Science and Technology (2005), S. 321–348

[49] Special report on carbon dioxide capture and storage, Intergovernmental Panel on Climate Change, Montreal, Canada 2005

[50] Global CCS Institute: Large scale CCS projects. On line content (2016), website, 2016. https://www.globalccsinstitute.com/projects/large-scale-ccs-projects

[51] Report: CO_2 capture and storage. Decarbonising energy from fossil fuels, European Commission, website, 2009. http://www.ab.gov.tr/files/ardb/evt/1_avrupa_birligi/1_9_politikalar/1_9_6_enerji_politikasi/2009_co2_capture_and_storage.pdf

[52] Hirama, T., Hosada, H., Kitano, K:, Shimizu, T: Method of separating carbon dioxide from carbon dioxide containing gas and combustion apparatus: US Patent: 5665319, 1997

[53] Abanades, J. C., Alvarez, D.: Conversion limits in the reaction of CO_2 with lime. Energy & Fuels 17 (2003) 2, S. 308–315

[54] Grasa, G. S., Abanades, J. C.: CO_2 capture capacity of CaO in long series of carbonation/ calcination cycles. Industrial & Engineering Chemistry Research 45 (2006) 26, S. 8846–8851

[55] Lysikov, A. I., Salanov, A. N., Okunev, A. G.: Change of CO_2 carrying capacity of CaO in isothermal recarbonation−decomposition cycles. Industrial & Engineering Chemistry Research 46 (2007) 13, S. 4633–4638

[56] Charitos, A., Rodríguez, N., Hawthorne, C., Alonso, M., Zieba, M., Arias, B., Kopanakis, G., Scheffknecht, G. , Abanades, J. C.: Experimental validation of the calcium looping CO_2 capture process with two circulating fluidized bed carbonator reactors. Industrial & Engineering Chemistry Research 50 (2011) 16, S. 9685–9695

[57] Martínez, I., Grasa, G., Murillo, R., Arias, B. , Abanades, J. C.: Kinetics of calcination of partially carbonated particles in a Ca-Looping system for CO_2 capture. Energy & Fuels 26 (2012) 2, S. 1432–1440

[58] Kuramochi, T., Ramírez, A., Turkenburg, W., Faaij, A.: Comparative assessment of CO_2 capture technologies for carbon-intensive industrial processes. Progress in Energy and Combustion Science 38 (2012) 1, S. 87–112

[59] Martínez, A., Lara, Y., Lisbona, P., Romeo, L. M.: Energy penalty reduction in the calcium looping cycle. International Journal of Greenhouse Gas Control 7 (2012), S. 74–81

[60] Alvarez, D., Abanades, J. C.: Pore-size and shape effects on the recarbonation performance of calcium oxide submitted to repeated calcination/recarbonation cycles. Energy & Fuels 19 (2005) 1, S. 270–278

[61] Borgwardt, R.: Calcium oxide sintering in atmospheres containing water and carbon dioxide. Industrial & Engineering Chemistry Research (1989) 28, S. 493–500

[62] Borgwardt, R.: Sintering of nascent calcium oxide. Chemical Engineering Science (1989) Volume 44, Issue 1, S. 53–60

[63] Chen, C., Zhao, C., Liang, C. , Pang, K.: Calcination and sintering characteristics of limestone under O_2/CO_2 combustion atmosphere. Fuel Processing Technology 88 (2007) 2, S. 171–178

[64] Li, Z.-S., Fang, F., Tang, X.-y. , Cai, N.-S.: Effect of temperature on the carbonation reaction of CaO with CO_2. Energy & Fuels 26 (2012) 4, S. 2473–2482

[65] Coppola, A., Palladino, L., Montagnaro, F., Scala, F. , Salatino, P.: Reactivation by steam hydration of sorbents for fluidized-bed calcium looping. Energy & Fuels 29 (2015) 7, S. 4436–4446

[66] González, B., Blamey, J., Al-Jeboori, M. J., Florin, N. H., Clough, P. T., Fennell, P. S.: Additive effects of steam addition and HBr doping for CaO-based sorbents for CO_2 capture. Chem. Eng. Process. (2015) 103, S. 21-26

[67] Scala, F., Montagnaro, F., Salatino, P.: Attrition of limestone by impact loading in fluidized beds. Energy & Fuels 21 (2007) 5, S. 2566–2572

[68]   Coppola, A., Montagnaro, F., Salatino, P., Scala, F.: Attrition of limestone during fluidized bed calcium looping cycles for CO_2 capture. Combustion Science and Technology (2012) vol.184, Issue 7-8

[69]   Coppola, A., Montagnaro, F., Salatino, P., Scala, F.: Fluidized bed calcium looping: The effect of SO_2 on sorbent attrition and CO_2 capture capacity. Chemical Engineering Journal 207-208 (2012), S. 445–449

[70]   Global action to advance carbon capture and storage - A focus on industrial applications, International Energy Agency, Paris, France 2013

[71]   Rodríguez, N., Alonso, M., Abanades, J. C.: Experimental investigation of a circulating fluidizedbed reactor to capture CO_2 with CaO. AIChE Journal (2011a) 57, S. 1356–1366

[72]   Arias, B., Cordero, J. M., Alonso, M., Diego, M. E., Abanades, J. C.: Investigation of SO_2 capture in a circulating fluidized bed carbonator of a Ca looping cycle. Industrial & Engineering Chemistry Research 52 (2013) 7, S. 2700–2706

[73]   Sánchez-Biezma, A., Ballesteros, J. C., Diaz, L., Zárraga, E. de, Álvarez, F. J., López, J., Arias, B., Grasa, G., Abanades, J. C.: Postcombustion CO_2 capture with CaO. Status of the technology and next steps towards large scale demonstration. Energy Procedia 4 (2011), S. 852–859

[74]   Ylätalo, J.: Model based analysis of the post combustion calcium looping process for carbon dioxide capture, Lappeenranta University of Technology Dissertation. Lappeenranta, Finland 2013

[75]   Yang, Y., Zhai, R., Duan, L., Kavosh, M., Patchigolla, K., Oakey, J.: Integration and evaluation of a power plant with a CaO-based CO_2 capture system. International Journal of Greenhouse Gas Control 4 (2010) 4, S. 603–612

[76]   Alonso, M., Rodríguez, N., Grasa, G., Abanades, J. C.: Modelling of a fluidized bed carbonator reactor to capture CO_2 from a combustion flue gas. Chemical Engineering Science 64 (2009) 5, S. 883–891

[77]   Martínez, I., Grasa, G., Murillo, R., Arias, B., Abanades, J. C.: Kinetics of Calcination of Partially Carbonated Particles in a Ca-Looping System for CO_2 Capture. Energy & Fuels 26 (2012) 2, S. 1432–1440

[78]   Diego, M. E., Arias, B., Abanades, J.C.: Modeling the solids circulation rates and solids inventories of an interconnected circulating fluidized bed reactor system for CO_2 capture by calcium looping. Chemical Engineering Journal 198-199 (2012), S. 228–235

[79]   Romano, M.: Coal-fired power plant with calcium oxide carbonation for postcombustion CO_2 capture. Energy Procedia 1 (2009) 1, S. 1099–1106

[80]   Romano, M.: Ultra-high CO_2 capture efficiency in CFB oxy-fuel power plants by calcium looping process for CO_2 recovery from purification units vent gas. International Journal of Greenhouse Gas Control 18 (2013), S. 57–67

[81]   Vorrias, I., Atsonios, K., Nikolopoulos, A., Nikolopoulos, N., Grammelis, P., Kakaras, E.: Calcium looping for CO_2 capture from a lignite fired power plant. Fuel 113 (2013), S. 826–836

[82]   Ströhle, J., Galloy, A., Epple, B.: Feasibility study on the carbonate looping process for post-combustion CO_2 capture from coal-fired power plants. Energy Procedia 1 (2009) 1, S. 1313–1320

[83]   Lasheras, A., Ströhle, J., Galloy, A., Epple, B.: Carbonate looping process simulation using a 1D fluidized bed model for the carbonator. International Journal of Greenhouse Gas Control 5 (2011) 4, S. 686–693

[84]   Kari Myöhänen: Modelling of combustion and sorbent reactions in three dimensional flow environment of a circulating fluidized bed furnace. Dissertation, Lappeenrante University of Technology. Lappeenrante, Finland 2011

[85]   Ylätalo, J., Ritvanen, J., Tynjälä, T., Hyppänen, T.: Model based scale-up study of the calcium looping process. Fuel 115 (2014), S. 329–337

[86]   Ylätalo, J., Parkkinen, J., Ritvanen, J., Tynjälä, T., Hyppänen, T.: Modeling of the oxy-combustion calciner in the post-combustion calcium looping process. Fuel 113 (2013), S. 770–779

[87]   Nikolopoulos, A., Nikolopoulos, N., Charitos, A., Grammelis, P., Kakaras, E., Bidwe, A. R., Varela, G.: High-resolution 3-D full-loop simulation of a CFB carbonator cold model. Chemical Engineering Science 90 (2013), S. 137–150

[88]   Atsonios, K., Zeneli, M., Nikolopoulos, A., Nikolopoulos, N., Grammelis, P., Kakaras, E.: Calcium looping process simulation based on an advanced thermodynamic model combined with CFD analysis. Fuel 153 (2015), S. 370–381

[89]   Rodríguez, N., Alonso, M., Abanades, J.C., Charitos, A., Hawthorne, C., Scheffknecht, G., Lu, D. Y., Anthony, E.J.: Comparison of experimental results from three dual fluidized bed test facilities capturing CO_2 with CaO. Energy Procedia 4 (2011), S. 393–401

[90]   Duelli (Varela), G., Bidwe, A. R., Papandreou, I., Dieter, H., Scheffknecht, G.: Characterization of the oxy-fired regenerator at a 10 kW_{th} dual fluidized bed calcium looping facility. Applied Thermal Engineering (2014) 74, S. 54–60

[91]   Charitos, A., Hawthorne, C., Bidwe, A., Sivalingam, S., Schuster, A., Spliethoff, H., Scheffknecht, G.: Parametric investigation of the calcium looping process for CO_2 capture in a 10kWth dual fluidized bed. International Journal of Greenhouse Gas Control 4 (2010) 5, S. 776–784

[92]   Scala, F., Cammarota, A., Chirone, R., Salatino, P.: Comminution of limestone during batch fluidized bed calcination and sulfation. AIChE Journal (1997) 43 (2), S. 363–373

[93]   González, B., Alonso, M., Abanades, J. C.: Sorbent attrition in a carbonation/calcination pilot plant for capturing CO_2 from flue gases. Fuel 89 (2010) 10, S. 2918–2924

[94]   Jia, L., Hughes, R., Lu, D., Anthony, E.J., Lau, I.: Attrition of Calcining Limestones in Circulating Fluidized-Bed Systems. Industrial & Engineering Chemistry Research 46 (2007) 15, S. 5199–5209

[95]   Cook, J.L., Khang, S.J., Lee, S.K., Keener, T.C.: Attrition and Changes in Particle-Size Distribution of Lime Sorbents in a Circulating Fluidized-Bed Absorber. Powder Technology 89 (1996) 1, S. 1–8

[96]   Chen, Z., Grace, J. R., Jim Lim, C.: Limestone particle attrition and size distribution in a small circulating fluidized bed. Fuel 87 (2008) 7, S. 1360–1371

[97]   Darroudi, T., Searcy, A.: Effect of CO_2 pressure on the rate of decomposition of calcite. Journal of Physical Chemistry (1981) 85 (26), S. 3971–3974

[98]   Donat, F., Florin, N. H., Anthony, E. J., Fennell, P.S.: Influence of high-temperature steam on the reactivity of CaO sorbent for CO_2 capture. Environmental Science & Technology 46 (2012) 2, S. 1262–1269

[99]   Champagne, S.: Steam enhanced calcination for CO_2 capture with CaO, University of Ottawa Master Thesis. Ottawa, Canada 2014

[100] García-Labiano, F., Abad, A., Diego, L., Gayán, P., Adánez, J.: Calcination of calcium-based sorbents at pressure in a broad range of CO_2 concentrations. Chemical Engineering Science 57 (2002) 13, S. 2381–2393

[101] Arias, B., Grasa, G., Abanades, J.C., Manovic, V., Anthony, E.J.: The effect of steam on the fast carbonation reaction rates of CaO. Industrial & Engineering Chemistry Research 51 (2012) 5, S. 2478–2482

[102] Manovic, V., Anthony, E.J.: Carbonation of CaO-based sorbents enhanced by steam addition. Industrial & Engineering Chemistry Research 49 (2010) 19, S. 9105–9110

[103] Khinast, J., Krammer, G., Brunner, C., Staudinger, G.: Decomposition of limestone: The influence of CO_2 and particle size on the reaction rate. Chemical Engineering Science 51 (1996) 4, S. 623–634

[104] MacIntire, W. , Stansel, T.: Steam catalysis in calcination of dolomite and limestone fines. Industrial and Engineering Chemistry (1953), S. 1548–1555

[105] Duelli (Varela), G., Charitos, A., Diego, M. E., Stavroulakis, E., Dieter, H., Scheffknecht, G.: Investigations at a 10kWth calcium looping dual fluidized bed facility: limestone calcination and CO_2 capture under high CO_2 and water vapor atmosphere. International Journal of Greenhouse Gas Control 33 (2015), S. 103–112

[106] Itskos, G., Grammelis, P., Scala, F., Pawlak-Kruczek, H., Coppola, A., Salatino, P., Kakaras, E.: A comparative characterization study of Ca-looping natural sorbents. Applied Energy 108 (2013), S. 373–382

[107] Deliverable 2.1: Report on bench/pilot scale test results. CAL-MOD: Modelling and experimental validation of calcium looping CO_2-capture process for near-zero CO_2 emission power plants, Duelli (Varela), G., 2013

[108] Champagne, S., Lu, D. Y., Macchi, A., Symonds, R. T., Anthony, E. J.: Influence of steam injection during calcination on the reactivity of CaO-based sorbent for carbon capture. Industrial & Engineering Chemistry Research 52 (2013) 6, S. 2241–2246

[109] Chen, Z., Jim Lim, C., Grace, J. R.: Study of limestone particle impact attrition. Chemical Engineering Science 62 (2007) 3, S. 867–877

[110] Benedetto, A., Salatino, P.: Modelling attrition of limestone during calcination and sulfation in a fluidized bed reactor. Powder Technology (1998) 95, S. 119

[111] Lee, S.-K., Jiang, X., Kleener, T., Khangr, S.: Attrition of lime sorbents during fluidization in a circulating fluidized bed absorber. Industrial & Engineering Chemistry Research (1987) 49, S. 193

[112] Duelli (Varela), G., Charitos, A., Armbrust, N., Dieter, H., Scheffknecht, G.: Analysis of the calcium looping system behavior by implementing simple reactor and attrition models at a 10 kW_{th} dual fluidized bed facility under continuous operation. Fuel 169 (2016), S. 79–86

[113] Coppola, A., Montagnaro, F., Salatino, P.,Scala, F.: Fluidized Bed Calcium Looping Cycles for CO_2 Capture: A Comparison between Dolomite and Limestone

[114] Wang, Y., Lin, S., Suzuki, Y.: Limestone Calcination with CO_2 Capture (II): decomposition in CO_2/ steam and CO_2/ N_2 atmospheres. Energy & Fuels 22 (2008) 4, S. 2326–2331

[115] Diego, M. E., Arias, B., Alonso, M. , Abanades, J. C.: The impact of calcium sulfate and inert solids accumulation in post-combustion calcium looping systems. Fuel 109 (2013), S. 184–190

[116] Arias, B., Abanades, J., Grasa, G.: An analysis of the effect of carbonation conditions on CaO deactivation curves. Chemical Engineering Journal 167 (2011) 1, S. 255–261

[117] Alonso, M., Criado, Y. A., Abanades, J. C. , Grasa, G.: Undesired effects in the determination of CO_2 carrying capacities of CaO during TG testing. Fuel 127 (2014), S. 52–61

[118] Abanades, J. C.: The maximum capture efficiency of CO_2 using a carbonation/calcination cycle of CaO/CaCO3. Chemical Engineering Journal 90 (2002) 3, S. 303–306

[119] Hills, A.: The mechanism of the thermal decomposition of calcium carbonate. Chemical Engineering Science 23 (1968) 4, S. 297–320

[120] Lu, D. Y., Hughes, R. W., Anthony, E. J.: Ca-based sorbent looping combustion for CO_2 capture in pilot-scale dual fluidized beds. Fuel Processing Technology 89 (2008) 12, S. 1386–1395

[121] Alonso, M., Rodríguez, N., González, B., Grasa, G., Murillo, R., Abanades, J. C.: Carbon dioxide capture from combustion flue gases with a calcium oxide chemical loop. Experimental results and process development. International Journal of Greenhouse Gas Control 4 (2010) 2, S. 167–173

[122] Duelli (Varela), G., Bernard, L., Bidwe, A. R., Stack-Lara, V., Hawthorne, C., Zieba, M., Scheffknecht, G.: Calcium Looping Process: Experimental investigation of limestone performance regenerated under high CO_2 partial pressure and validation of a carbonator model. Energy Procedia 37 (2013), S. 190–198

[123] Rodríguez, N., Alonso, M., Abanades, J.: Average activity of CaO particles in a calcium looping system. Chemical Engineering Journal 156 (2010) 2, S. 388–394

[124] Fennell, P. S., Anthony, E. J.: Calcium and chemical looping technology for power generation and carbon diocide (CO_2) capture. Cambridge, UK, Waltham, USA, Kindlington, UK: Woodhead Publishing Series in Energy 2015

[125] Stavroulakis, E.: Experimental investigation of the effect of water vapor on the Ca-looping process at a $10KW_{th}$ dual fluidized bed faciliy, University of Stuttgart Diploma thesis. Stuttgart, Germany 2013

[126] Papandreou, I.: Experimental study of the calcium looping process under high CO_2 concentrations at a 10KWth dual fluidized bed facility, University of Stuttgart Diploma thesis. Stuttgart, Germany 2014

[127] Bernard, L.: Post combustion calcium looping process. The effect of high partial pressure of CO_2 during regeneration on the main process characteristics, University of Stuttgart Bachelor thesis. Stuttgart, Germany 2012

[128] VGB Scientific Advisory Board: Power Plants 2020+. Power plant options for the future and the related demand for research, Statement of the advisory board. Essen, Germany 2010

[129] Stanger, R., Wall, T., Spörl, R., Paneru, M., Grathwohl, S., Weidmann, M., Scheffknecht, G., McDonald, D., Myöhänen, K., Ritvanen, J., Rahiala, S., Hyppänen, T., Mletzko, J., Kather, A. , Santos, S.: Oxy-fuel combustion for CO_2 capture in power plants. International Journal of Greenhouse Gas Control 40 (2015), S. 55–125

[130] Vaux, W. G.: Attrition of particles in the bubbling zone of a fluidized bed. American power congress, 40:793 (1978)

[131] "Modeling and experimental validation of calcium looping CO_2-capture process for near-zero CO_2- emission power plants". Research programme of the Research Fund for Coal and Steel, CALMOD: RFCR-CT-2010-00013. Final report, Univeristy of Stuttgart, Stuttgart, Germany 2014

[132] Duelli (Varela), G., Papandreou, I., Stack-Lara, V., Dieter, H., Scheffknecht, G.: Calcium looping process for CO_2 capture: Experimental characterization of the regenerator operation under oxy-fuel conditions, in a 10 kW_{th} dual fluidized bed facility. 6th Int. Conf. on CCT, Thessaloniki, Greece: 2013

[133] Duelli (Varela), G., Bernard, L., Bidwe, A. R., Stack-Lara, V., Hawthorne, C., Zieba, M., Scheffknecht, G.: Calcium looping process: Experimental investigation of limestone performance regenerated under high CO_2 partial pressure and validation of a carbonator model. GHGT-11 conference, Osaka, Japan: 2012

[134] Atsonios, K., Grammelis, P., Antiohos, S. K., Nikolopoulos, N., Kakaras, E.: Integration of calcium looping technology in existing cement plant for CO_2 capture: Process modeling and technical considerations. Fuel 153 (2015), S. 210–223

[135] Blamey, J., Anthony, E., Wang, J., Fennell, P.: The calcium looping cycle for large-scale CO_2 capture. Progress in Energy and Combustion Science 36 (2010) 2, S. 260–279

[136] Dieter, H., Hawthorne, C., Zieba, M., Scheffknecht, G.: Progress in Calcium looping post combustion CO_2 capture: successful pilot scale demonstration. Energy Procedia (2013) 37, S. 48–56

[138] Ströhle, J., Junk, M., Kremer, J., Galloy, A., Epple, B.: Carbonate looping experiments in a 1 MW_{th} pilot plant and model validation. Fuel 127 (2014), S. 13–22

[140] Zeneli, M., Nikolopoulos, A., Nikolopoulos, N., Grammelis, P., Kakaras, E.: Application of an advanced coupled EMMS-TFM model to a pilot scale CFB carbonator. Chemical Engineering Science 138 (2015), S. 482–498

[141] Martínez, I., Grasa, G., Murillo, R., Arias, B., Abanades, J.: Modelling the continuous calcination of CaCO3 in a Ca-looping system. Chemical Engineering Journal 215-216 (2013), S. 174–181

[142] Wen-Ching, Y. (Hrsg.): Fluidization solids handling and processing. Industrial applications. Westwood, New Jersey, USA: Noyes Publications 1999

[143] Coppola, A., Gais, E., Mancino, G., Montagnaro, F., Scala, F., Salatino, P.:Effect of steam on the performance of Ca-based sornbents in calcium looping process. Powder Technology (2016), http://dx.doi.org/10.1016/j.powtec.2016.11.062